

STATUS OF THESIS

Title of thesis 

Improving Data Quality for Shallow Seismic Refraction Survey in Noisy Environment
--

I, WAN SURIANI BINTI A RAMAN

hereby allow my thesis to be placed at the Information Resource Center (IRC) of Universiti Teknologi PETRONAS (UTP) with the following conditions:

1. The thesis becomes the property of UTP
2. The IRC of UTP may make copies of the thesis for academic purposes only.
3. This thesis is classified as

Confidential

Non-confidential

If this thesis is confidential, please state the reason:

\_\_\_\_\_  
\_\_\_\_\_

The contents of the thesis will remain confidential for \_\_\_\_\_ years.

Remarks on disclosure:

\_\_\_\_\_  
\_\_\_\_\_

Endorsed by

\_\_\_\_\_

\_\_\_\_\_

Signature of Author

Signature of Supervisor

Permanent address: Lot 915,

Name of Supervisor

Kampung Sawah Dato',

Assoc. Prof. Dr. Zuhar Zahir

86800 Mersing,

Bin Tuan Harith

Johor, Malaysia

Date : \_\_\_\_\_

Date : \_\_\_\_\_

UNIVERSITI TEKNOLOGI PETRONAS  
IMPROVING DATA QUALITY FOR SHALLOW SEISMIC REFRACTION  
SURVEY IN NOISY ENVIRONMENT

by

WAN SURIANI BINTI A RAMAN

The undersigned certify that they have read, and recommend to the Postgraduate Studies Programme for acceptance this thesis for the fulfillment of the requirements for the degree stated.

Signature:

\_\_\_\_\_

Main Supervisor:

Assoc. Prof. Dr. Zuhar Zahir Bin Tuan Harith

Signature:

\_\_\_\_\_

Head of Department:

Assoc. Prof. Dr. Abdul Hadi Bin Abd Rahman

Date:

\_\_\_\_\_

IMPROVING DATA QUALITY FOR SHALLOW SEISMIC REFRACTION  
SURVEY IN NOISY ENVIRONMENT

by

WAN SURIANI BINTI A RAMAN

A Thesis

Submitted to the Postgraduate Studies Programme

as a Requirement for the Degree of

MASTER OF SCIENCE

DEPARTMENT OF PETROLEUM GEOSCIENCES

UNIVERSITI TEKNOLOGI PETRONAS

BANDAR SERI ISKANDAR

PERAK

MARCH 2013

DECLARATION OF THESIS

Title of thesis 

Improving Data Quality for Shallow Seismic Refraction Survey in Noisy Environment
--

I, WAN SURIANI BINTI A RAMAN  
hereby declare that the thesis is based on my original work except for quotations and citations which have been duly acknowledged. I also declare that it has not been previously or concurrently submitted for any other degree at UTP or other institutions.

Witnessed by

\_\_\_\_\_  
Signature of Author  
Permanent address: Lot 915,  
Kampung Sawah Dato',  
86800 Mersing,  
Johor, Malaysia

\_\_\_\_\_  
Signature of Supervisor  
Assoc. Prof. Dr. Zuhar Zahir  
Bin Tuan Harith

Date : \_\_\_\_\_

Date : \_\_\_\_\_

## DEDICATION

*To those who still believe in themselves who've no regret for that which have  
happened before in their life...*

*Keep your chin up and keep on moving...*

*"In three words I can sum up everything I've learned about life: it goes on."*

*— Robert Frost*

## ACKNOWLEDGEMENT



This thesis marks the opening and beginning of a new chapter in life at the end of this exhausting but deeply fulfilling journey of obtaining my MSc. It is an immense pleasure to express my greatest thanks to all those who have given me their support, encouragement and have contributed to my success and well-being throughout this journey.

I am extremely indebted to my supervisor Assoc. Prof. Dr. Zuhar Zahir Bin Tuan Harith for his kind understanding, encouragement and guidance that has served as a solid foundation for the pursuance and completion of my MSc tenure. I am grateful to Mr. Deva A. for his help and guidance during the early stages of my research. I would like to thank Prof. Dr. Noorhana for her motherly care and concern. Not to forget all crew members that was involved during the acquisition stage.

I would also like to take this opportunity to express my most sincere appreciation to my lab mates who have patiently bear with the only rose in the lab. Warmly thanks to Sajid, Pak Maman, Pak Eko, Amin, Ifti and Luluan for their valuable help and support.

My warmest appreciation too goes to my roommate Kak Sureena for all her guidance and support. I would like to extend my heartfelt, huge, and warm thanks to my girlfriends for their precious friendship; Tlya, Yana, Wanie, Sara and Didi. Our journey is just starting. Rise and shine ladies!

My special thanks to Ken who has always been by my side during my happy and hard moments, showered me with generous care, to push and motivate me. We will leave our trail where no path has ever been taken before. A journey is easier and more beautiful when shared together.

Last but not least, my special gratitude, and high regards to my family for their sincere understanding and encouragement. This is for you Abah, Ibu, Along, Anje, Kak Meme, Y and Jiha. For brothers-in-law, Bacu, Ameir and Zaed, you guys are awesome! My little pumpkins, Adam, Danish, Darwish and Delyscha you guys always make me happy. No one can ever replace them and I owe everything to them.

*“Everything I know, I know because of love”*

-Leo Tolstoy-

## ABSTRACT

The data used in this research was acquired in an urban area, Damansara, and is highly contaminated by noise due to the location and this made it hard to identify the first break signal. The objectives of this research are to design the field acquisition parameter for noisy area, to formulate new approach for noise reduction using MatLab software, to image the granite interface in the noisy environment and to investigate the possible correlation between Standard Penetration Test (SPT) values obtain from borehole data and velocity values obtain from seismic survey.

Four parameters, geophone array, source, equipment and trigger were tested in the field. From the test, single geophone array, aluminium striker plate with sledge hammer, 48-channel seismograph and analogue trigger are the best parameters to be use in noisy environment. Addition, subtraction and frequency scaling technique were develop using the MatLab software and the data acquired was tested. The frequency scaling shows a good improvement on the noise reduction for the seismic data.

A further investigation on the correlation between Standard Penetration Test (SPT) and seismic velocity should be done since the preliminary work on these shows a small correlation coefficient between these two values. Subsurface image of the area were then develop using the information obtain from the seismic survey and borehole survey. Maps represent the thickness overburden, thickness of the saturated soil layer and bedrock elevation was produce using both data information.

## ABSTRAK

Data yang digunakan merupakan data yang diperolehi dari kawasan kajian yang terletak di Damansara dan mengandungi kadar hingar yang tinggi lalu menyebabkan kesukaran untuk mengenal pasti isyarat pertama. Objektif kajian ini adalah untuk merekabentuk parameter lapangan bagi pengumpulan data di kawasan yang mempunyai kadar hingar yang tinggi, membangunkan pendekatan baru bagi mengurangkan hingar menggunakan perisian MatLab, menghasilkan imej permukaan granit di kawasan berhingar tinggi dan mengkaji kemungkinan korelasi antara nilai SPT yang diperolehi dari proses penggerudian dan nilai halaju daripada kajian seismik.

Empat parameter berbeza, susunan geofon, sumber tenaga, peralatan dan pemicu telah diuji di lapangan. Dari ujikaji tersebut, susunan geofon tunggal, plat penahan aluminium bersama tukul baji, 48-*channel* seismograf dan pemicu analog adalah parameter terbaik digunakan di persekitaran berhingar tinggi. Teknik penambahan, penolakan dan pecahan frekuensi berskala telah dibangunkan dengan menggunakan perisian MatLab dan data yang diperolehi diuji. Teknik pecahan frekuensi berskala menunjukkan peningkatan yang baik pada pengurangan hingar dalam data.

Satu ujikaji terhadap korelasi antara nilai SPT dari maklumat penggerudian dan halaju seismik dari kaedah pembiasan seismik dilakukan dengan keputusan nilai pekali korelasi yang kecil antara keduanya. Imej subpermukaan kawasan kajian dihasilkan daripada maklumat yang diperolehi dari kajian kaedah pembiasan seismik dan penggerudian. Peta ketebalan bebanan, ketebalan lapisan tepu dan ketinggian batuan hampar dihasilkan menggunakan maklumat daripada kedua-dua kaedah.

In compliance with the terms of the Copyright Act 1987 and the IP Policy of the university, the copyright of this thesis has been reassigned by the author to the legal entity of the university,

Institute of Technology PETRONAS Sdn Bhd.

Due acknowledgement shall always be made of the use of any material contained in, or derived from, this thesis.

© WAN SURIANI BINTI A RAMAN, 2012

Institute of Technology PETRONAS Sdn Bhd

All rights reserved.

## TABLE OF CONTENTS

STATUS OF THESIS.....	i
APPOVAL PAGE.....	ii
TITLE PAGE.....	iii
DECLARATION OF THESIS.....	iv
DEDICATION.....	v
ACKNOWLEDGEMENT.....	vi
ABSTRACT.....	viii
ABSTRAK.....	ix
COPYRIGHT PAGE.....	x
TABLE OF CONTENTS.....	xi
LIST OF TABLES.....	xiv
LIST OF FIGURES.....	xv
CHAPTER 1 INTRODUCTION.....	1
1.1 Introduction.....	1
1.2 Study Area.....	2
1.2.1 Geological Background.....	2
1.3 Problem Statement.....	3
1.4 Objectives.....	8
1.5 Thesis Outline.....	8
CHAPTER 2 LITERATURE REVIEW.....	10
2.1 Introduction.....	10
2.2 Shallow Seismic Refraction.....	11
2.2.1 The First Kick.....	17
2.2.2 Interpretation Method.....	18
2.3 Geophone Coupling Problem.....	19
2.4 Noise Type.....	21
2.5 Use of Seismic Refraction Survey.....	22
2.6 Standard Penetration Test vs. Seismic Velocity.....	23

CHAPTER 3 METHODOLOGY .....	26
3.1 Introduction.....	26
3.2 Testing Acquisition Parameter .....	29
3.2.1 Geophone Array Testing .....	29
3.2.2 Source Testing .....	32
3.2.2.1 Striker Plate.....	33
3.2.3 Seismograph .....	35
3.2.4 Trigger Type.....	37
3.2.5 Spread Layout and Shot Point Configuration System.....	38
3.3 Normal Processing Cycle .....	41
3.4 Advanced Data Improvement .....	43
3.4.1 Subtraction and Addition Technique.....	43
3.4.2 Frequency Scaling Technique .....	44
3.5 Correlation between Standard Penetration Tests (SPT) With Seismic Velocity .....	46
 CHAPTER 4 RESULTS AND DISCUSSIONS.....	 49
4.1 Introduction.....	49
4.2 Acquisition Parameter Design for Noisy Area .....	49
4.2.1 Geophone Array Testing .....	50
4.2.2 Source Testing .....	51
4.2.2.1 Striker Plate.....	54
4.2.3 Trigger Type.....	59
4.2.4 Equipment and Spread Layout .....	63
4.3 Normal Processing Cycle .....	67
4.4 Advanced Data Improvement .....	75
4.4.1 Subtraction Technique and Addition Technique.....	75
4.4.2 Frequency Scaling Technique .....	86
4.4.3 Comparison between Subtraction and Addition Technique with Frequency Scaling Technique.....	98
4.5 3D Subsurface Images after Data Enhancement .....	98
4.6 Correlation between Standard Penetration Tests (SPT) with Seismic Velocity .....	103

CHAPTER 5 CONCLUSIONS AND RECOMMENDATIONS .....	109
5.1 Conclusions .....	109
5.2 Recommendations.....	111
REFERENCES .....	112
APPENDIX A.....	117
APPENDIX B.....	121
APPENDIX C.....	124

## LIST OF TABLES

Table 1.1: Borehole log example .....	6
Table 2.1: Site classification scheme (after Glenn, 2006) .....	24
Table 3.1: Striker plate's characteristic .....	32
Table 3.2: Equipment characteristic .....	34
Table 3.3: Trigger characteristic .....	37
Table 3.4: 24 channel seismograph shot points position .....	39
Table 3.5: 48 channel seismograph shot points position .....	39
Table 4.1: Striker plates parameter testing result.....	54
Table 4.2: Trigger type parameter testing result.....	59
Table 4.3: Equipment test result .....	63
Table 4.4: RMS fitting error and average error values for original data and after application of subtraction and addition technique .....	75
Table 4.5: RMS fitting error and average error values for original data and after frequency scaling technique's application .....	87

## LIST OF FIGURES

Figure 1.1: Study area.....	4
Figure 1.2: Typical classification of weathering profile (after Huat et. al) .....	5
Figure 2.1: Snell’s Law diagram (modified from Encyclopedia Britannica, Inc.,2006) .....	13
Figure 2.2: Critical refraction (Sjögren,1984) .....	15
Figure 2.3: Applying Huygen’s Principle in determining the second wavefront arrival time, $t_2$ after the interval time of $\Delta t$ from the first arrival, $t_1$ (Burger, 1992).....	15
Figure 2.4: $X_{crit}$ , $x_{cross}$ and $t_1$ position in a t-x curve.....	16
Figure 2.5: Position of seismic wave’s arrivals [45].....	16
Figure 2.6: Picking the first break.....	18
Figure 3.1: General view of the research area, surrounded by residential area, bussiness development area and arrows indicates where the noises coming from.....	26
Figure 3.2: Research flow chart .....	27
Figure 3.3 : (a) Constructive concept of wave (b) : Destructive concept of wave .....	29
Figure 3.4 : (a) Single geophone array (b): Schematic diagram showing array of single geophone.....	30
Figure 3.5: (a) Triple geophone array (b): Schematic diagram showing triple array geophone.....	30
Figure 3.6: (a) Aluminium striker plate .....	33
Figure 3.6: (b) Steel striker plate .....	33
Figure 3.6: (c) Wooden striker plate .....	33
Figure 3.7: Two seismographs systems interconnected to each other at the trigger port during the testing phase .....	35
Figure 3.8: 24 channel seismograph diagram .....	35
Figure 3.9: 48 channel seismograph diagram .....	35
Figure 3.10: Interconnection of both seismographs diagram.....	35

Figure 3.11: (a) Analogue trigger position next to the striker plate (b) Trigger switch position near to the sledge hammer head .....	36
Figure 3.12: Schematic diagram for spread layout using 24 and 48-channel seismograph .....	38
Figure 3.13: Normal processing flow chart .....	41
Figure 3.14: Advanced data improvement flow chart .....	44
Figure 3.15: Correlation flow chart .....	46
Figure 3.16: Correlation between SPT and seismic velocity .....	47
Figure 4.1:(a) Single geophone array seismic record using 48-channel seismograph (b): Frequency spectrum .....	51
Figure 4.2:(a) Triple geophone array seismic record using 48-channel seismograph (b): Frequency spectrum .....	52
Figure 4.3: (a) Wooden striker plate seismic record using 48-channel seismograph (b) Frequency spectrum .....	55
Figure 4.4: (a) Aluminium striker plate seismic record using 48-channel seismograph (b) Frequency spectrum .....	56
Figure 4.5: (a) Steel striker plate seismic record using 48-channel seismograph (b) Frequency spectrum .....	57
Figure 4.6: (a) Analogue trigger at 1” away from striker plate seismic record using 48-channel seismograph (b) Frequency spectrum .....	61
Figure 4.7: (a) Analogue trigger at 6” away from striker plate seismic record using 48-channel seismograph (b) Frequency spectrum .....	62
Figure 4.8: (a) 24-channel seismograph (b) Frequency spectrum .....	65
Figure 4.9: (a) 48-channel seismograph (b) Frequency spectrum .....	65
Figure 4.10 : GRM interpreted depth model for line 3 .....	68
Figure 4.11 : 2D inverted model for line 3 .....	69
Figure 4.12: GRM interpreted depth model for line 47 .....	70
Figure 4.13 : 2D inverted model for line 47 .....	71
Figure 4.14: Shot point in between geophone 1 and 2 for seismic line 3 .....	72
Figure 4. 15 : Shot point in between geophone 35 and 36 for seismic line 3 .....	72
Figure 4.16: Shot point in between geophone 12 and 13 for seismic line 3 .....	72
Figure 4. 17 : Shot point in between geophone 46 and 47 for seismic line 3 .....	72
Figure 4. 18: Shot point in between geophone 24 and 25 for seismic line 3 .....	72

Figure 4.19 : Shot point at 5 meters away from geophone 48 for seismic line 3 .....	72
Figure 4.20 : Shot point in between geophone 1 and 2 for seismic line 47 .....	73
Figure 4.21: Shot point in between geophone 35 and 36 for seismic line 47 .....	73
Figure 4.22 : Shot point in between geophone 11 and 12 for seismic line 47 .....	73
Figure 4.23 : Shot point in between geophone 47 and 48 for seismic line 47 .....	73
Figure 4.24 : Shot point in between geophone 25 and 26 for seismic line 47 .....	73
Figure 4.25 : Shot point at 5 meters away from geophone 48 for seismic line 47 .....	73
Figure 4.26: Recorded signal data at shot point 2 for seismic line number 35.....	76
Figure 4.27: Recorded noisy data at shot point 2 for seismic line number 35.....	76
Figure 4.28: 2D inverted model for seismic line number 35 .....	77
Figure 4.29: GRM interpreted depth model for seismic line number 35.....	78
Figure 4.30: (a) Shot point record after subtraction technique (b) Spectrum plot.....	79
Figure 4.31: (a) Shot point record after addition technique (b) Spectrum plot.....	80
Figure 4.32: 2D inverted model after subtraction technique .....	81
Figure 4.33: GRM interpreted depth model after subtraction technique .....	82
Figure 4.34: 2D inverted model after addition technique .....	83
Figure 4.35: GRM interpreted depth model after addition technique.....	84
Figure 4.36: (a) Frequency scaling technique using trace number 43 as the noisy trace (b) Spectrum plot .....	88
Figure 4.37: 2D inverted model after frequency scaling technique using trace number 43 as noisy trace.....	89
Figure 4.38: GRM interpreted depth model after frequency scaling technique using trace number 43 as noisy trace.....	90
Figure 4.39: (a) Frequency scaling technique using trace number 42 as the noisy trace (b) Spectrum plot .....	92
Figure 4.40: 2D inverted model after frequency scaling technique using trace number 42 as noisy trace.....	92
Figure 4.41: GRM interpreted depth model after frequency scaling technique using trace number 42 as noisy trace.....	93
Figure 4.42: (a) Frequency scaling technique using trace number 47 as the noisy trace (b) Spectrum plot .....	95
Figure 4.43: 2D inverted model after frequency scaling technique using trace number 47 as noisy trace.....	95

Figure 4.44: GRM interpreted depth model after frequency scaling technique using trace number 47 as noisy trace.....	96
Figure 4.45: View of the research area with seismic lines superimposed .....	99
Figure 4.46: Isopach 2 map represents the thickness of overburden .....	101
Figure 4.47: Isobach map represents the bedrock elevation .....	102
Figure 4.48: Location plan of seismic line superimposed with borehole survey.....	105
Figure 4.49: Isopach 2 map represents the thickness of the saturated soil layer .....	105
Figure 4.50 : Example of processed data .....	106
Figure 4.51: Correlation graph between SPT value and velocity value .....	107

# CHAPTER 1

## INTRODUCTION

### 1.1 Introduction

Due to its deep penetration, high accuracy and high resolution, seismic method is by far the most important technique in geophysical world. The history of seismic methods started in 1910 with seismic refraction method and since then, the method evolved and is widely used until now [41]. Principally, the use of this method is mainly in exploring petroleum, however the widespread use of this method, made it important in other civil engineering work, groundwater searches and locating subsurface geological features[8] [30] [37] [41] [44].

The seismic method used controllable and movable source of energy, small recording points and continuous recording along profile's line [41] [44]. Reconstructions of the subsurface images is based on the velocity of travel time obtain from the energy source to the detector. Initially, manual calculation method was used to extract the information gain from the survey, data were plotted by hand and interpretation was done graphically [3]. Nowadays, more promising and faster method using computer processing was used in extracting the information needed from the survey. In land based work, geophone is primarily used as the detector with different type of energy source mainly from explosive or non-explosive source to generate the seismic waves [2]. The paths where the seismic waves propagate are dependent on the elastic properties of the paths itself.

No doubt that seismic method can be extremely useful and provide valuable information needed in most cases. However, it is good to know and recognize the limitations of this method. Common limitation is when lack of contrast in elastic properties occurs, the nonuniqueness of interpretation techniques, resolution and noise

problem which vary as the noise is site dependent. With this concern limitations, the field procedure of seismic survey must be designed to overcome the limitations and in addition to obtain reliable and informative information.

## **1.2 Study Area**

The research area is located within the township development area of Mutiara Damansara, Petaling Jaya, Selangor, Malaysia. It is closely located to Damansara Utama and Sungai Penchala and can easily be reached via Sprint Expressway. The area can be accessed by the road network of Damansara-Puchong Expressway (LDP) and Persiaran Surian.

The study area is surrounded by the robust construction development, business park including offices and residential area which contributes to the noise contamination of the data. As it offers good justification for the research objective, the area was chosen as the study area. Figure 1.1 shows the Google map of the research area.

### **1.2.1 Geological Background**

The geology of the area is underlain by the KL granite formation. Figure 1.2 shows the typical weathering profile of granite in tropical region. The borehole data show that the granite bedrock is generally from 20 to 25 meters below the ground surface. The granite appears to be moderately weathered and boulders were not found. From the borehole logs, it shows a different result from the normal weathering profile classification. The example of the borehole log is shown in Table 1.1. The soil layers overlying the granite predominantly consist of soft to very stiff silt and/or sand with gravel. The test was done at every 1.5 meter of the sample. The number of blow needed (N value) for each test was clearly stated. Comparison between borehole log example and weathering profile shows the absent of class IV from the weathering profile in the borehole log example. Therefore, no clear cut-off fraction between the inner layers of the sampling area is identified.

### **1.3 Problem Statement**

With the high-density of populations and high level noise environment, it is very challenging to get a good seismic signal. Most of the signals recorded have been contaminated by the unwanted signals, noise. There are many type of noise, thus removing the noise itself is very challenging in the seismic world. Therefore, a good plan is required before the research in order to minimize the noise contamination. The four different seismic acquisition parameters were tested in the field in order to minimize the noise level. Due to its limitation on the space, the study area's is fully utilized in order to get the optimum data.

Once the data are collected and observed, there are a lot of noises identified in the data. Even though primary action in ensuring the low noise contamination was taken, further action was proposed and tested. New techniques in reducing the noise level was formulated and tested on the data.

General understanding on the value of velocity is it will increase with the stiffness or hardness of the Earth's layer. The same understanding was applied in the Standard Penetration Test (SPT) where the number of blow (N-value) of the test will increase with the hardness of the sample. As for now, there is no work done in correlating both velocity and value from the refraction survey and N-value from the SPT in the study area. Therefore, a correlation between those two values was carried out.



Figure 1.1: Study area with coordinates of 3.1622.31,101.614543) denotes with green arrow and it 2.5cm to 100 m scale in Google image on the right side.

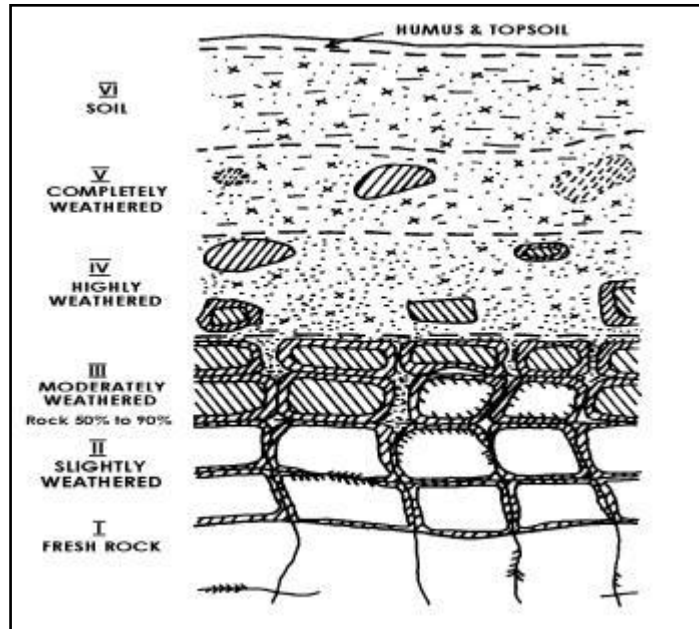


Figure 1.2: Schematic diagram showing the typical classification of weathering profile (after Bujang et. al., 2005).

Table 1.1: Borehole log example.

							BOREHOLE NO	BH B14		
							STARTING DATE	19/11/2009		
TYPE OF BORING		Rotary Wash-boring/Coring	COORDINATE		E -9734 202	FINISHING DATE		20/11/2009		
TYPE OF RIG		YBM-2JES			N -1193.850	WATER LEVEL		NIL		
DIA. OF BORING		0.0875m (NW)	REDUCED LEVEL (m)		57	SUPERVISOR		Azlan		
Date & Time	W.Level (M)	Drilling Method	Depth (M)	Sample & Test Number	Result	Rec (%)	RQD (%)	Legend	Description	
19/11/09 0610pm	1.10m	NW	0.00					O O O O O X O O O O O O X O O O O O O X O O O O O	Top Soil: Medium brown,	
			1.00							
			1.50	SPT1/ DS1	1,1,2,1,1,1 N=5	Rec=0.37/0.45	●	82	X X X X X X . X X X X X X X O X X X X X X X . X X X X X X	Medium stiff, medium brown, sandy SILT with some gravels.
			1.95							
			2.00							
			3.00	SPT2/ DS2	1,2,2,2,1,2 N=7	Rec=0.41/0.45	●	91	X X X X X X O X X X X X X X . X X X X X X	- Ditto -
			3.45							
			4.00							
			4.50	SPT3/ DS3	1,2,3,2,3,3 N=11	Rec=0.38/0.45	●	84	X X X X X X O X X X X X X X . X X X X X X X O X X X X X X X . X	- Ditto - (Stiff)
			4.95							
5.00										
0815am 20/11/09	1.16m	NMLC  NW  NMLC	6.00	SPT4/ DS4	2,2,3,2,4,6 N=15	Rec=0.19/0.45	●	42	..... . X . X . ..... . X . X . ..... . X . X . .....	Medium dense, medium brown, silty SAND.
			6.45							
			7.00							
			7.50	SPT5/ DS5	2,3,4,4,5,8 N=21	Rec=0.15/0.45	●	33	O O O O O X O	Medium dense, light grey, silty GRAVEL.
			7.95							
8.00										
0815am 20/11/09	1.16m	NMLC  NW  NMLC	8.00	C1	Rec=0.40/0.60 RQD=0/0.60	⊗	67	0	+++++ +++++	Encountered rock formation at 8.00m. Light grey spotted dark grey, highly weathered, GRANITE, weak.
			8.60							
			9.00	C2	Rec=1.50/1.50 RQD=1.00/1.50	⊗	100	67	+++++ +++++ +++++ +++++	Re-encountered rock formation at 9.00m. Dark grey with pale grey, moderately weathered, GRANITE, medium strong.
10.00										

Cohesive soil (N)	0 - 2 = V. Soft 2 - 4 = Soft 4 - 8 = M. Stiff 8 - 15 = Stiff 15 - 30 = V. Stiff > 30 = Hard	Legend	Standard Penetration Test	●	Remarks
Non Cohesive Soil (N) <td>0 - 4 = V. loose 4 - 10 = Loose 10 - 30 = M. dense 30 - 50 = Dense &gt; 50 = V. dense</td> <td></td> <td>Undisturbed Sample</td> <td>○</td> <td></td>	0 - 4 = V. loose 4 - 10 = Loose 10 - 30 = M. dense 30 - 50 = Dense > 50 = V. dense		Undisturbed Sample	○	
			Mazier Sample	⊗	
			Vane Shear Test	⊠	
			Coring into Rock	⊗	

20/11/09 0445pm	NIL	NMLC	10.00	C3	Rec=1.50/1.50 RQD=0.74/1.50	100	49	+++++	Dark grey with pale grey, highly weathered, GRANITE, weak.
			10.50					+++++	
			11.00					+++++	
			12.00	C4	Rec=1.50/1.50 RQD=1.30/1.50	100	87	+++++	- Ditto - (slightly weathered, GRANITE, strong)
			13.00					+++++	
			13.50					+++++	
			14.00					+++++	END OF BOREHOLE AT 13.50m.
			15.00					+++++	
			16.00					+++++	
			17.00					+++++	
			18.00					+++++	
			19.00					+++++	
			20.00					+++++	
Cohesive soil (N)			Legend		Standard Penetration Test		Remarks		
0 - 2 = V. Soft					Undisturbed Sample				
2 - 4 = Soft					Mazier Sample				
4 - 8 = M. Stiff					Vane Shear Test				
8 - 15 = Stiff					Coring into Rock				
15 - 30 = V. Stiff									
> 30 = Hard									
Non Cohesive Soil (N)									
0 - 4 = V. loose									
4 - 10 = Loose									
10 - 30 = M. dense									
30 - 50 = Dense									
> 50 = V. dense									

## **1.4 Objectives**

The objectives of this research are:

1. To design the acquisition parameter for noisy area.
2. To formulate new approach for noise reduction using MatLab software.
3. To investigate the possible correlation between Standard Penetration Test (SPT) values obtain from borehole data and velocity values obtain from seismic survey.
4. To image the granite interface in the noisy environment.

In order to reach the objective, four sub-objectives had been identified. The sub-objectives are:

1. To determine the suitable source/plate to be use with hammer.
2. To find the best mechanisms for getting optimum number of stacking.
3. To investigate the sustainability of the geophone used.
4. To compare the normal processing result with the new develop technique.

## **1.5 Thesis Outline**

This thesis consists of five chapters. Chapter 1 features the introduction, study area, objectives and problem statement. Thesis outline also stated in this chapter.

Chapter 2 presents the literature review made on the related field. The previous works of other researchers also present in order to give overview on the research gap. The used of method in different environments and the advantages of the interpretation method available in industry is also described.

The research methodology taken in this work is discussed in Chapter 3. The steps taken in each stage is present in detail work flow chart. This includes detail discussion on field procedure, processing and interpretation of the data as well as the new data enhancement technique.

Chapter 4 elaborates the results achieved for each objective. The final suitable parameters to be used in urban area are present in details and discussed. The comparison of result before and after the data enhancement using the new technique is also discussed and compared. The finding on correlation between seismic velocity and SPT value is present too.

Chapter 5 ends the research findings with conclusion and recommendations for future works and better direction of the field of study.

## CHAPTER 2

### LITERATURE REVIEW

#### **2.1 Introduction**

In the early days, the seismic refraction method which has been discovered by the German geophysicist, L Mintrop was widely used in oil exploration and detecting salt dome [41]. Over time, after the method was well established, it has become one of the tools in applied geophysics. Then, it was replaced by seismic reflection for the main oil prospecting method. The rapid advancement and refinement in equipment and interpretation technique of this refraction method proved that it is one of the best reliable, non-invasive and relatively minimal cost of data collection for shallow activities. The applicability of this method made it suitable in solving petroleum, mineral, hydrology and engineering problems [3] [8] [30] [37] [41]. The use of seismic refraction instrument in shallow target studies is traced back from early 1950's to 1980. Started from 1980, the use of multichannel, signal enhancement seismograph and microcomputer with capabilities in executing Generalized Reciprocal Method (GRM) for interpreting the data made it possible for detail subsurface mapping [25].

Seismic refraction method is widely used in petroleum, mineral and engineering investigations. This includes the application in civil engineering projects, geothermal area, mineral deposition, mining projects, groundwater studies and dam projects. Ackermann [1] discussed the application of this method in geothermal area at the Raft River, Southern Idaho. Hayashi and Takahashi [13] stated the widely use of this method in civil engineering projects in mountainous areas, including railway and highway tunnel, dam constructions and landslides protection in Japan. Kilty et. al.[21] used this seismic refraction method in upgrading the roadways and retaining wall to the Horse Mesa Dam, Arizona.

M. Kamen Kaye [20] extended the use of this method in the study of the relationship between post-basement velocities and compaction on the deposition affect at Orinoco basin, Venezuela. Gendzwill [7] in the other hand extended the use of seismic refraction method to monitor the thickness of salt formation over the potash mine in Saskatchewan.

Several interpretation methods were introduced and still applicable to be used up till today. The first method introduced was "method of differences" in 1930s. The classical evolution of the interpretation method was active in between 1930 and 1970 with the enhancement to suit the shooting configurations and field arrangement [3] [4]. However, the variations with no difference in its fundamental concept were different in graphical approaches in order to compensate the lack of computer machines during that time [3]. Such interpretation methods are Barthelmes' Procedure, Wyrobek-Gardner Method, Slotnick Method, Tarrant Method, Hales' Method, and Wavefront Method. In 1980, Palmer's first publication of "Generalized Reciprocal Method" was published and since then, the interpretation method view is changed. The encouragement of using this method on a regular basis is particularly based on its ability to solve hidden layer problem [4].

## **2.2 Shallow Seismic Refraction**

Selection of shallow seismic refraction source for a survey within the project's constraint can be a very crucial decision for geophysicist. Many sources were discussed and they agreed that every survey's site have their own characteristics and the source use might be varying from one site to another site [33]. The applicability of this method made it suitable in solving petroleum, mineral, environmental, hydrology and engineering problems [8] [26] [37] [41].

Utilizing the propagation of elastic waves through the Earth as the medium, this method is based on the following fundamental postulates [41]:

The waves are propagated with different velocity for each different layer.

The velocities contrast between the layers is large.

The layer velocities increase with depth.

By using the basic concept of wave travelling under the Earth's layer and measure some elastic properties of the Earth's subsurface layer, the data is obtained where the energy required is either from impact, explosives or mechanical source [2][8][41]. The seismic waves produced by this energy source will travel along the subsurface and two different types of seismic waves are expected to be transmitted, the longitudinal waves and transverse wave. In longitudinal wave, usually termed in P-waves (primary waves), the particles move back and forth along the direction of propagation. For transverse wave, termed as S-waves (secondary waves), the particle move perpendicular to the direction of propagation. Both of the seismic waves will return to the ground and the signal is captured by the detector.

The velocities of P-waves and S-waves in terms of density,  $\rho$  and elastic coefficient can be calculated by using the following equations [2].

$$V_p = \sqrt{\frac{K + \frac{4}{3}G}{\rho}} = \sqrt{\frac{E(1-\mu)}{\rho(1-2\mu)(1+\mu)}}$$

$$V_s = \sqrt{\frac{G}{\rho}} = \sqrt{\frac{E}{\rho} \frac{1}{2(1+\mu)}}$$

with

$V_p$  = Velocities of P-waves

$V_s$  = Velocities of S-waves

$K$  = Bulk modulus

$G$  = Rigidity modulus

$E$  = Young's modulus

$\rho$  = Density

$\mu$  = Poisson's ratio

The travel time between the detector and seismic source is recorded by the array of geophones (detector) which lies in a straight line on the ground. The signals are captured and stored by a seismograph. Later, the signals are transferred to the computer for processing purposes. In the early days, the available interpretation methods cannot solve complex problem such as hidden layer problem. But, with the advent more sophisticated technology, this problem can be solved and allows interpretation of the data easier, thus more detail information is obtain.

Though there has been new interpretation technique proposed and developed to solve complex cases, the same technique of basic field practice and interpretation has not changed and is still used as it was before. Based on the law of light rays propagation, Snell's Law together with critical incidence phenomenon, the foundation of seismic refraction survey was discovered [12] [37] [41]. Figure 2.1 shows the Snell's Law diagram.

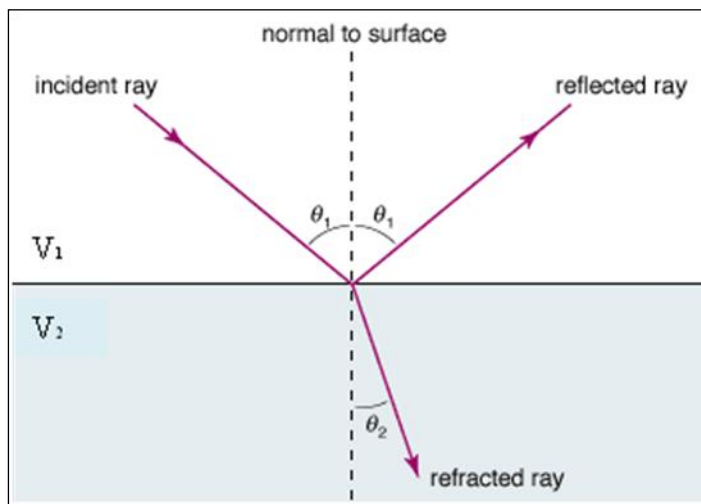


Figure 2.1: Snell's Law diagram (modified from Encyclopedia Britannica, Inc., 2006).

$$\frac{\sin \theta_1}{\sin \theta_2} = \frac{v_1}{v_2} \quad \text{Equation 1}$$

with

$\theta_1$  = angle of incidence

$\theta_2$  = angle of refraction

$v_1$  = velocity of medium 1

$v_2$  = velocity of medium 2

The critical incidence only occurs when there is an increase in velocity at the lower refracting layer ( $V_2$  is greater than  $V_1$ ) and the angle of refraction is  $90^\circ$ . With this assumption, therefore the Equation 1 becomes:

$$\sin \theta_1 = \frac{V_1}{V_2} \quad \text{Equation 2}$$

Figure 2.2 shows the illustration of the seismic refraction based on the stated condition above [41].

Two other principles that are important in seismic refraction are Fermat's Principle and Huygen's Principle. Huygen, in his principle stated that all points in wavefront can be considered as the point source for the secondary wavefront. Fermat developed the well known principle of least time, where he stated that in propagation of waves, the path travelled by the waves will always be the shortest path. Figure 2.3 show sthe application of Huygen's principle in determining the position of second wavefront.

In shallow seismic work, most of the wave involved is the P-waves. Even the S-waves is not involved directly to this work, the appearance of this waves gives more understanding on the data itself. These S-waves have less speed and appears later in the seismogram [2]. The first arrival of the P-waves indicates the travel time between the source and the detector. This travel time is very important for the seismic refraction survey method as it will give the information needed about the survey area. Thus, the equipment, energy source, trigger and geophone array are very important in field design procedure and the decision on the parameter used will influence the data acquired at the said area.

The first type of wave that will appear first in the seismogram is the direct wave. At greater distance, refracted waves will arrives before the direct waves due to the high velocity boundaries they travel in. The point where refracted waves appear first is called crossover distance,  $x_{\text{cros}}$ , intercept time,  $t_i$  is time where the refracted waves cut the y-axis. Critical distance,  $x_{\text{crit}}$  is a minimum distance from energy source to the first refraction can be received [2] [4]. The position of  $x_{\text{cros}}$ ,  $x_{\text{crit}}$  and  $t_i$  is illustrated in Figure 2.4.

Figure 2.5 shows the position of different type of seismic wave arrival in common seismic record. From the figure, we can identify the position of direct wave, refraction, reflection and ground roll.

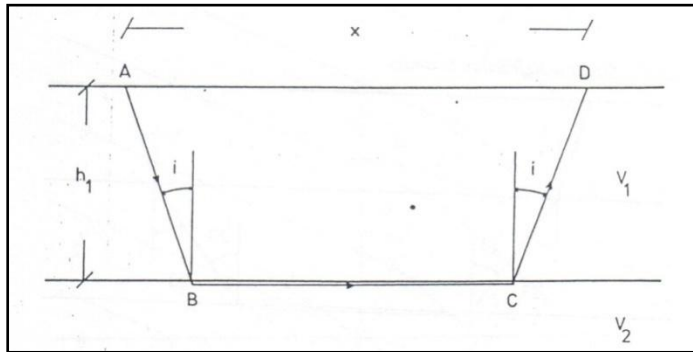


Figure 2.2: Critical refraction (Sjögren,1984).

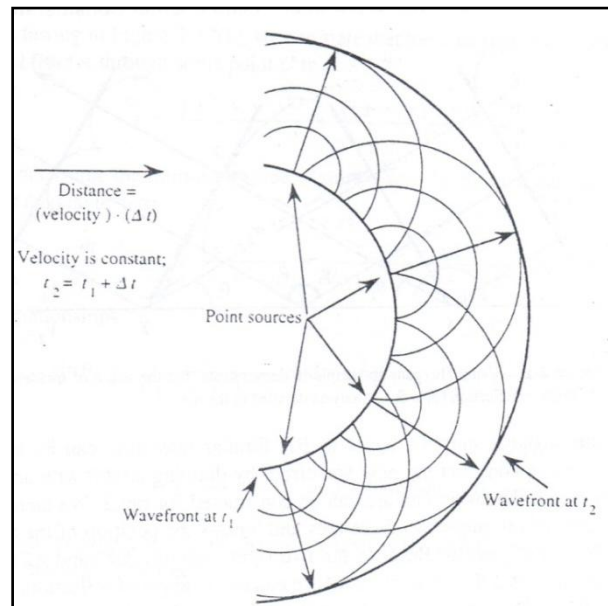


Figure 2.3: Applying Huygen's Principle in determining the second wavefront arrival time,  $t_2$  after the interval time of  $\Delta t$  from the first arrival,  $t_1$  (Burger, 1992).

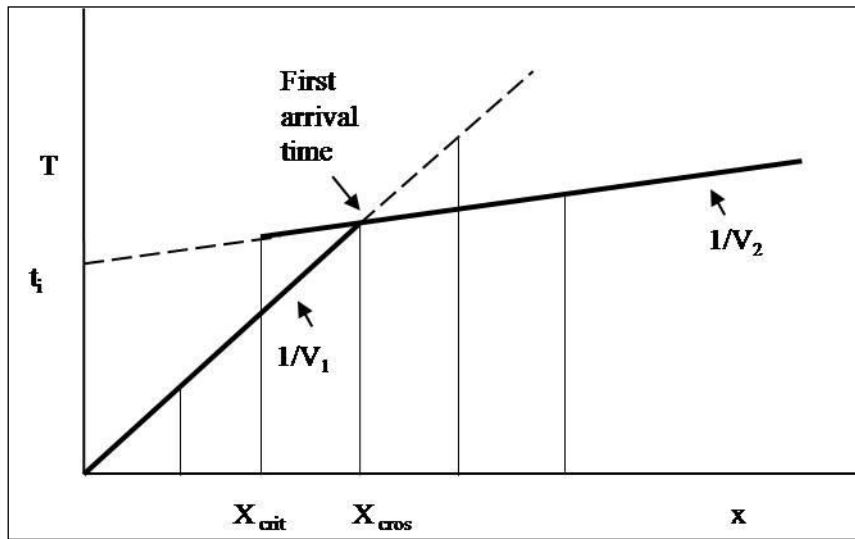


Figure 2.4:  $X_{crit}$ ,  $x_{cros}$  and  $t_i$  position in a  $t$ - $x$  curve.

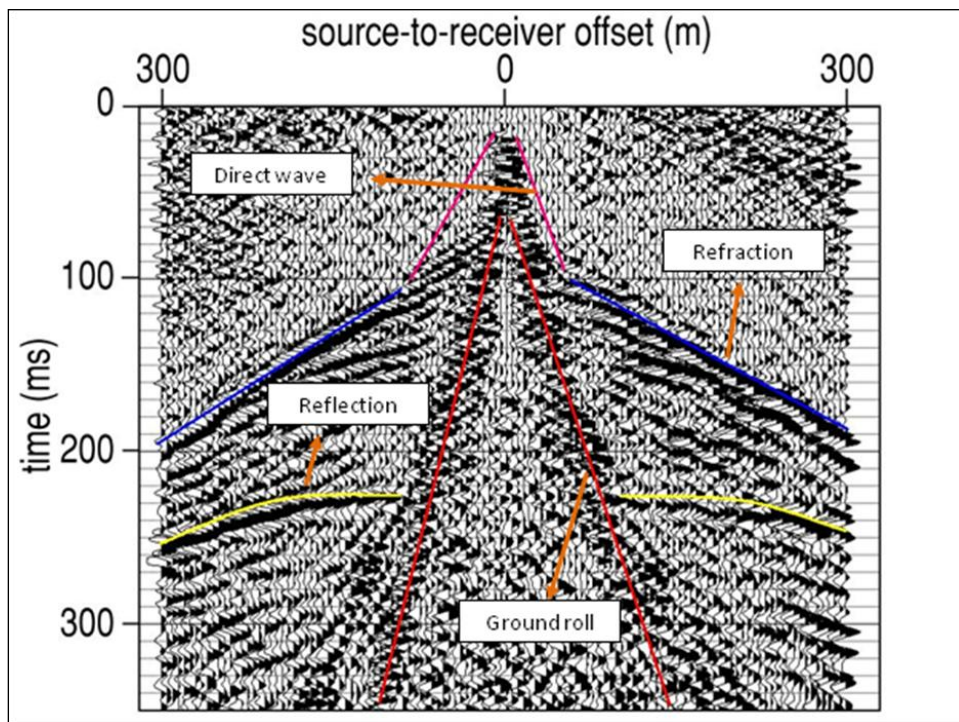


Figure 2.5: Position of seismic wave's arrivals (Washburn and Wiley, 1941).

### 2.2.1 The First Kick

Since the signal that we are interested in shallow seismic refraction is the first arrival signal, it is good to have a view on this signal. This first signal, known as first break is defined as the first kick on a trace or the first noticeable signal from the background noise, it depends primarily upon the signal-to-noise ratio and amplifier gain. Shot and receivers location, size of charge or energy source and noise level are the factors that affect the signal-to-noise ratio [9] [11]. Figure 2.6 shows the example of the picking on the first break on a data.

In general, the task of picking this first break where the energy is associated with the refracted waves or direct waves that travel from shot point to receiver is crucial. Shallow seismic refraction survey uses the arrival time of first signal for the analysis of the subsurface depth.

The above definition of the first kick event may not be useful given under some circumstances: (1) “no sudden takeoff of the trace when the disturbance arrives. The motion begins gradually and if the first kick arrival time is attempted, the time picked will depend upon the over-all magnification of the seismograph [38], (2) the delay of the arrival due to noise disturbance, (3) amplitudes and phase picked as a first event vary from trace to trace, (4) some practical limit on how weak the signal is and the early part may not be present [11].

Some problem arises when the hand picking is done due to the stated circumstance; Ricker [38] defines the first event as the intercept first kick which is obtained when picking the time where the first motion intercepts the time axis through the inflection point. This objective definition somehow has problems due to the time consumed for constructing the tangent manually and the intercept first kick arrives later than the true first kick when compared.

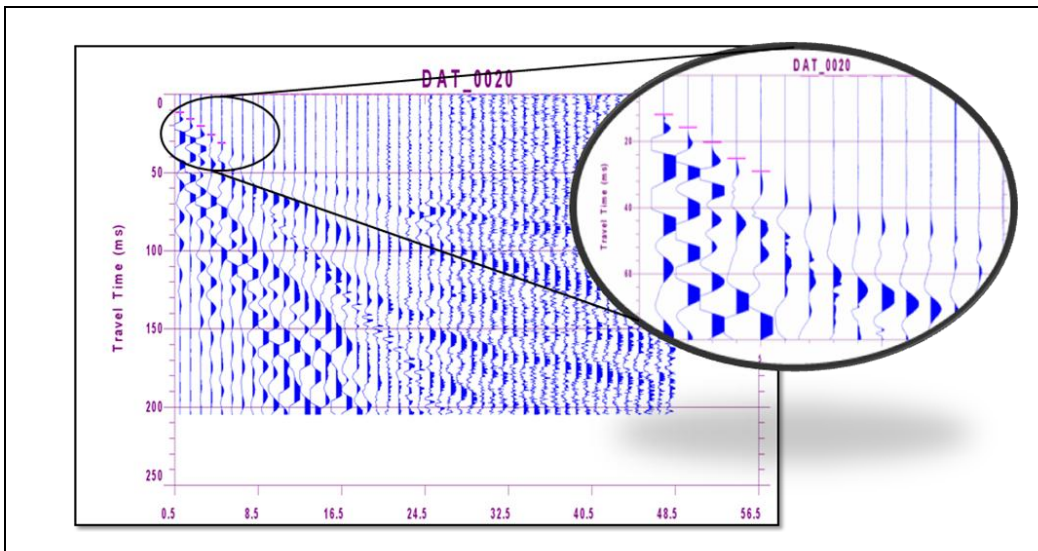


Figure 2.6: Picking the first break.

### 2.2.2 Interpretation Method

The basic process of interpretation was to plot the first arrival from the picking in the function of geophone position. Different velocity layers were defined by fit straight line to the data. The computer revolution made it possible for interpretation to be done faster than before. However, the cultural and economic barrier made most practitioners to continue using the old methods, which use hand plots, graphically interpretation, and hand calculators for calculation [9].

The development of the interpretation method is rapid and active during the years of 1930-1970 with many researchers trying to compensate the basic method introduced. As reported by Dobecki and Romig [9] the GRM method, introduced by Palmer (1981) was the successor of the improved, first introduced method by Edge and Labi (1931) known as “method of difference”. The method proposed by Palmer is one of the biggest contributions in the interpretation method for seismic refraction and have been used in many environment and case study by other researchers.

Palmer [35] introduced the generalized reciprocal method, a technique for interpret and process the in-line seismic refraction data which include forward and reverse travel times. This method uses computation velocity analysis function and generalized time-depth in unit of time as the processing aspect. The major advantage of this method is the ability to measure the depth conversion of dips up to 20 degree.

On the other hand, other researcher or institution focused on the development of the equipment they have at that time. As reported by Moore (1952) in Stam [42], the earliest development was done by the Physical Research Branch of the Bureau of Public Roads, Washington D.C. which developed a portable three-channel seismograph. The equipment has successfully fulfilled the need in United States with several combined characteristics of seismic refraction with the use of fixed geophone technique and movable shot point.

Common interpretation methods apply since the appearance of seismic refraction method and advancement in computing including Intercept Time Method (ITM), Delay Time Method, Generalized Reciprocal Method (GRM) and Hagiwara Method. However, GRM have been widely use in routine basic as the ability of this method in solving hidden layer problem [26].

### **2.3 Geophone Coupling Problem**

In the early stage of the application of this method, many problems arise as the initial equipment consists of single channel equipment. The problem is partially resolved over the years by adding more channels into each record. The multi-channel system undoubtedly has increased the record's quality and longer spreads can be used. However, many questions concerning the geophone's design and methods to plant in for optimum results were discussed. Several researches both on the theoretical and experimental level have done research since the early days [14] [24] [45].

The theoretical modeling studies of the geophone ground coupling and modeling have dominated the discussion rather than the experimental work. Nonetheless, early experimental work by Washburn and Wiley [45] discovered a resonant system is formed by the geophone ground coupling and the ground. They also demonstrated the amplitude and phase of seismic signal record could be seriously distorted by the difference among individual geophone. They also discussed about the influence factor of this characteristic, which are type and condition of the ground surface, the method of planting the geophone, the geophone weight and base area.

The following experimental work by Krohn [24] defined the geophone ground coupling as the accuracy with which the geophones measure the actual ground

motion. Even though the conventional geophone used frequency less than the resonant frequency, the crew should plant the geophone firmly to the ground to avoid the coupling effect as it will limit the geophone response to the ground motion. Krohn suggested conventional technique of planting the geophone in firm soil is acceptable for frequency less than 100 Hz and for frequency more than 100 Hz, the geophone should be buried to achieve better coupling as the firmness of the soil is increase with increasing depth. Krohn concludes that the coupling is dependence on the soil type, geophone placement, spike length, geophone radius and geophone mass. As long as the geophone is firmly coupling with the soil, the effect of the geophone coupling could be disregarded as the conventional seismology used frequency less than its resonant frequency.

Another experimental work by Hoover and O'Brien [14] discusses the other factors that mostly influence the signals, which are the geophone coupling, dimension of earth contact, local soil consolidation and properties dependent upon the geophone mass. They stated that the filtering effects on seismic data is equivalent to the damped oscillatory system by using theoretical calculation on the earth-geophone coupling based on the way theory approach. Three different techniques of measuring ground coupling stated by Krohn, Washburn and Wiley, and Hoover and O'Brien is modified and deploy by Drijkoningen [5]. Continuing from Krohn's work, he concludes that the behavior of poor planted geophones is determined by its weight while the good planted geophones are determined by the shear along the spike.

The previous theoretical studies model the geophone as the cylinder lying on the Earth's surface [14] [46]. In his study, Krohn mentioned about taken spike into modeling. Even though Krohn mentioned about spike should be taken into account of modeling, Tan [43] is the first to carry this out in his work, followed by Rademakers et al [36], who also quantified the ground-coupling phenomenon which is not taken into account by Tan.

## **2.4 Noise Type**

In seismic refraction survey, noise always creates the most problem. Different types of noise will give different types of signature signal yet give the same problem

on the data acquired. Contamination of the data with noise makes the researcher find the way to reduce if not eliminate the noise. As the different type of noise gives different signature of signal in the data, researcher believes that noise comes from any direction and can be reduced with a proper survey planning and reduction techniques.

Most noise is not due to equipment, but more due to human activities and natural phenomena and normally can be eliminated by careful survey planning [2]. Two common major type of seismic noise have been identified as 1) coherent and 2) incoherent. The coherent noise normally follows some trend and sometimes subdivided into energy that travels horizontally and energy that reach the spread more or less vertically. Surface waves, noise from vehicular traffic and multiples are the examples of coherent noise. Incoherent noise on the other hand often refers as random and repeatable due to near-surface irregularities scattering and inhomogeneities. Non-repeatable incoherent noise may occur due to the wind, movement of trees and people walking near geophone [44].

Dobrin and Savit [4] define noise as the spurious seismic signals from ground motion not associated with reflections in seismic prospecting context. They propose expert tuning and adjustment of noise suppression techniques as the signal and noise frequency, direction of arrival as well as the other relevant factors are varied from place to place. To conceal the signal beneath the noise, they propose an averaging concept in order to get a better estimation.

Scales and Snieder [40] agree that noise is the features that we not bother to explain. In deterministic process, it is not clear how the unmodeled Earth response can be treated as noise if the reproducible between the experiment and corresponds is high. They review three implications on geophysics in this paper which is 1) stacking of data where the averaging of the stacking can reduce noise when compared to the signal. The noise is different in each experiments, 2) prescription of a priori in Bayesian inversion where it is fine to include signal-generated “noise” in the joint distribution function of the data error and 3) making the decision how well to fit the data where one need to differentiate which part of the data is real and which part is not and should be consider as noise. This is important in order to identify data and noise in a more subtle way.

Li and Couzens [27] define ground roll as the strong coherent noise, which always degrades the seismic data quality. Routinely, bandpass filters are used to attenuate this noise as it is dominated by low frequency energy range and only little useful signal can be extracted. Other than that, time-variant spectral whitening (TVSW) is also used to attenuate the ground roll noise. In this paper, they introduced a new method, time-frequency adaptive noise suppression (T-FANS) used in seismic data where it isolate and attenuate localized high-amplitude noise. In their perspective localized means limited range of space, time and frequency domain.

## **2.5 Use of Seismic Refraction Survey**

A paper by D. Linehan, S.J. and V. J. Murphy [28] discussed the application of the seismic refraction survey in two different geologic environment and field conditions of noisy area. The proposed skyscraper at the Bay Back area, Prudential Centre, Boston, Massachusetts was once tidal land and is a reclaimed land. The limitation faced by the operator is the loose fill materials area which limits the charges used. The proposed additional building at the St. Mary's College, Montreal, Quebec on the other hand faced different problem with the existing structure and busy roadways on all side of the sites. For both sites, the operator need to be creative where they have to wait until quite moment occurs when the railroad traffic stopped coincidentally with minimum local vehicular traffic to avoid noise contamination. The charges used also small in quantity so that it does not endangered the existing structure, operator personnel and surroundings area.

Martí et al. [31] used seismic reflection method in finding detail characterizations of subsurface for subway tunnel drilling in Barcelona, Spain. They highlighted the difficulties encountered when work with this urban area such as cultural noise and street layout which limit the ability of instrument deployment. Other than that, poor subsurface knowledge, distribution of existing infrastructures, streets and buildings, location of utilities services, building foundations and subterranean garage severely alter the wavefield which lead to the scattering effects and make it difficult to obtain good seismic signal. In order to obtain better quality seismic data, they conducted the acquisition during midnight to early morning as it the quietest time they can have.

Mossman et al. [34] presents the application of seismic refraction and reflection method for proposed Deep Tunnel System in Chicago using vibroseis. The intense urban development in the area precluded the use of explosive or percussion type energy source, thus the used of vibroseis. The seismic survey was designed to aid the city streets and boulevards. Split spread with nine detector were deployed at each separation for reliable results to be obtained.

Work done by Hager-Ritcher Geoscience, Inc. [16] at the Mid-Western city for locating underground leaking storage tank is one of the example of seismic refraction survey in noisy, paved and partially located on fill which lead to difficulties in acquire data. For the solution, they used both close line spacing and close geophone spacing. As a result, a high resolution seismic refraction survey was done in two days and yield to the detailed and accurate bedrock surface map.

During summer 2009, a planned seismic survey was taken at the Long Beach/Signal Hill, California [6]. This is a revisited survey from 2006 due to the public concerns towards the effects felt and heard from seismic vibrator. During the recent survey, the responsible company, Signal Hill Petroleum has taken several actions in making the survey successful. They redefine the vibrator sweep to meet the residents concern and deployment of nodal survey, utilizing 100% cable free, passive recording system. Mutual agreement with municipal, residents and the contractor involved yield to the successful of this survey.

## **2.6 Standard Penetration Test vs. Seismic Velocity**

For a routine geotechnical site investigation, the used of number of blows (N) of Standard Penetration Test (SPT) and undrained shear strength ( $s_u$ ) is more common as the many engineering consultant is more familiar with this method [38] [39]. In addition, this old test is relatively cheap in comparison with borehole drilling besides the practicality of this old method [19] [23]. Basically, the N-value obtained from SPT is related to the strength and deformation properties of the ground as stated by Koukis et. al [23]. The site classification is shown in Table 2.1 as reported by Glenn [39] is based on the International Building Code 2003.

As this correlation is important for the ground motion assessments, many researchers have done an empirical correlation of these two parameters at different region in the world consisting different type of sediments and area [10] [19] [23] [29]. Although it is good to have the dynamic soil parameter test in situ, it is often not preferable as it is not economic at all locations. With these correlations, researchers are hoping to get a more reliable correlation that considerable advantage.

Table 2.1: Site classification scheme (after Glenn, 2006).

Site Class	Description	Average properties in the top 30 m		
		Shear wave velocity, $V_s$ (m/sec)	Standard penetration resistance, N	Undrained shear strength, $S_u$ (psf)
A	Hard rock	$V_s > 1500$	Not applicable	Not applicable
B	Rock	$760 < V_s \leq 1500$	Not applicable	Not applicable
C	Very dense soil and soft rock	$360 < V_s \leq 760$	$N > 50$	$S_u > 2000$
D	Stiff soil	$180 < V_s \leq 360$	$15 < N \leq 50$	$1000 < S_u \leq 2000$
E	Soft soil	$V_s \leq 180$	$N \leq 15$	$S_u \leq 1000$
E	-	Any profile with more than 10ft of soil having the following characteristics: <ul style="list-style-type: none"> <li>1. Plasticity index <math>PI &gt; 20</math>;</li> <li>2. Moisture content <math>w &gt; 40\%</math>; and</li> <li>3. Undrained shear strength <math>S_u &lt; 500</math> psf</li> </ul>		
F	-	Any profile containing soils having one or more of the following characteristics: <ul style="list-style-type: none"> <li>1. Soils vulnerable to potential failure or collapse under seismic loading.</li> <li>2. Peats and/or highly organic clays.</li> <li>3. Very high plasticity clays.</li> <li>4. Very thick soft/medium stiff clays.</li> </ul>		

## CHAPTER 3

### METHODOLOGY

#### **3.1 Introduction**

This chapter describes the methodologies and equipments used in this work. The data used are primarily from the data acquired in the research area. The first section will describe the steps taken in order to achieve the first objective which is, to design the acquisition parameter for noisy area. This stage is very important since the research area is in urban area and there are a lot of noises coming from all directions. The general view of the research area, surrounded by traffic, residential areas and business development area are shown in Figure 3.1. In this study, an acquisition parameter that is practical to be use in this kind of environment will be designed.

The second section will focus on the second objective which is, to formulate new technique for noise reduction using MatLab software. Since the data acquired in the urban area is normally contaminated by noise, we need to have a tool that can filter the recorded noise.

The third section will represent the method used in order to achieve the third objective which is, to investigate the correlation between Standard Penetration Test (SPT) values obtain from borehole data and velocity values obtain from seismic survey. The methodology used in the research was summarized as a research flow chart and shown in the Figure 3.2.

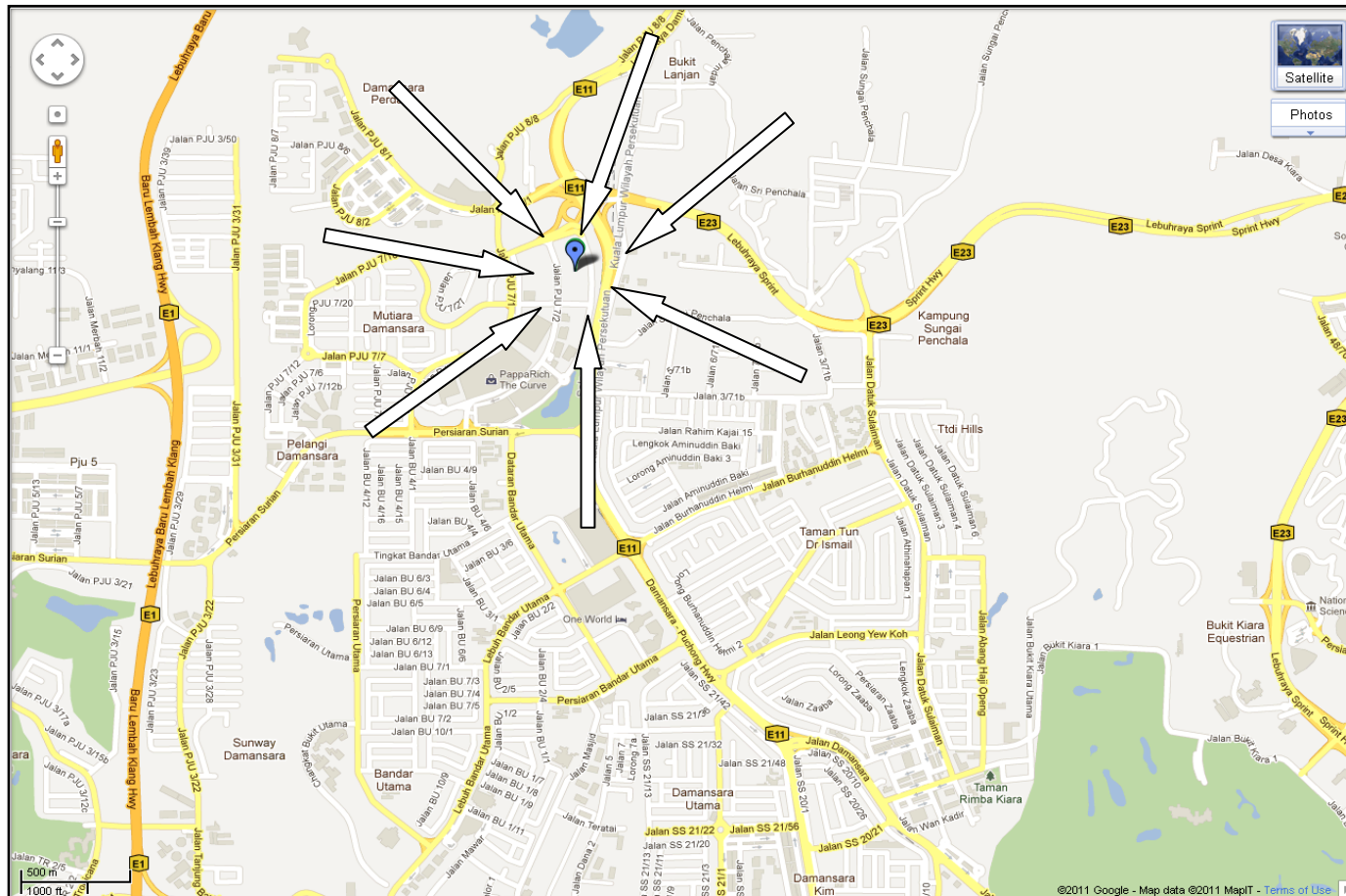


Figure 3.1: General view of the research area, surrounded by residential areas, business development area and arrows indicates where the noises coming from.

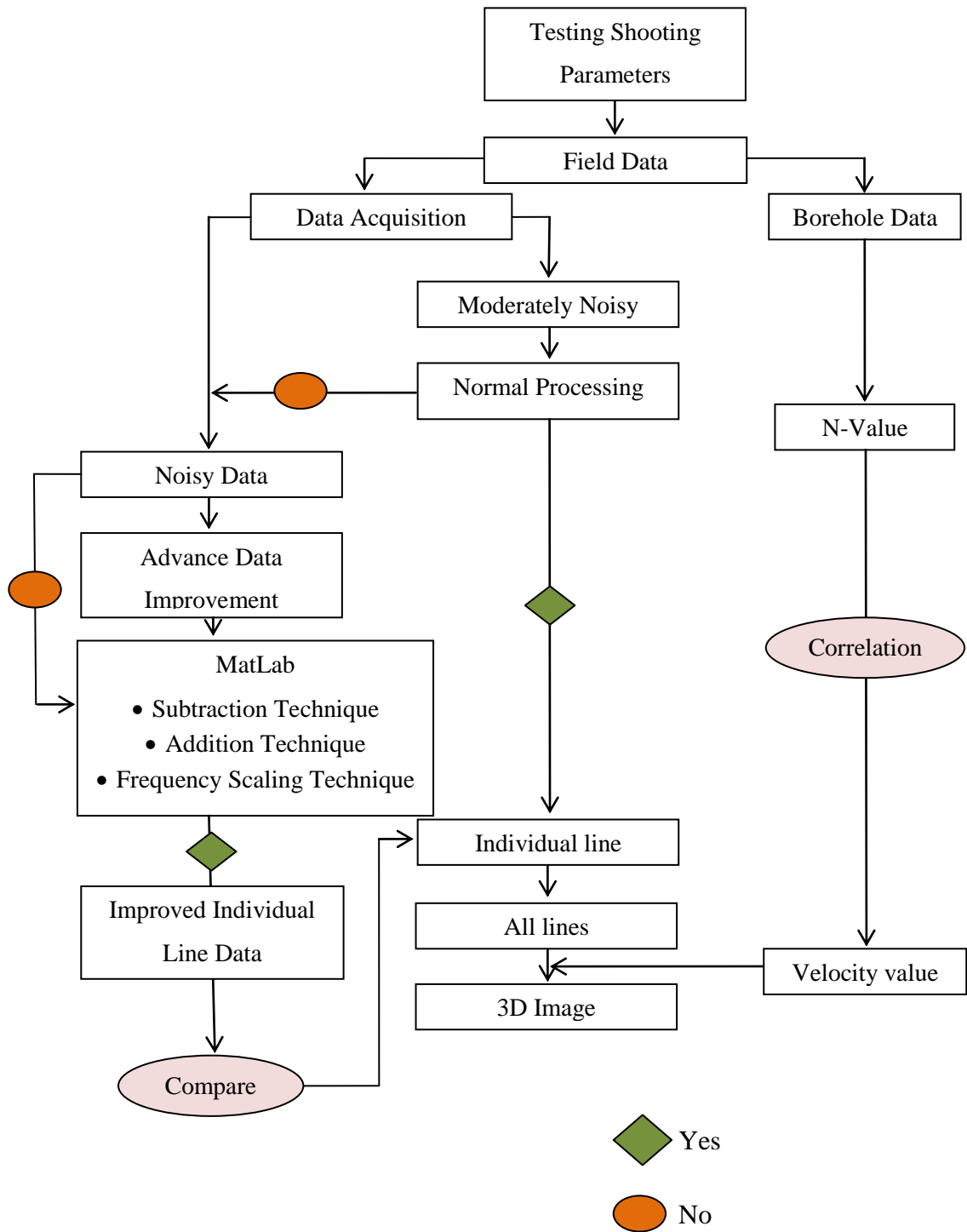


Figure 3.2: Research flow chart

### **3.2 Testing Acquisition Parameter**

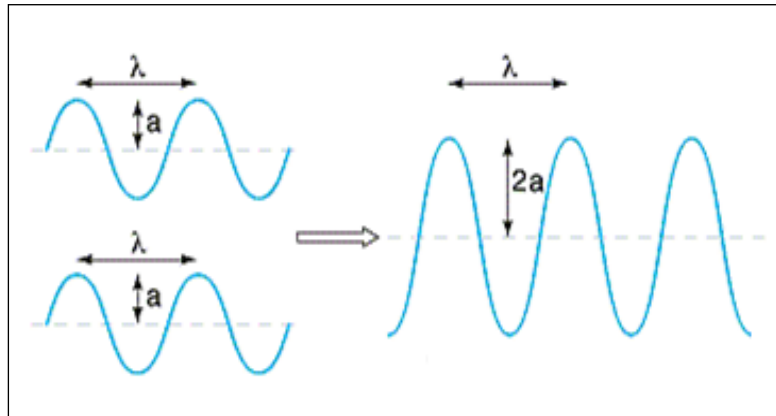
The research area is located at the urban area; this makes the data acquired easily contaminated with different type of noise. In order to gain a good signal record with less noise, the acquisition parameter and field set up need to be design in such away to meet the purpose. There are four types of testing done in the field, 1) the geophone array testing, 2) source testing, 3) equipment testing and 4) trigger testing. The result of these tests will be discussed in the following chapter.

#### **3.2.1 Geophone Array Testing**

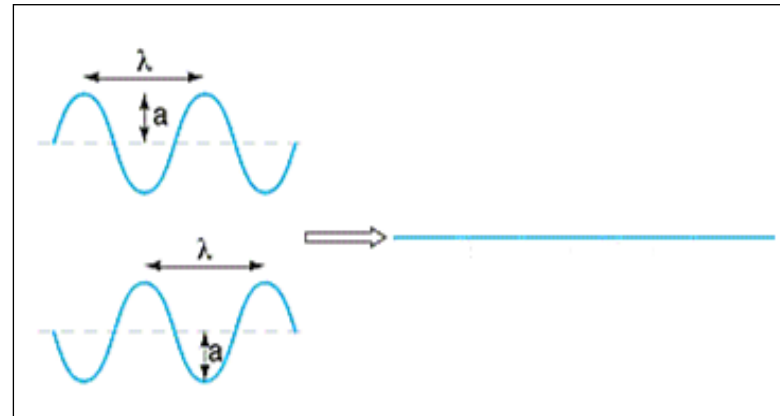
Two different geophone (14-Hz) arrays (single-geophone array and triple geophone array) were tested in order to determine which array captured most of the desired signals since the research area is small and the noise is coming from all direction. Triple geophone array was chosen as it can be arrange in triangle group and the available equipment only permit up to triple geophone array.

In order to compare the quality of the data recorded, the test was done at the same site and on the same line. For the triple geophone array, the geophones are planted as in triangle group rather than vertically or horizontally in line. The idea of doing so is that the noise reached the geophones can be eliminate as the noises suspected coming from all of the direction.

The concept of vertical stacking is applied in this testing. Based on the concept of constructive and destructive of wave, it is understandable that coherent noise will enhance, thus construct the signal after several stacking. For the random signal, it will be minimize and destruct the signal after several stacking. This wave's concept is shown in Figure 3.3. The schematic diagram for single geophone array and triple geophone array is given in Figure 3.4 and Figure 3.5 respectively.



(a)

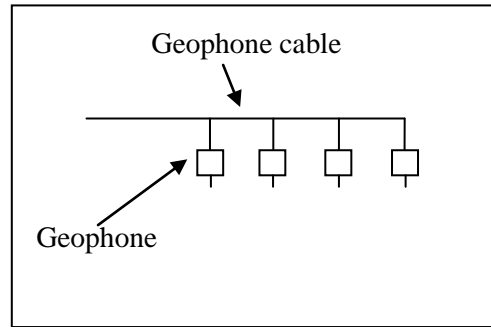


(b)

Figure 3.3 : (a) Constructive concept of wave (b) : Destructive concept of wave.



(a)

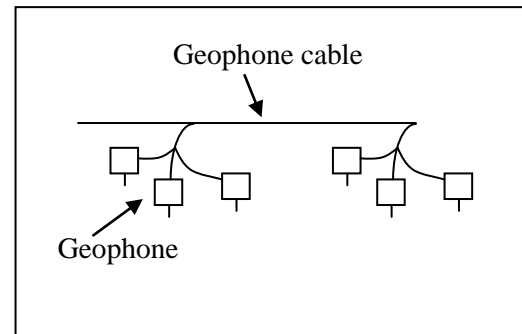


(b)

Figure 3.4 : (a) Single geophone array (b): Schematic diagram showing array of single geophone.



(a)



(b)

Figure 3.5: (a) Triple geophone array (b): Schematic diagram showing triple array geophone.

### **3.2.2 Source Testing**

As the energy used in this research was mainly from induced source energy, sledge hammer and the striker plate play a critical role. This test was carried out with three different types of striker plate before and along the acquisition in order to determine the best striker plate to be paired with sledge hammer. A good striker plate will give a good signal when the energy is induced.

There are several types of induced land source. Dynamite, short gun, sledge hammer and weight drop are the examples of commonly used energy sources in land acquisition. Due to the research area, mobility and safety, sledge hammer was chosen as the primary energy source in this research. The fact that this source did not give great energy imparted cannot be denied. But, this source is a very good and reliable for shallow acquisition since it can sum up the ground motion and enhance the waveforms of the records after a number of impacts.

There are several reasons why sledge hammer was chosen as the primary induced source energy rather than other induced sources like dynamite, vibrator and weight drop. One of the factors is the mobility of the sledge hammer. The sledge hammer can be handled by one field crew as the weight and shape of it is easy to move.

The cost of the sledge hammer is very cheap in comparison to the other induced energy sources. The handling cost for dynamite is relatively higher because only licensed personnel can handle the source as it is dangerous. Other than that, the area of the study (urban area) makes it unsuitable to use dynamite or shot gun.

The other factor is safety of using the source. Since the sledge hammer gives low impact of induced energy compared to dynamite and shot gun, it is very suitable to use in urban type research area. This source will not create and gain attention from the residents and it is very safe.

### 3.2.2.1 Striker Plate

Three different type of striker plate were used in this test which is 1) wooden plate, 2) aluminium plate and 3) steel plate. These plates were tested based on their diameter, weight, thickness, durability towards the impact from the sledge hammer, ability to give good signals and the ductility of the material. These parameters are very important in order to gain good signals and speed up the acquisition. Table 3.1 represents the characteristics for each striker plate. Figure 3.6 (a), (b) and (c) shows the striker plate used during the acquisition phase.

There are three important parameters to look at during this test. The quality of the seismic signals obtain when the energy is impacted by the sledge hammer, the toughness of the striker plates towards the impact from sledge hammer and the mobility of the striker plate in the field.

Table 3.1: Striker plate's characteristic.

	Aluminium	Steel	Wood
Diameter (meter)	0.28	0.31	0.20
Thickness (meter)	0.038	0.038	0.15
Weight (kilogram)	5.97	21.15	2.74



Figure 3.6: (a) Aluminium striker plate.



Figure 3.6 : (b) Steel striker plate.



Figure 3.6 : (c) Wooden striker plate.

### 3.2.3 Seismograph

The equipment used is sets of seismograph system from ABEM. Two different seismographs are tested in order to determine data quality given by the equipment, visibility of the first seismic signal which is known as the first break and the capability of the seismograph in helping the speed of the acquisition phase. This testing is needed in order to have a good quality of data sets and maximize the recorded signals for the next processing step.

A common seismic line was chosen as the test line. Both seismographs are linked together so that they are interconnected to each other. This action was taken so that the energy level is at the same for both seismographs and the signals captured are from the same amount of energy and travel at the same speed. Several shots points were shot. From the recorded signals, the signals captured were analyzed and the equipment is determined to be the main equipment for acquisition, except when the data acquisition has to be completed in a specific duration of time, both equipments were used.

A set of 24-channel seismograph system and 48-channel seismograph system were tested during this testing stage. The characteristics of both seismographs are shown in Table 3.2. Figure 3.7 show how the two seismographs systems were connected during the testing phase. Figure 3.8 and Figure 3.9 shows the diagram for both seismograph systems. While Figure 3.10 show the interconnection of both seismographs.

Table 3.2: Equipment characteristic.

Type	24-channel	48-channel
Weight (Kilogram)	16	23
Dimensions (Meter)	0.48 x 0.26 x 0.33	0.48 x 0.26 x 0.47

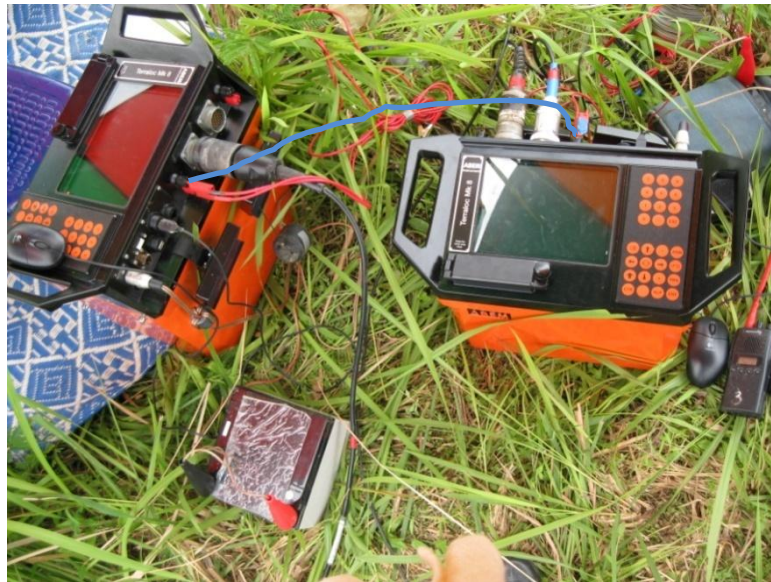


Figure 3.7: Two seismographs systems interconnected to each other at the trigger port during the testing phase.

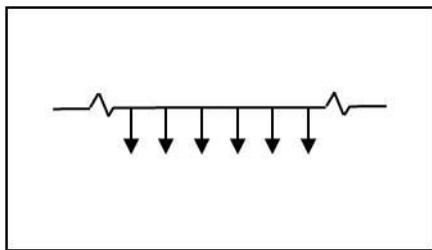


Figure 3.8: 24 channel seismograph diagram.

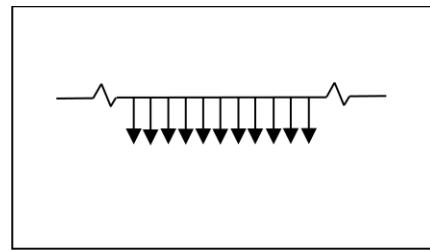


Figure 3.9: 48 channel seismograph diagram.

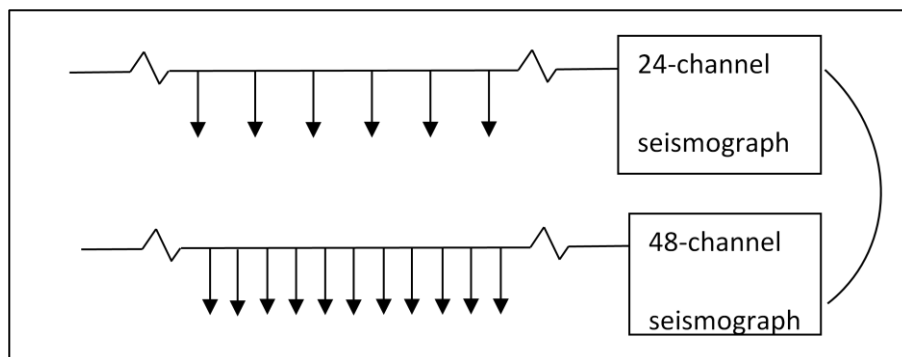


Figure 3.10: Interconnection of both seismographs diagram.

### 3.2.4 Trigger Type

For the triggering purposes, a test was done in order to determine the most suitable trigger to be used during the acquisition. A commercial trigger switch and a geophone were used for the testing. The trigger switch acts as the make/break trigger and it is attached to the sledge hammer. The geophone, on the other hand, acts as the analogue trigger and is placed near to the striker plate. Figure 3.11 shows the position of the trigger respectively. This trigger is very important since it is the only device that helps the triggering process, captures the signal and sends it to the seismograph.

There are three parameters that we look at the trigger type during the testing, there is 1) The sensitivity level of the trigger, 2) time needed to move the trigger from one point to another and 3) time required recovering to the initial condition. The characteristics for each trigger are shown in Table 3.3.



(a)



(b)

Figure 3.11: (a) Analogue trigger position next to the striker plate (b) Trigger switch position near to the sledge hammer head.

Table 3.3: Trigger characteristic.

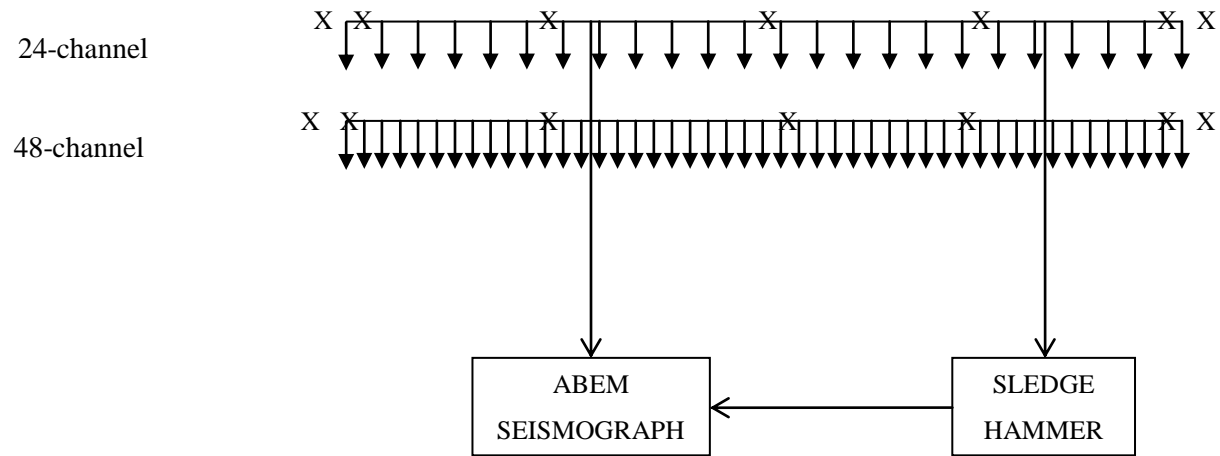
Type	Switch	Analog
Weight (kilogram)	0.07	0.28
Size	Small	Medium
Trigger level input (Hz)	10	14
Position	Near to hammer's head	Planted on the ground

### 3.2.5 Spread Layout and Shot Point Configuration System

Total of seven shot points were used for each seismic line. All shots points are placed in line with the seismic spread. In some condition, the shot point will relocate at different position. The layout spread orientation has been decided on the site itself. The decision has made in order to obtain good seismic data. The shot point locations for both channel systems are referred to the start of line and the length is in meter.

Since there are two different channel of seismograph that has been used, two different orientation of the spread layout is used. The geophone interval for both seismographs is different from each other. For 24 channel system, the geophone spacing intervals are constant at 5 meters spacing. While for the 48 channel system, the geophones spacing intervals are constant at 2.5 meters. The schematic diagram of this channel system is shown in Figure 3.12.

The positions of the shot point for both seismographs are different since the geophone spacing intervals are different. The positions of the shot point are shown in the following Table 3.4 and Table 3.5.



X Shot point position  
 ↓ Geophone

Figure 3.12: Schematic diagram for spread layout using 24 and 48-channel seismograph.

Table 3.4: 24 channel seismograph shot points position.

	24 Geophones	
Shot point	In meters	In geophone position
1	-15	15m away from geophone 1
2	2.5	In between geophone 1 & 2
3	27.5	In between geophone 6 & 7
4	57.5	In between geophone 12 & 13
5	87.5	In between geophone 18 & 19
6	112.5	In between geophone 23 & 24
7	130	15m away from geophone 24

Table 3.5: 48 channel seismograph shot points position.

	48 Geophones	
Shot point	In meters	In geophone position
1	-15	15m away from geophone 1
2	1.25	In between geophone 1 & 2
3	28.75	In between geophone 12 & 13
4	58.75	In between geophone 24 & 25
5	86.25	In between geophone 35 & 36
6	116.25	In between geophone 47 & 48
7	132.5	15m away from geophone 48

### **3.3 Normal Processing Cycle**

The data obtain from the acquisition had gone through the normal processing cycle which is using computer software before the advanced data improvement take place. The flow for this stage is shown in Figure 3.13. The software used in this processing was IXRefrax from Interpex Limited. This software is using Generalized Reciprocal Method (GRM) as their primary method.

The raw data with moderate noise level from the seismograph is saved and manual first break picking is done. The raw data is printed out before the process takes place. Using the software, the data for each line is processed and analyzed. The first break picking using the software is based on the manual first break picking that done before.

After the processing, the information gained from it is used in the model development of that particular line. There are two types of model generated from the information that we are interested in, 2D inverted model and GRM interpreted depth model. From these two models, the velocity for each layer and depth under each of the geophone is obtained.

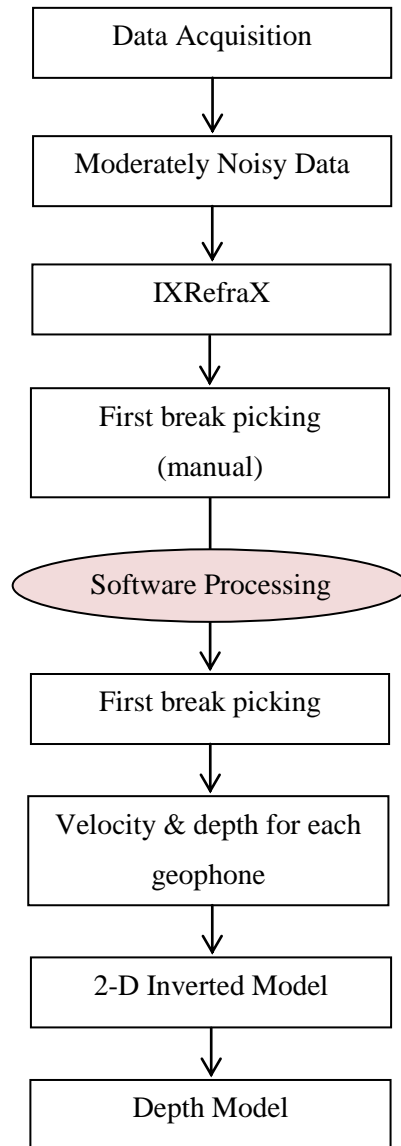


Figure 3.13: Normal processing flow chart.

### **3.4 Advanced Data Improvement**

This method is used to achieve the second objective of the research, to formulate new noise reduction technique using MatLab software. Three different techniques were developed and tested, which are 1) subtraction technique, 2) addition technique and 3) frequency scaling technique.

During the acquisition process, apart from the recorded signal at the shot point, the noise data (noise record) were also recorded. This noise record records the noise level at that particular shot point. Based on comparison of data quality between the noisy data and noise record, the new techniques are formulated.

The data recorded is first converted to the .SGY file format from .SG2 file format using IXSeg2SegY software. After the conversion, the data is then ready to be use in MatLab software where the algorithm for the method is developed.

#### **3.4.1 Subtraction and Addition Technique**

The subtraction technique and addition technique was built based on the simple mathematical expression shown below. Both of this technique used the original time-distance domain as the medium of application. The recorded signal data is subtracted or added by the recorded noisy data for that particular shot point. The initial hypothesis for this technique was, we will get a better clean first break signal after the application of both techniques. The final result after the application of this technique is compared and discussed.

$$A - B = C \quad (1)$$

$$A + B = D \quad (2)$$

with

A = Recorded data with moderately noise

B = Recorded noise data

C = Product of subtraction

D = Product of addition

### 3.4.2 Frequency Scaling Technique

For the frequency scaling technique, the process is divided into two parts. The first part is to identify the noisiest trace from the recorded seismic trace. The second part is to carry out the treatment for all the noisy traces. As the discrimination evidence of noisy trace, the threshold value of this treatment is selected and fixed at 3. The threshold value is determined using the following expression and is the value where the cut off frequency is defined:

$$A(f) = B_1(f) / B_2(f) \quad (3)$$

where  $A(f)$  is the amplitude factor,  $B_1(f)$  is the average frequency of clean trace and  $B_2(f)$  is the average frequency of noisy trace. For every trace that has the threshold value more than 3, the treatment will apply to that trace. If the threshold value is less than 3, the trace will be preserved as its original state.

The new trace is the dot product of  $A(f)$  and each single traces that need the treatment. This treatment is done in time domain. To revert back the new traces to frequency domain after the treatment, inverse FFT is applied. This technique is done using MatLab software. Figure 3.14 explain how the data improvement stage was carried out.

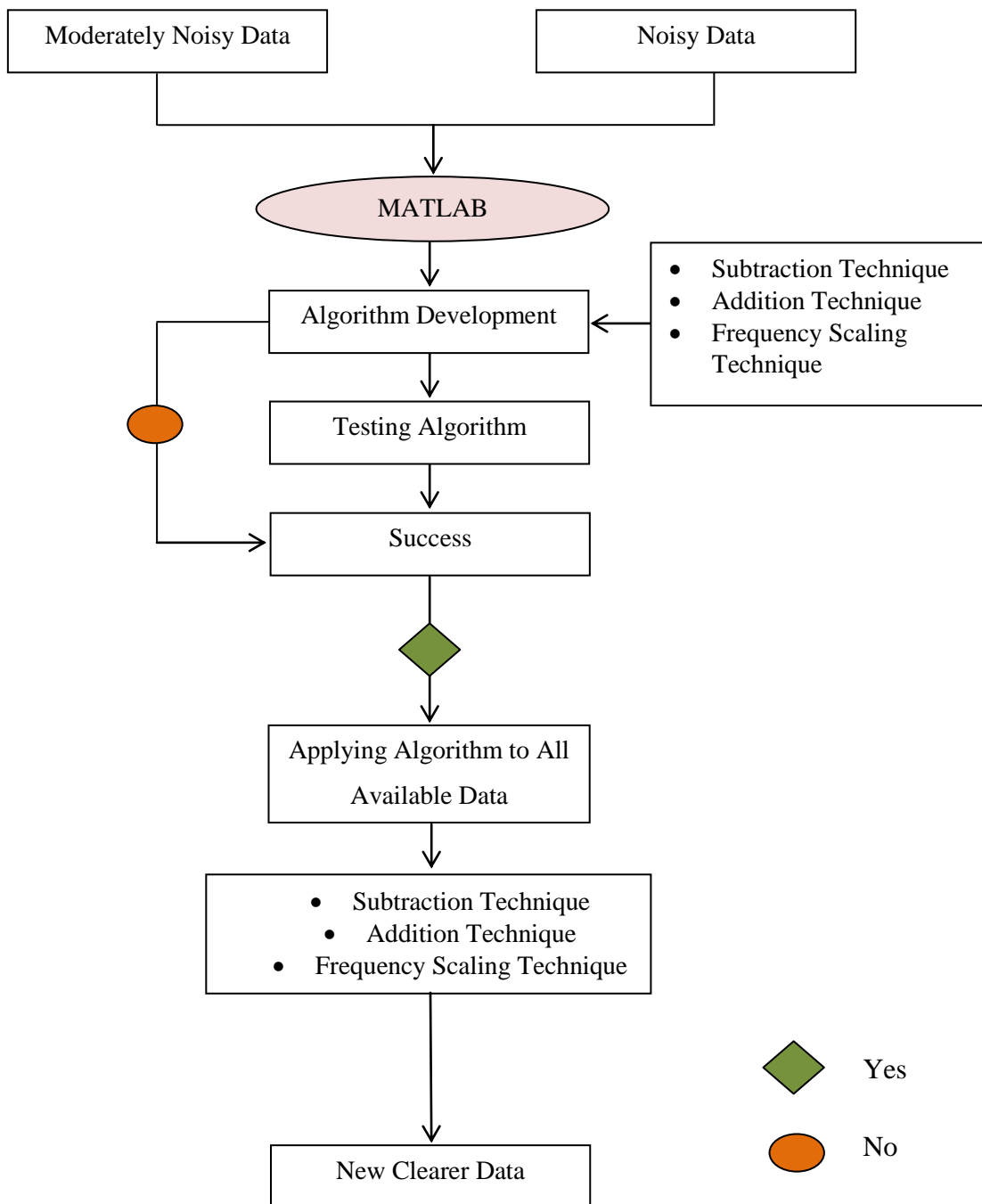


Figure 3.14: Advanced data improvement flow chart.

### **3.5 Correlation between Standard Penetration Tests (SPT) With Seismic Velocity**

In total, there are 99 surveyed seismic lines and 95 boreholes data that were collected around the research area. From the surveyed lines, the velocity value for each layers and depth under the geophone of the area are obtain. On the other hand, from the boreholes data, the value of Standard Penetration Test (SPT) is obtained. The action taken for this objective is shown by Figure 3.15.

From the information, a correlation between velocity value from seismic survey and Standard Penetration Test (SPT) from boreholes survey was done. The SPT is referring to the number of blows needed for a certain penetration depth of the bottom of the borehole by a slide hammer with standard weight and falling distances. The SPT blow count value is commonly known as N-value.

The SPT is done for every 1.5 meter of depth. The depth where the seismic encountered the second layer is compared to the depth where the SPT is done. If the depth of the encountered second layer is in between the SPT is done, the upper value is taken into account. Both the value of the SPT at the cut off level of seismic is summed up.

From the seismic survey, the value obtain is velocity. This velocity value is gained from the density contrast of the subsurface. The value is higher for denser material compared to lower one. From the SPT, the N-value also counts from the density of the sample. The harder the sample, the more blows you need for that sample. We are expecting there is a correlation between this two after the graph is plot. The result of this correlation will be discussed in the following chapter. Figure 3.16 shows an example of correlation panel between SPT and Seismic Velocity.

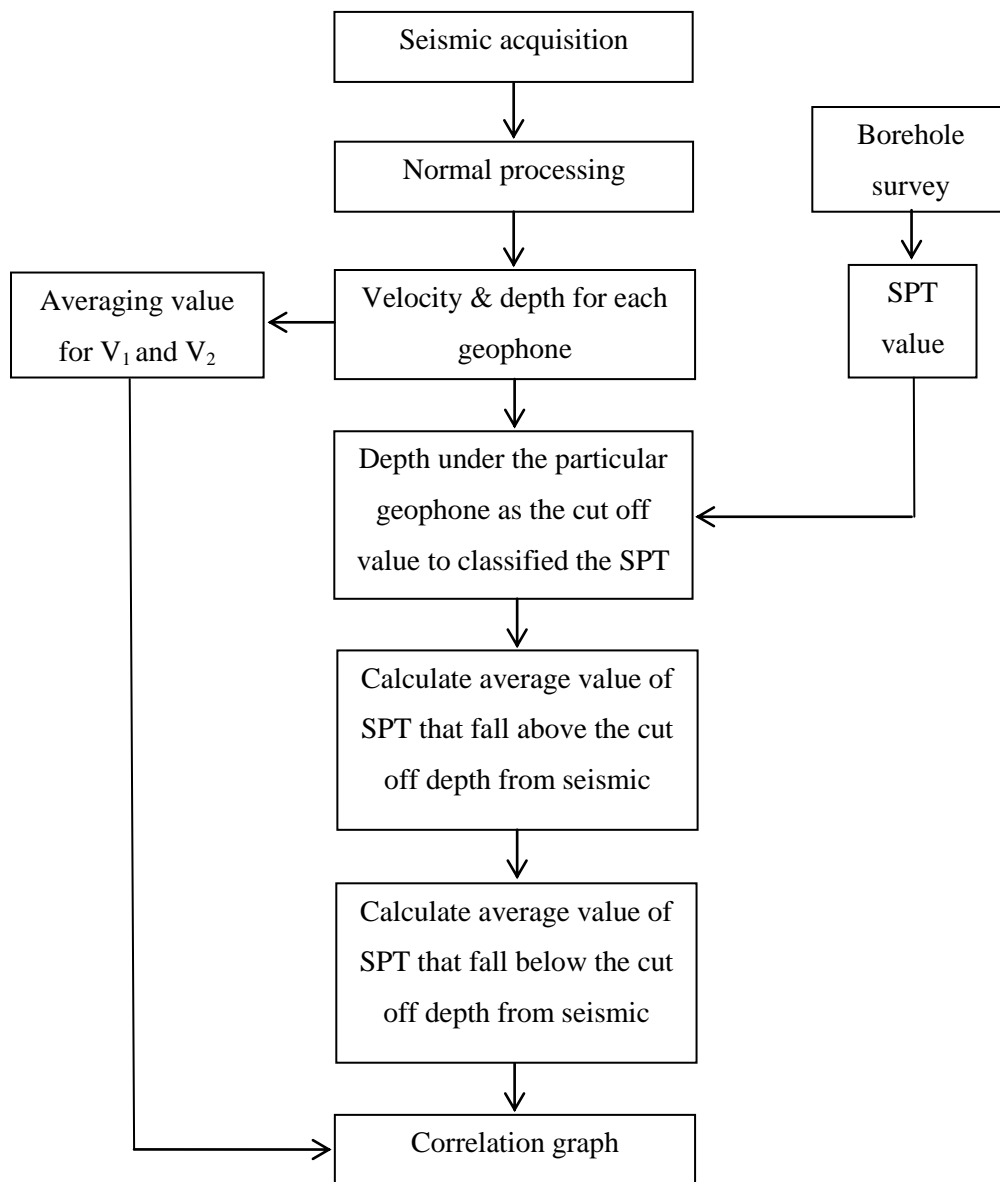


Figure 3.15: Correlation flow chart.

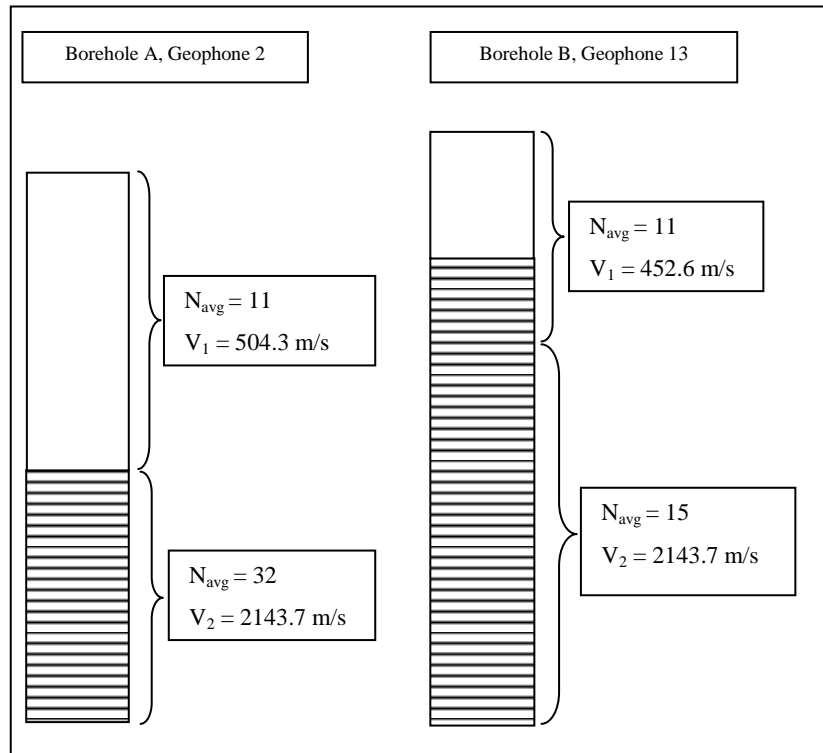


Figure 3.16: Correlation between SPT and seismic velocity.

## CHAPTER 4

### RESULTS AND DISCUSSIONS

#### **4.1 Introduction**

This chapter presents the result obtained from the work done. Discussion of the results will be given in three sections. The first section discussed the result of steps taken to achieve the first objective which is to design the acquisition parameter for noisy area. The second section focused on the results of the development of a new approached noise reduction technique using MatLab software. The last section discusses the outcome of investigating the possible correlation between Standard Penetration Test (SPT) values obtain from borehole data and velocity values obtain from seismic survey.

#### **4.2 Acquisition Parameter Design for Noisy Area**

Field parameter used to acquire seismic refraction data will determine the quality of the data recorded. In some area, good quality data are easily obtained. In some other area, it is not easy to obtain any good data. The quality of the recorded data is dependent on the acquisition parameters used as well as the site characteristic. Since every area / site has their own character, the acquisition parameters should be designed to meet those characteristic. One should be aware of the capabilities and limitations of the equipment used since the seismic data acquisition equipment has finite capabilities. Each aspect of these capabilities can yield to good quality of data [1].

Since the research area is located in urban area there are a lot of noise signals coming from all direction that should be considered. Choosing the right acquisition parameters of this area is very crucial in acquisition phase, even when the locations are bad for seismic survey. Thus, deciding the right acquisition parameters is very important. Four acquisition parameters were tested which are 1) geophone array, 2) source, 3) equipment and 4) trigger.

#### **4.2.1 Geophone Array Testing**

Two different geophone arrays were tested in the field which is single array and triple array. These arrays were tested in order to determine which array captured most of the desired seismic signals. The seismic signals recorded for both array are shown in Figure 4.1(a) for single array and Figure 4.2(a) for triple array.

The triple geophone array captures clearer signal as all three geophone recorded the signal at the same time and stacks the signals at the same time which enhance the quality of the seismic signal recorded. The single geophone array on the hand, also give a good quality of data even though not as good as the triple geophone array. The first break signals are still visible and easily picked up.

Frequency spectrum of both seismic signals is plotted as in Figure 4.1(b) and Figure 4.2 (b). Both of the geophone arrays are giving same seismic signal behavior. Both frequency spectrums show the presence of two peaks which dominated at frequency range of 10 Hz to 50 Hz and 50 Hz to 100 Hz.

In single array, the highest amplitude reached by the low frequency is 0 dB at frequency of 45 Hz and the highest amplitude by the high frequency is -2 dB at frequency 60 Hz. The triple geophone array reached the highest amplitude of low frequency at 0 dB at 30 Hz and high frequency of -1 dB at 70 Hz.

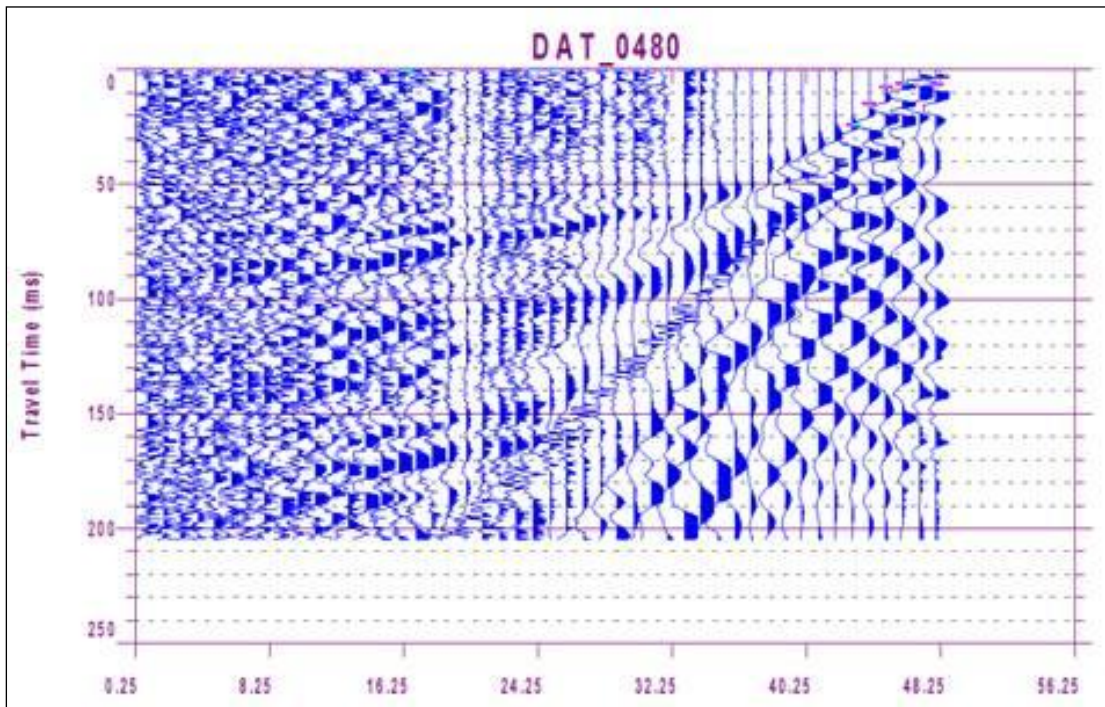
From the plot, it shows very minimal changes in amplitude carried by both geophone arrays. Since there are only minimum changes, single geophone array was chosen as this array has shorter time in setup and can help in speeding up the acquisition.

### **4.2.2 Source Testing**

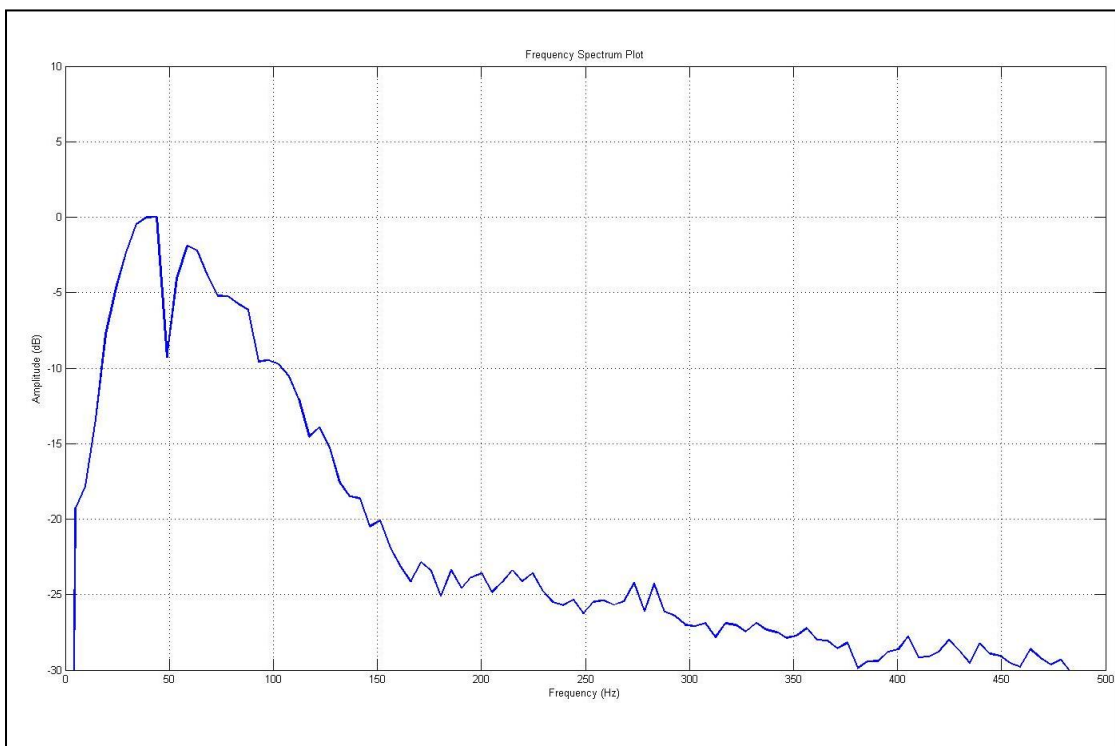
Choosing the right source for the seismic acquisition is important. In every seismic acquisition, working under specific budget constraints is a normal practice, and cost is one of the most important factor. Often, before a seismic acquisition started, all of this constraints will be taken under consideration in order to get the best data.

As the study area is situated in urban area, this characteristic itself dictates the energy source. The traditional, sledge hammer was used as the source due to some constraints that have been discuss in previous chapter. Even though the hammer strike would not give a great energy imparted, this classical way of seismic acquisition is still a useful inexpensive instrument that can enhanced the signals recorded via summation of the ground motion and safe to be used in urban area [3].

Other considerations that was taken into account are time saving for moving the source, convenience and efficiency of the source to enter the research area, man power that needed for the mobility of the source and environment concerns. In this study, the sledge hammer was used for the source testing due to the constrain for other type of sources.

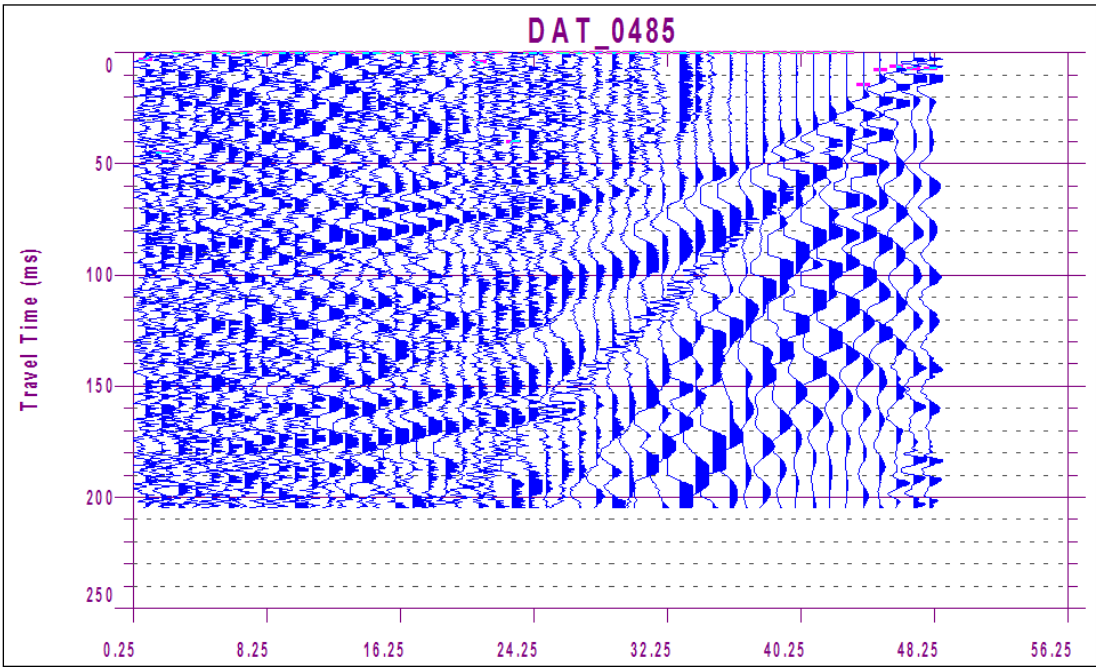


(a)

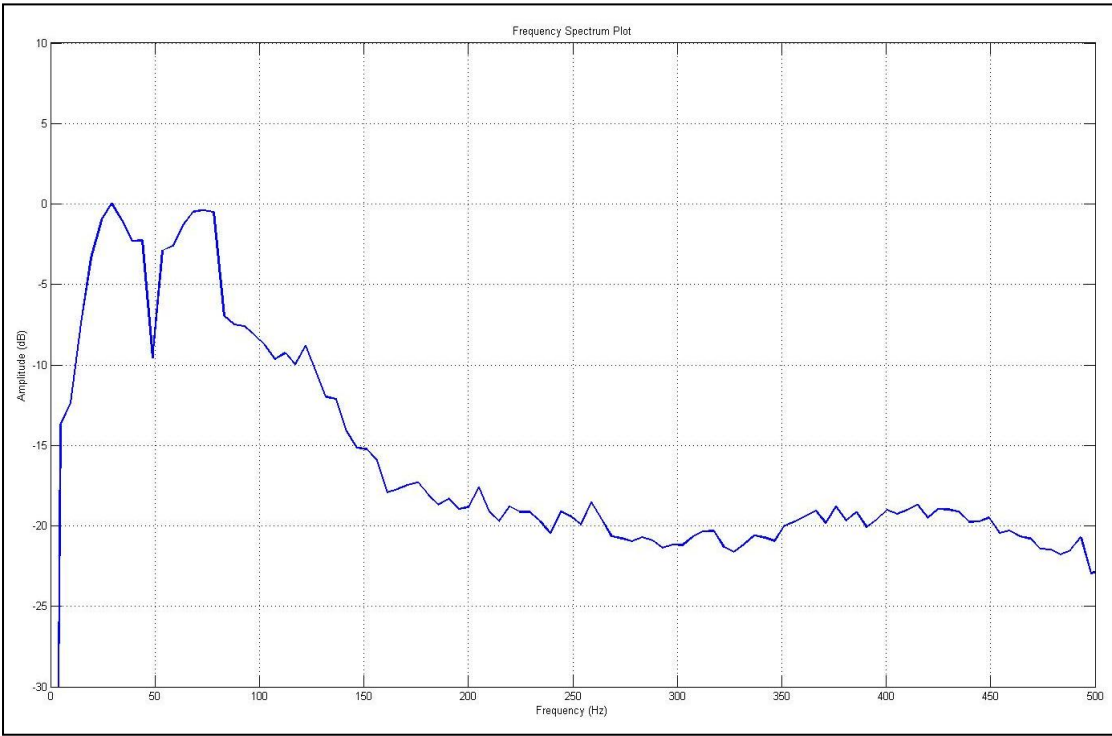


(b)

Figure 4.1:(a) Single geophone array seismic record using 48-channel seismograph  
(b): Frequency spectrum.



(a)



(b)

Figure 4.2:(a) Triple geophone array seismic record using 48-chann3l seismograph  
(b): Frequency spectrum.

#### ***4.2.2.1 Striker Plate***

Three different striker plates' were tested which are 1) wooden plate, 2) aluminium plate and 3) steel plate. The characteristics of those plates' were listed in Table 4.1. The important parameter of the striker plates in this study are the quality of the seismic signals obtain when the energy is imparted by the sledge hammer, the toughness of the striker plates towards the impact from sledge hammer and the mobility of the striker plates in the field.

The recorded data for all the striker plates are shown in Figure 4.3 (a), Figure 4.4 (a) and Figure 4.5 (a) respectively. The signals obtain from shot at the particular striker plate's are showing the same trend. The seismic signals obtain from all of the striker plate are clear and the first break are visibly seen. In order to compare the quality of the seismic signals obtain when the energy is imparted by the sledge hammer, frequency spectrum for all the shots was plotted. The frequency spectrum plot of the recorded data is shown by Figure 4.3 (b), Figure 4.4 (b) and Figure 4.5 (b).

From frequency spectrum plot, all of the seismic signals captured show the same behavior. All plates show two dominant peaks of amplitude. Wooden striker plate and aluminium striker plate is having the highest amplitude of low dominant frequency at 0 dB. The steel striker plate is having the highest amplitude of -32 dB at low dominant frequency. The highest amplitude of high dominant frequency recorded is at -1 dB by wooden striker plate and -2.5 dB aluminium striker plate. The lowest amplitude of high dominant frequency is recorded at -35 dB by steel plate.

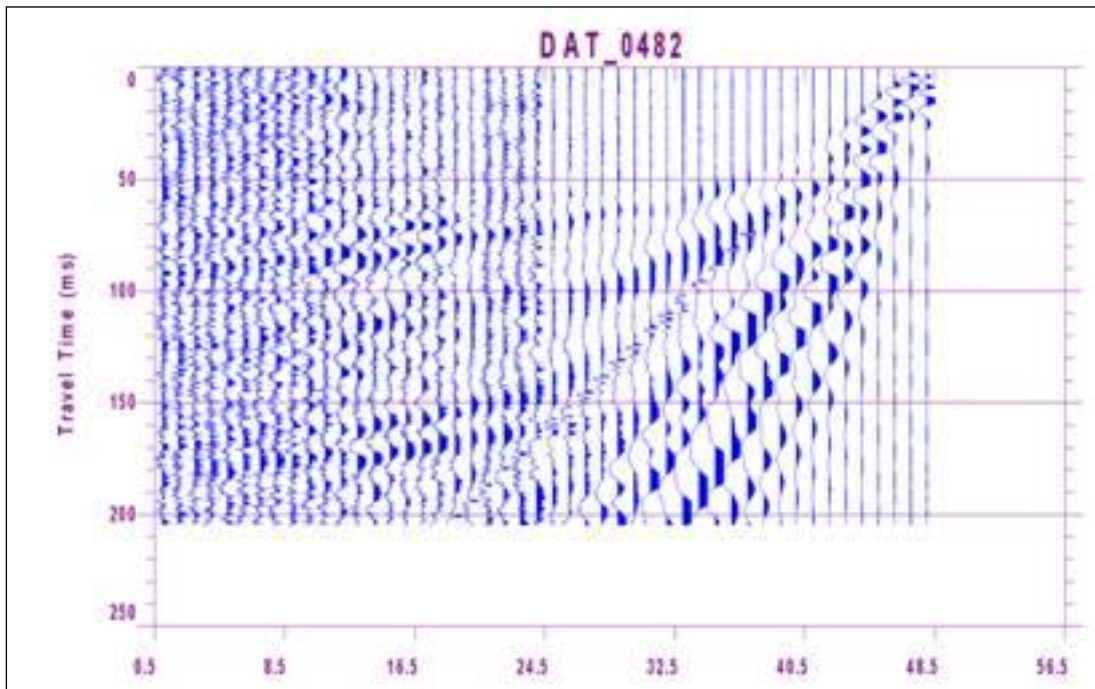
From the site's observation, wooden plate and steel plate is not suitable to be used as primary striker plate. The toughness of wooden striker plate is very low, thus make it easily broken after several impact from the sledge hammer. The wooden plate is also very fragile even though producing good quality of seismic signals. With 0.20 meter diameter, 0.15 meter thickness and 2.74 kilogram weight, this striker is easy to handle. The mobility rate of this striker plate is at very easy level since it is light. Steel plate on the other hand is heavy, thus make it difficult to move from one location to another location. Furthermore, the steel plate is not that durable, because after several lines acquire, it break into two pieces.

From the frequency plot, the aluminium striker plate also shows the same behavior like the other two striker plates. The seismic signals obtain was good too. From the field's observation, the toughness of this plate is high compared to the other two striker plates'. It is still having the shape like before impacting by the sledge hammer with slightly changes. With diameter of 0.028 meter, 0.038 meter thickness and 5.97 kilogram weight, this striker plate is easy to managed and handled.

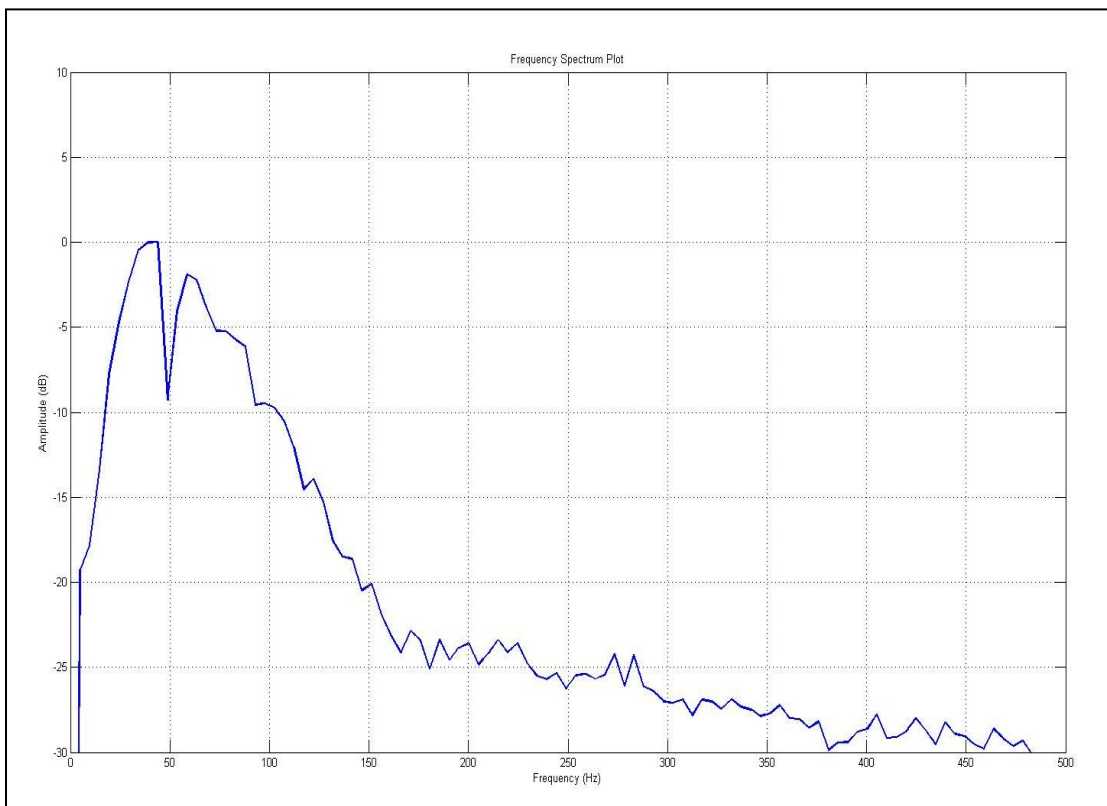
The field observation result is listed in the Table 4.1. From the observation and test, it shows that aluminium plate is the best striker plate to be use in the field. The signals obtain from this striker plate is good, high rate of toughness make it hard to break and medium weight make it mobility rate is medium is the key factor why we chose this striker plate instead of the other two.

Table 4.1: Striker plates parameter testing result.

Parameter tested	Striker plate		
	Wooden	Steel	Aluminium
Data quality	Good	Good	Good
Toughness rate	Very low	Low	High
Mobility Rate	Easy	Hard	Medium

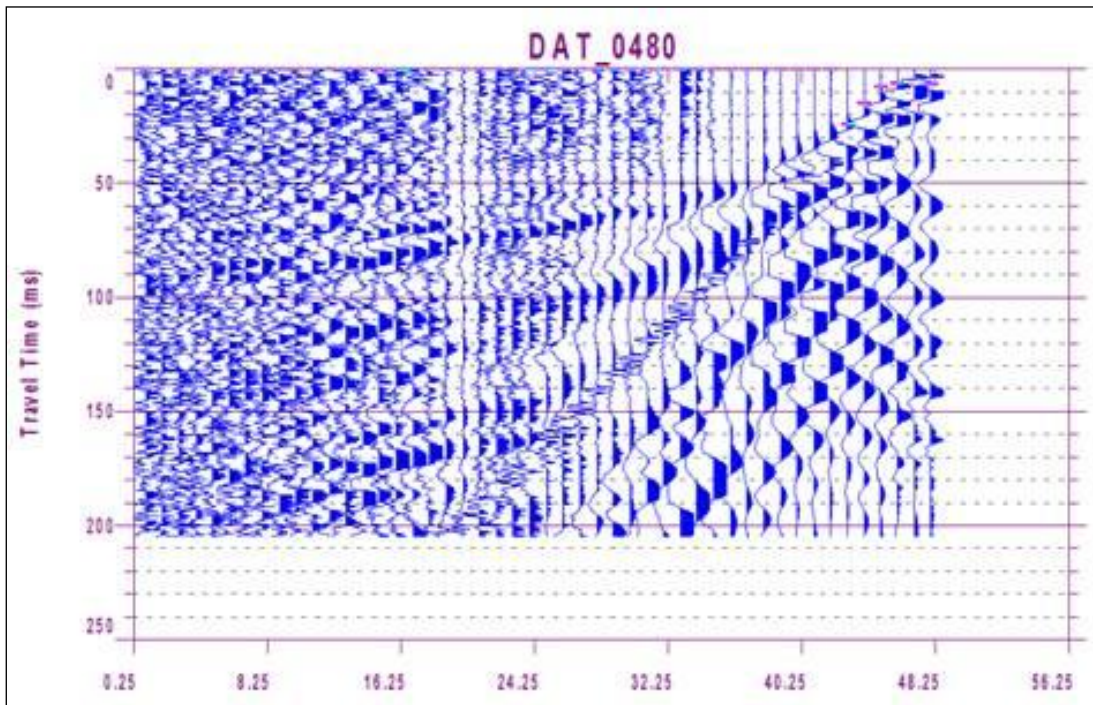


(a)

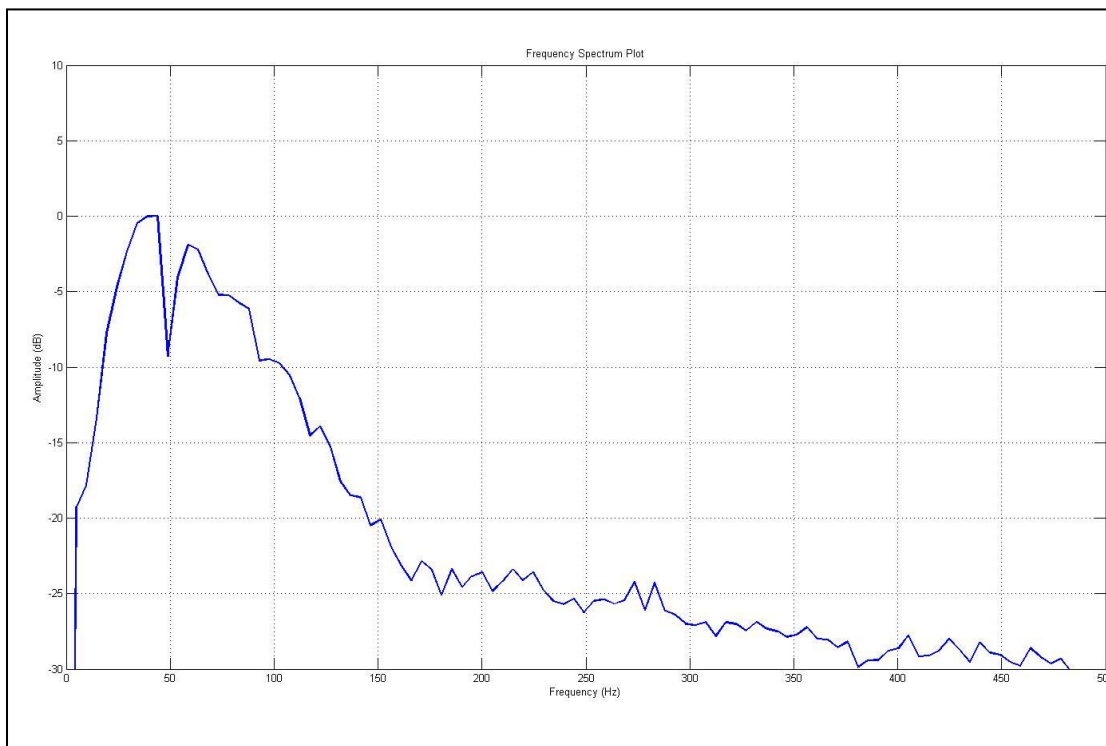


(b)

Figure 4.3: (a) Wooden striker plate seismic record using 48-channel seismograph  
(b) Frequency spectrum.

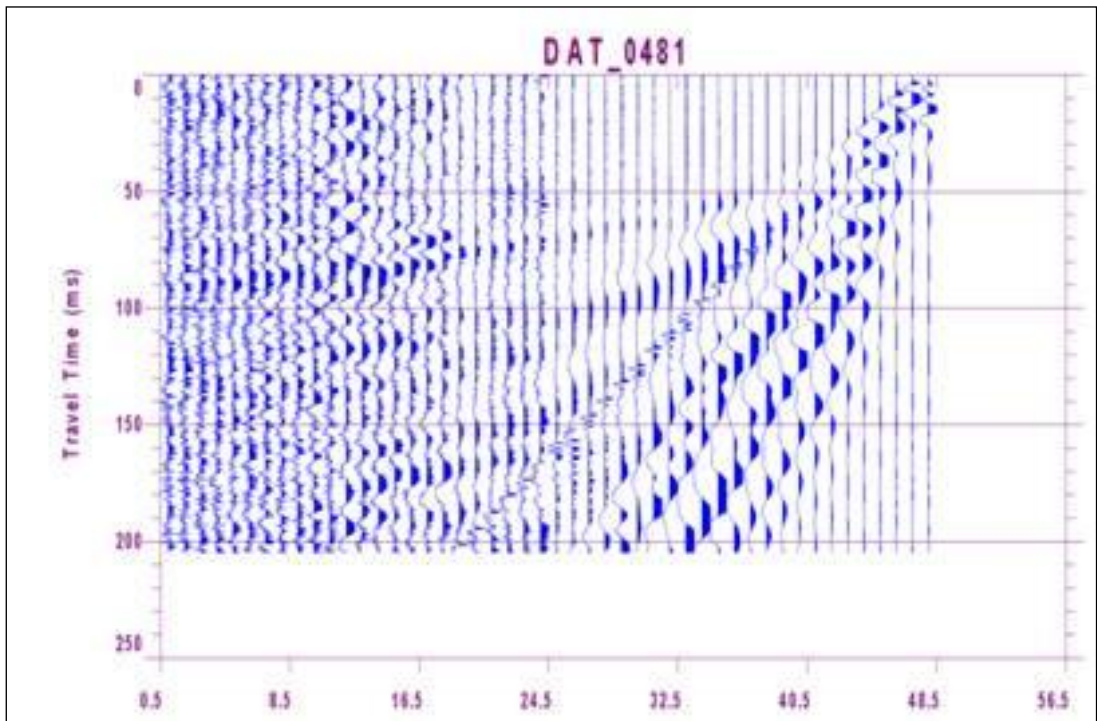


(a)

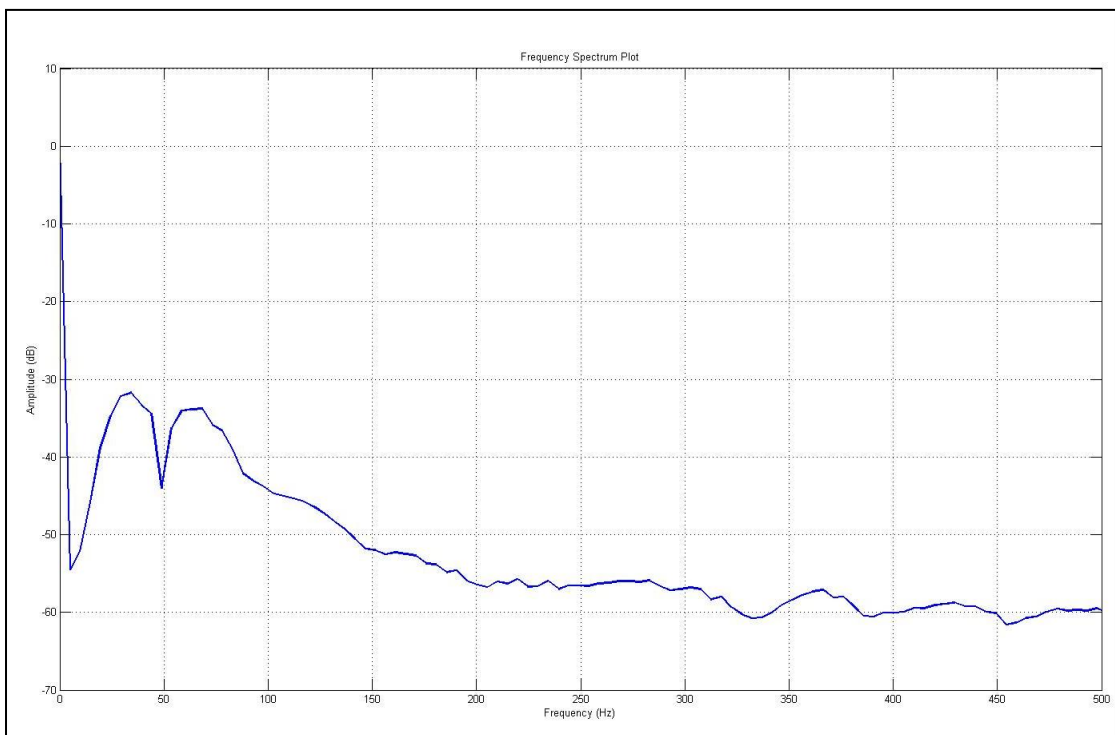


(b)

Figure 4.4: (a) Aluminium striker plate seismic record using 48-channel seismograph  
(b) Frequency spectrum.



(a)



(b)

Figure 4.5: (a) Steel striker plate seismic record using 48-channel seismograph  
(b) Frequency spectrum.

### 4.2.3 Trigger Type

Two different trigger types were tested in order to determine sensitivity level of the trigger, time needed to move the trigger from one point to another and time required recovering to the initial condition. There are commercial switch trigger and an analogue trigger. The characteristics of these two trigger are listed in Table 3.3.

For switch trigger, the trigger position is placed near to the hammer head. This trigger switch is working based on make/break principal. From the field observation, this trigger is very sensitive to movement. When the shooter swings the hammer, the trigger captured the signal from the hammer's movement. This makes it very difficult to acquire seismic signals.

For analogue trigger, a geophone was used as the analogue trigger. This analogue trigger is planted near to the striker plate when the acquisition takes place. The trigger must be coupled to the ground firmly as the response to ground motion will be limited if it is not firmly coupled. It will capture signal when the trigger level is exceeding the trigger level input that we set up in the instrument [4]. With this, the shooter has more control and freedom to do the shooting.

From the field test observation, even though the level of sensitivity of commercial trigger is very high, the time needed to move this trigger is very fast. This is due to the position of this trigger that is attached near to the hammer's head. The analogue trigger on the other need more time since more time is needed to plant the geophone trigger. The geophone need to be re-planted if the striker plate position changed too. On average, the time needed to complete one seismic line acquisition using commercial switch trigger is slightly faster than using analogue trigger. But, since the sensitivity level of commercial switch trigger is very high, the analogue trigger was chosen to be used throughout the acquisition phase. The trigger type parameter testing result is listed in Table 4.2.

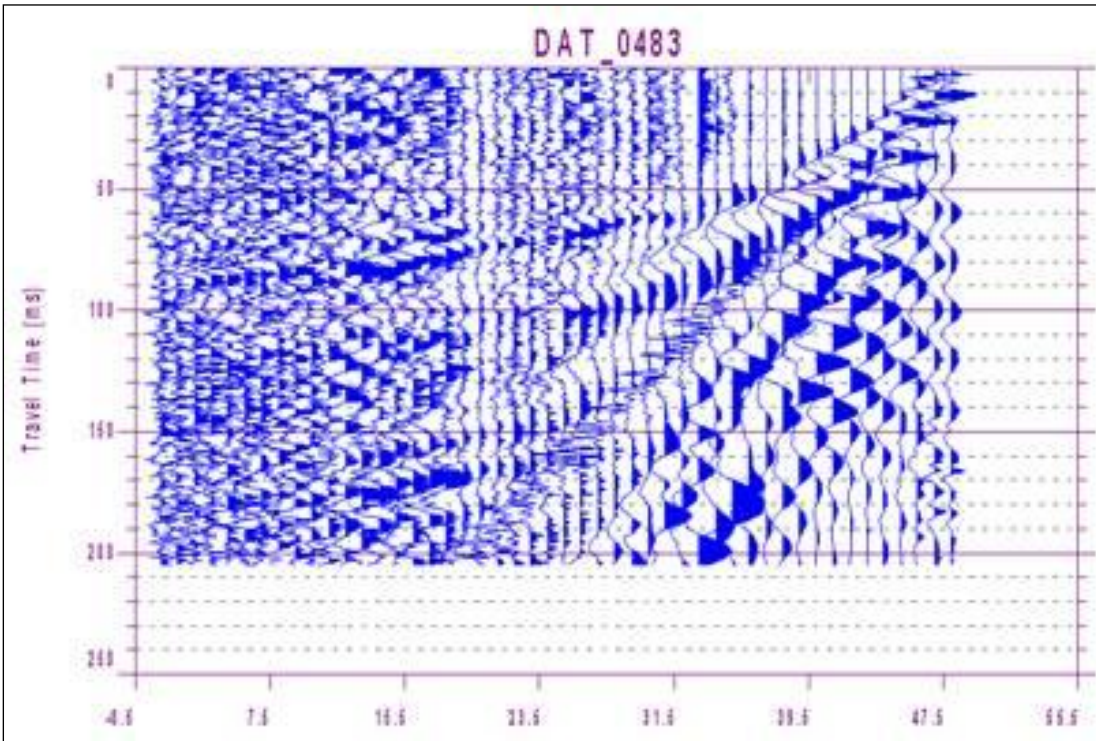
Further investigation is made for analogue trigger. A test about trigger distance from striker plate was also carried out. Two different distances was tested, 1 inch from the striker plate and 6 inch from the striker plate. The raw recorded data for both distances is shown by Figure 4.6(a) and Figure 4.7(a). The frequency spectrum plot is shown in Figure 4.6(b) and Figure 4.7(b).

The frequency spectrum obtain from this record shows same behavior of seismic signal and there is only slightly different in amplitude for both frequency spectrum. There are two peaks of two dominant frequencies which are at 20 Hz to 50 Hz and 50 Hz to 80Hz. Both of the spectrums show the value of -33 dB for low dominant frequency and -35 dB for high dominant frequency.

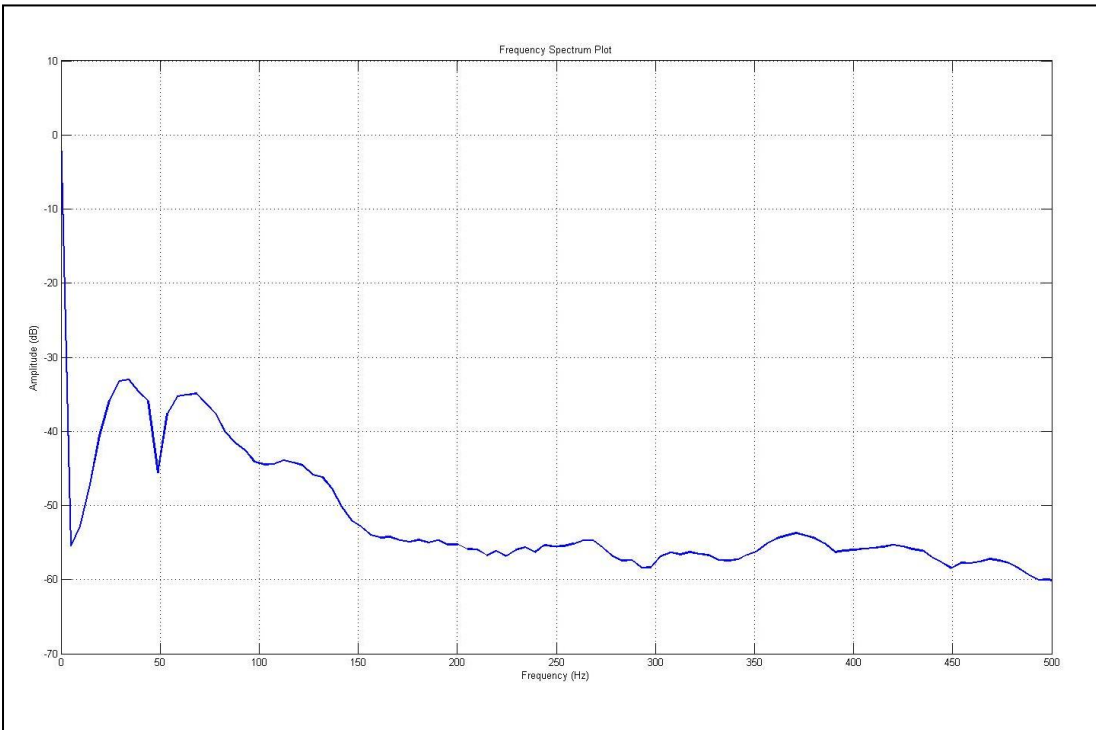
From this, we can deduce that, there is no differences in terms of positioning of the analogue trigger with the condition, the coupling of the trigger with the soil must be firm contact in order to maximize the ability of the geophone in capturing signal from the ground motion.

Table 4.2: Trigger type parameter testing result.

<b>Parameter tested</b>	<b>Trigger type</b>	
	<b>Switch</b>	<b>Analogue</b>
Sensitivity level	High	Moderate
Time required to recover to the initial condition (second)	20	10
Time needed to move (minutes)	10	20
Average time needed to complete one seismic line (minutes/line)	40	20

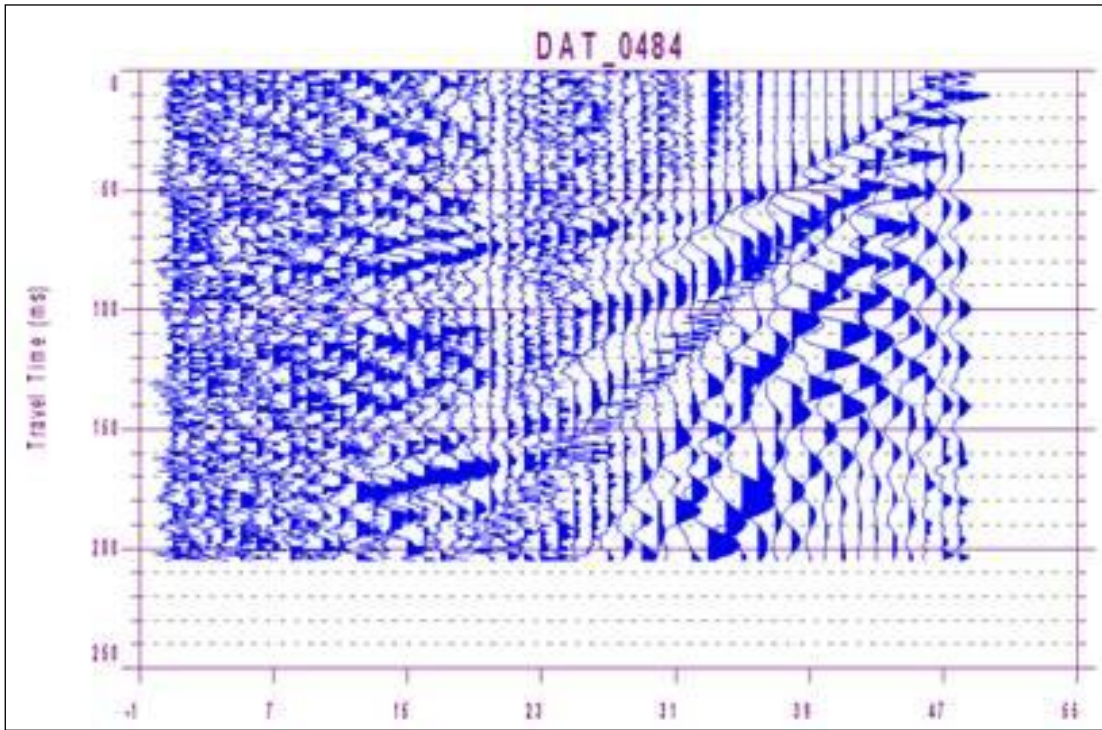


(a)

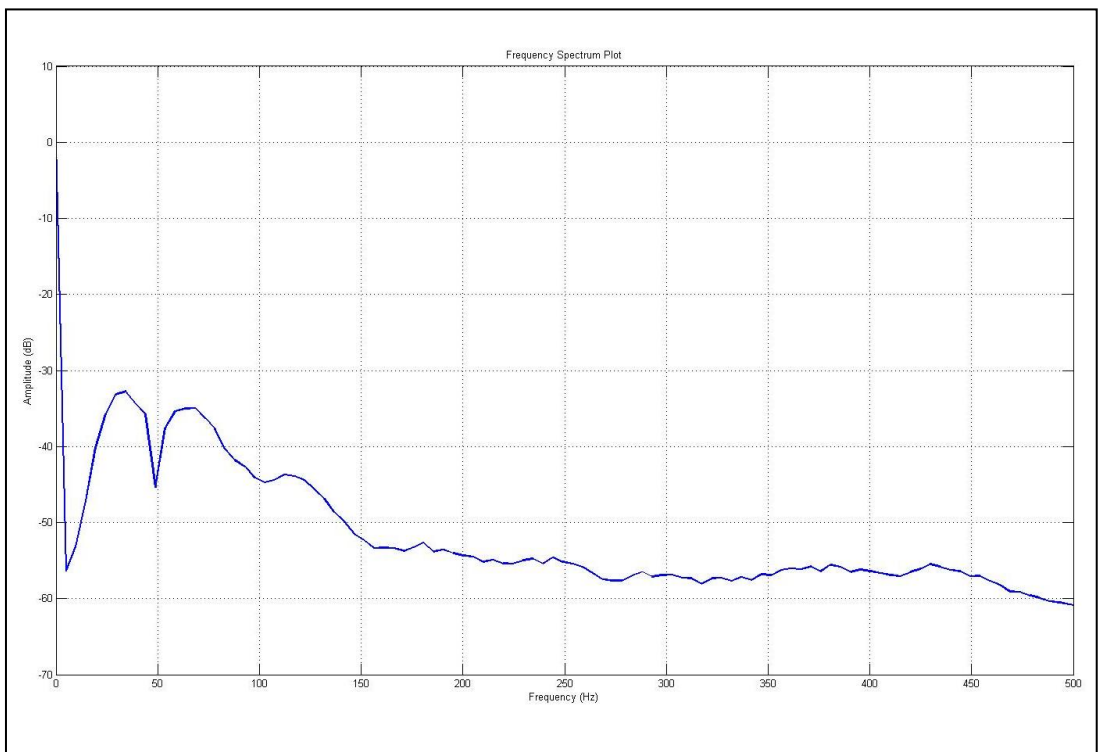


(b)

Figure 4.6: (a) Analogue trigger at 1" away from striker plate seismic record using 48-channel seismograph (b) Frequency spectrum.



(a)



(b)

Figure 4.7: (a) Analogue trigger at 6" away from striker plate seismic record using 48-channel seismograph (b) Frequency spectrum.

#### 4.2.4 Equipment and Spread Layout

Two different sets of seismographs system were tested in the field, 24-channel seismograph system and 48-channel seismograph system. The test was carried out in order to determine data quality recorded by the equipment, visibility of the first seismic signal which is known as the first break and the capability of the seismograph in helping the speed of the acquisition phase. The characteristics of the seismographs system are listed in Table 3.2.

The test was carried out with the seismographs system interconnected with each other. The data recorded was acquired at the same shot point with the same amount of energy. The recorded raw data of both seismographs systems are shown in Figure 4.8 (a) and Figure 4.9 (a). The frequency spectrum plot of the recorded data is shown in Figure 4.8 (b) and Figure 4.9 (b).

The data quality of both seismograph systems is good. Both of the system show the same trend of seismic signals captured. The data quality of 24-channel seismograph system is relatively less good compared to the 48-channel seismograph system. This is due to the difference in geophone spacing. The geophone spacing for 24-channel seismograph system is 5 meters and 2.5 meters for 48-channel seismograph system.

The first break signals are clearer seen in both seismograph systems. The first break trend in 48-channel seismograph system are clearer and easier to pick rather than first break in 24-channel seismograph system since the geophone spacing in 48-channel seismograph system are small compared to the geophone spacing in 24-channel seismograph system.

Even though there is a difference in geophone spacing, both of the seismographs are still very helpful in speeding up the acquisition process. Both of the seismograph system was used in the acquisition phase as we do have time constrains and need to finish the work in the given time frame.

The spread layout is determined based on the seismographs channel system. As for the 24-channel seismograph system, the geophone spacing was constant at 5 meters and the shot point's position is listed in Table 3.4. For the 48-channel

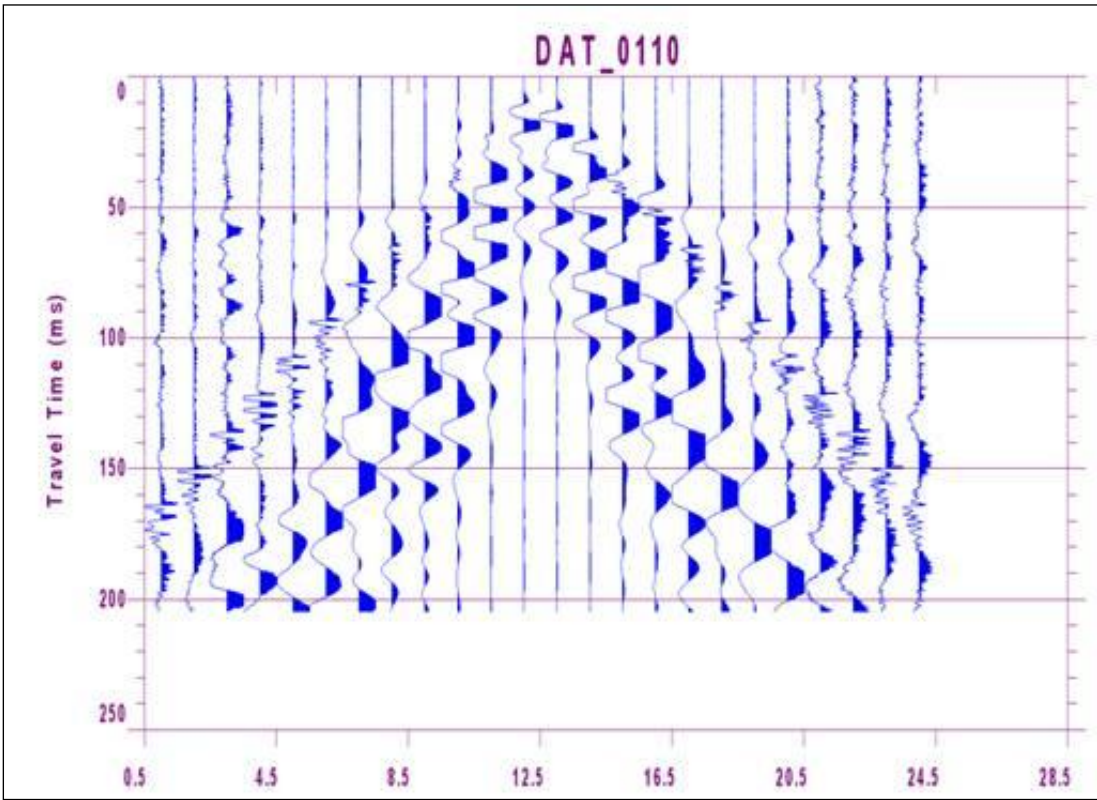
seismograph system, the geophone spacing was constant at 2.5 meters and the shot point's position is listed in Table 3.5.

As the research area is not a flat empty field, the shot points of a particular line may shift to suit the environment. Some restrictions on the sites are abandoned concrete, hard soil and buried water tunnel. These restrictions may results in delaying the acquisition and an appropriate action should be taken to overcome these restrictions.

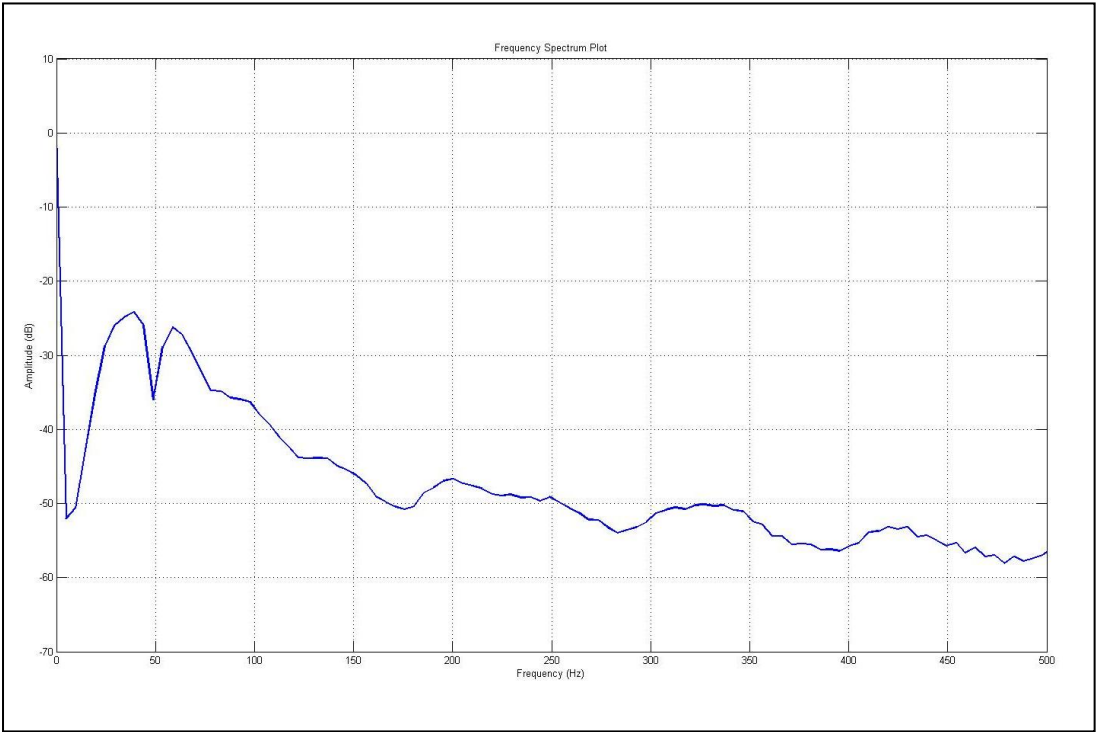
From all of the above tests, designing optimum parameters for seismic acquisition in urban area is very important. As a conclusion, single geophone array, aluminium plate, analogue trigger and 48-channel seismograph system are the best parameters to be used in this research. The parameters used are low in cost and the seismic signals obtain from the seismic acquisition phase are good. The equipment test result is listed in Table 4.3.

Table 4.3: Equipment test result.

Type	24-channel	48-channel
Data Quality	Good	Very Good
Visibility of the first signal	Good	Very Good
Capability to help speeding the acquisition	Yes	Yes

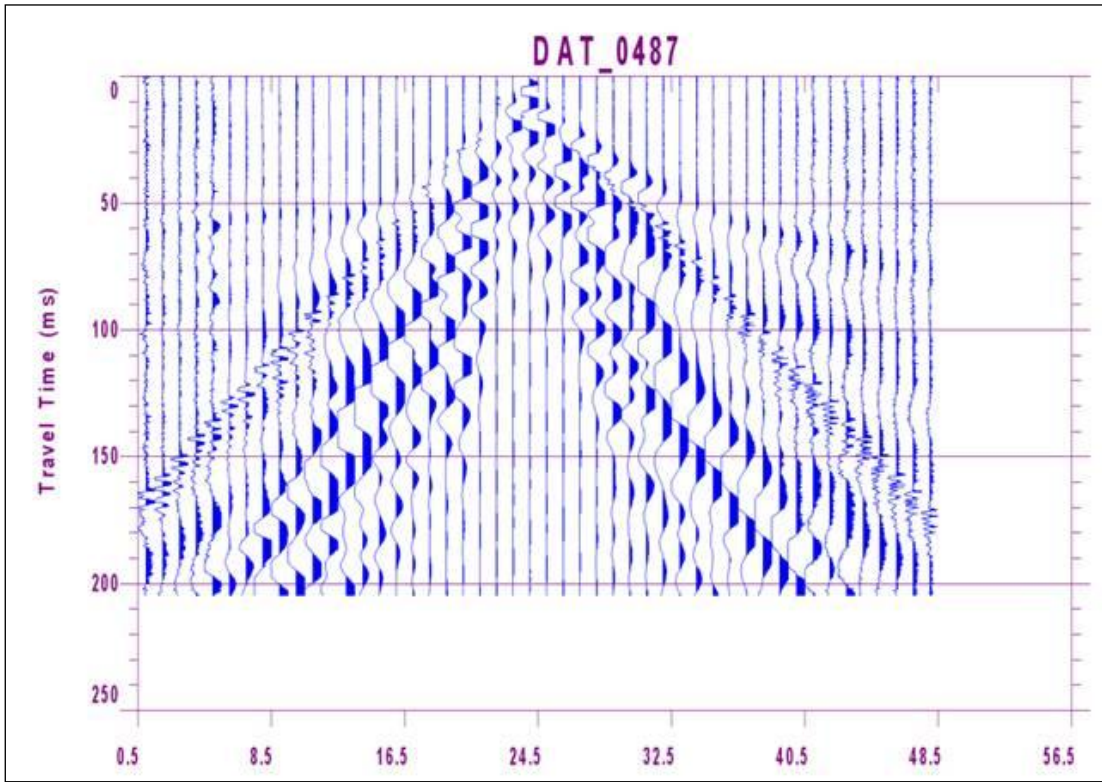


(a)

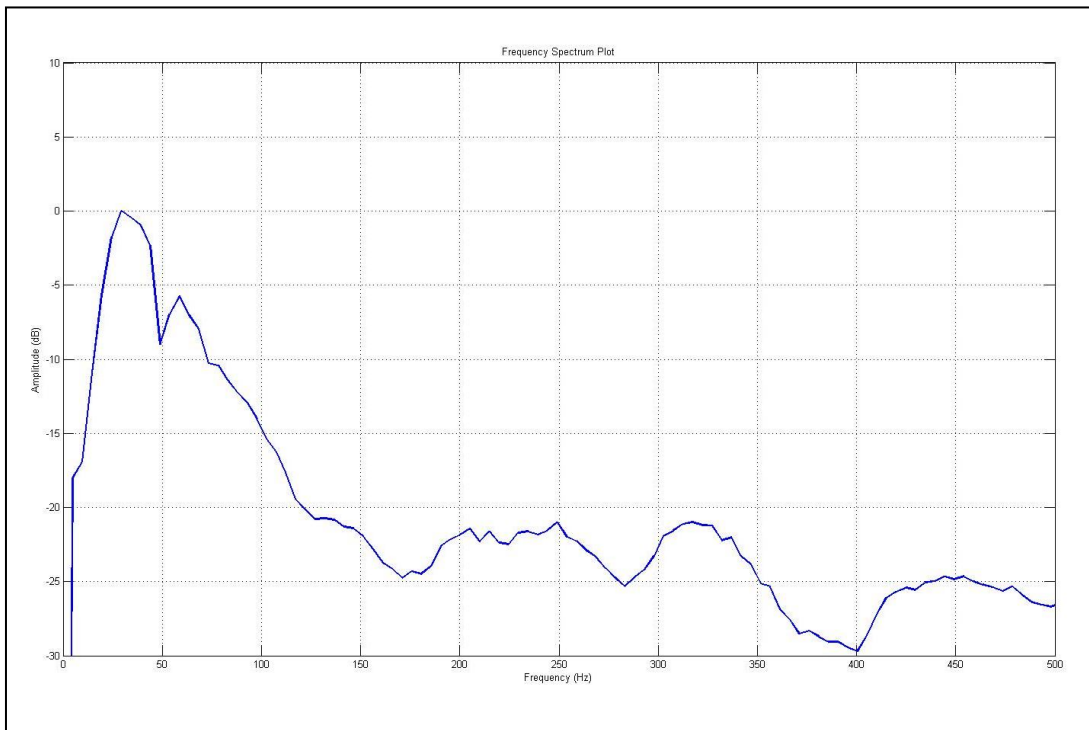


(b)

Figure 4.8: (a) 24 channel seismograph seismic record (b) Frequency spectrum.



(a)



(b)

Figure 4.9: (a) 48 channel seismograph seismic record (b) Frequency spectrum.

### 4.3 Normal Processing Cycle

The seismic lines acquired were processed and interpreted using commercial software, IXRefrax. Before the computerized processing is done, the manual picking of first break is done manually for every shot record. The manual picking will use to assist during the computerized picking using the software.

The data were interpreted separately for each line. The data were imported to the software and the first break picking is done. The software can help to generate 2D inverted model and GRM interpreted depth. The velocity for each layer of the subsurface and depth to the refractor was obtain for each seismic survey lines from both model.

The 2D inverted model will give information on velocity of first layer, velocity of second layer, depth and elevation of the subsurface. The GRM interpreted depth in the other hand will give information on velocity of first layer, velocity of second layer, depth, elevation and time taken to travel along the subsurface to the refractor depth.

Two different seismic line, line number 3 and line number 47 were use as the example. Figure 4.10 and Figure 4.11 shows model of seismic line number 3 interpret using the software. Figure 4.10 is corresponding to GRM interpreted depth model. It shows the depth model of the seismic refractor in GRM interpretation method. The information given including velocity of first layer, velocity of second layer, depth, elevation and time depth to the refractor.

The velocity of first layer is ranging from 401.2 m/s to 510.8 m/s and 1546.2 m/s to 2274.5 m/s for second layer. The depth to refractor is in between 7.7 meters to 12.8 meters below the subsurface. The time to the refractor in time unit is vary from 15.2 millisecond to 26 millisecond.

Figure 4.11 is corresponding to 2D inverted depth model. Velocity of first layer, velocity of second layer, depth and elevation to the refractor can be obtained from this model. The velocity of first layer is 424.1 m/s and the velocity value for second layer is 1712.7 m/s. The depth to the refractor is ranging from 5.6 meters to 11.2 meters below the subsurface.

This seismic line has a good seismic signal record and the first break picking is easy as the first break is clearly visible on the recorded data. From the fitting, the manual picking noted in square box is matching well with the computer picking. The record for every shot position is shown in Figure 4.14 to Figure 4.19.

Figure 4.12 is corresponding to GRM interpreted depth model and Figure 4.13 corresponding to 2D inverted depth model for seismic line number 47. For GRM interpreted depth model, the velocity for first layer is ranging from 487.6 m/s to 609.8 m/s and ranging from 1540.5 m/s to 2117.8 m/s for second layer. The depth to refractor is ranging from 8.5 meters to 12.2 meters below the subsurface with time to the refractor in time unit varying from 15.4 millisecond to 22.7 millisecond.

For the 2D inverted depth model, the velocity for first layer is 512.3 m/s and the velocity for second layer is 2095.9 m/s. The depth to the refractor is ranging from 7.3 meters to 12.3 meters below the subsurface. The fitting of first break picking for both models are showing differences between the manual picking and computerized picking.

The records for each shot position of seismic line number 47 are shown in Figure 4.20 to Figure 4.25. From these figures, the noise contamination of this seismic lines is higher, thus make the picking of first break difficult to be done confidently. A new proposed technique of noise reduction will be discussed in the next section in order to get better seismic signals which focuses on the first break picking.

Good results were obtained from some of the data after undergoing the normal processing phase. Some of the data shows error which is expected to comes from poorly picking of the first break due to the bad trace which contaminated with noise. A new approached to remove and minimize this bad trace is developed. With this new developed technique, it is hope that the new result of the data will be better and less noise contamination in the data is present.

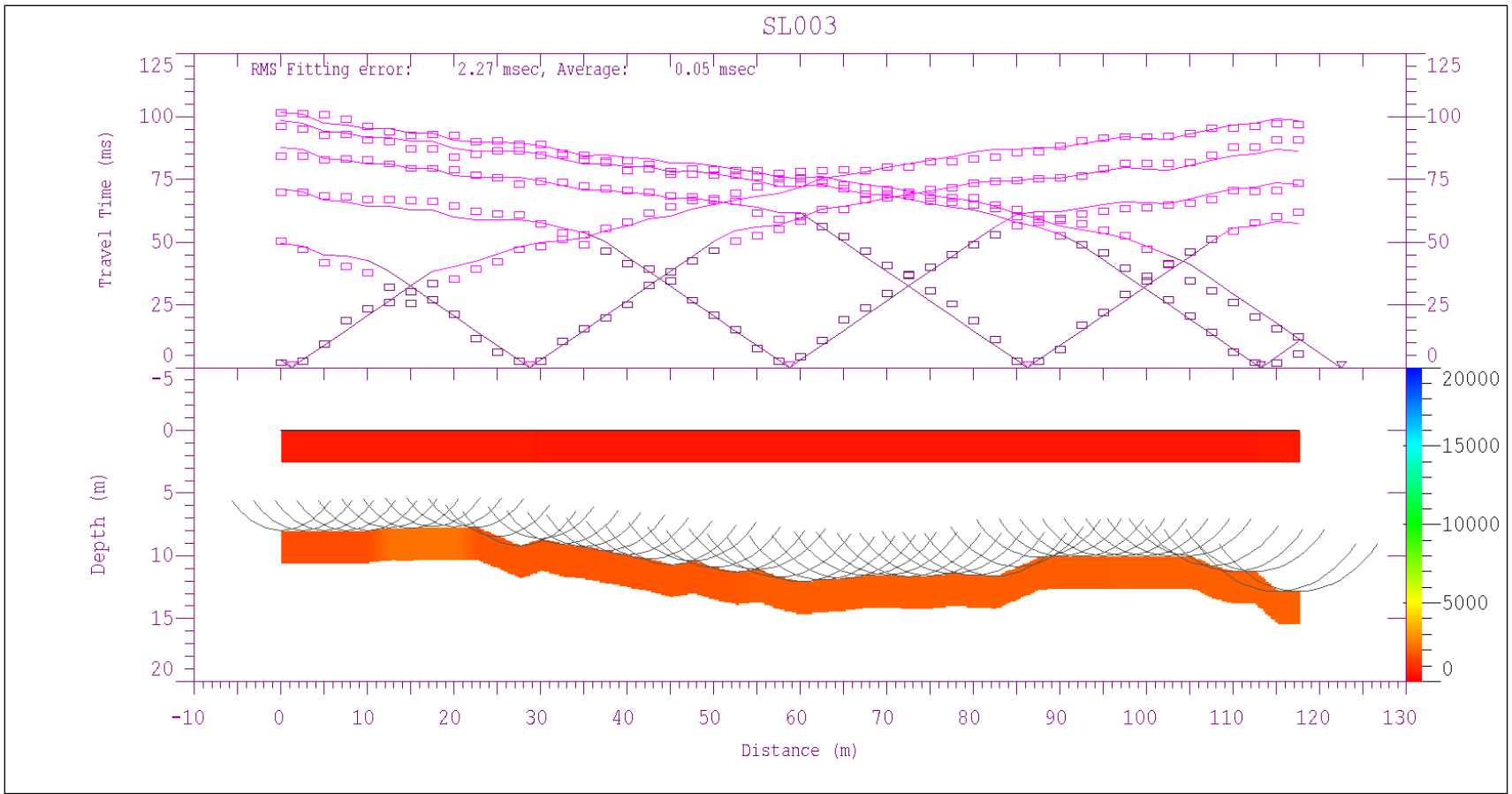


Figure 4.10 : GRM interpreted depth model for line 3.

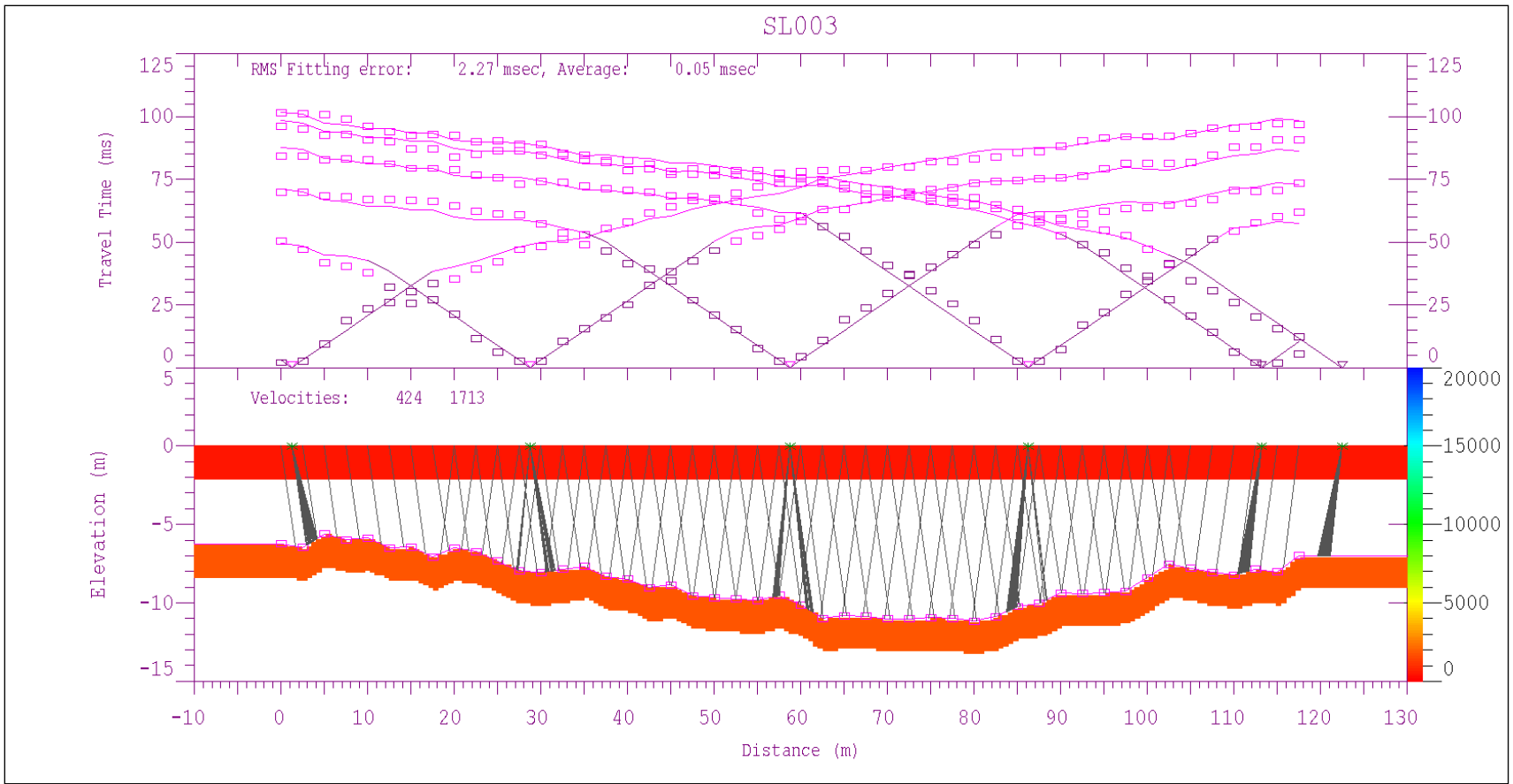


Figure 4.11 : 2D inverted model for line 3.

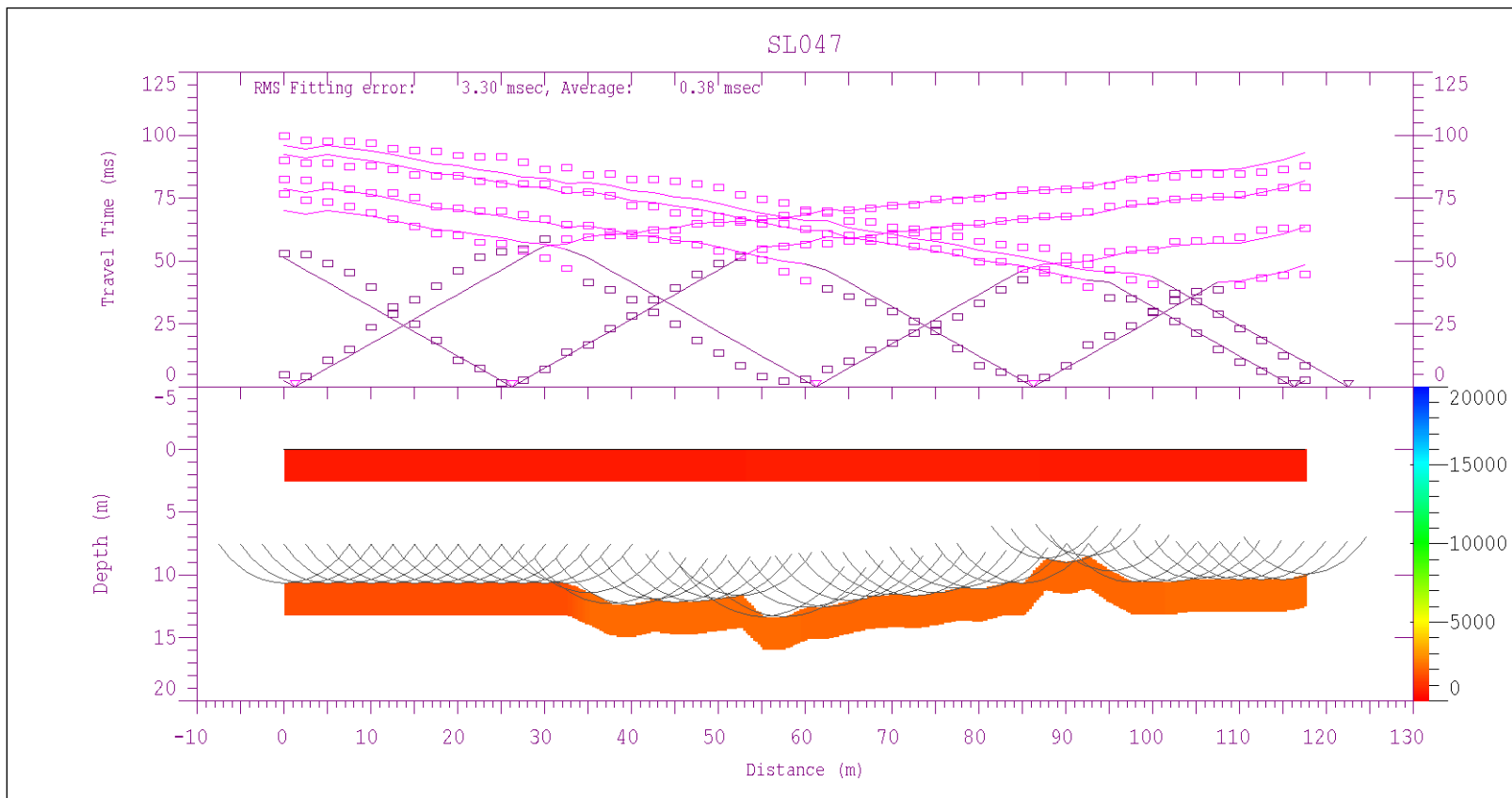


Figure 4.12: GRM interpreted depth model for line 47.

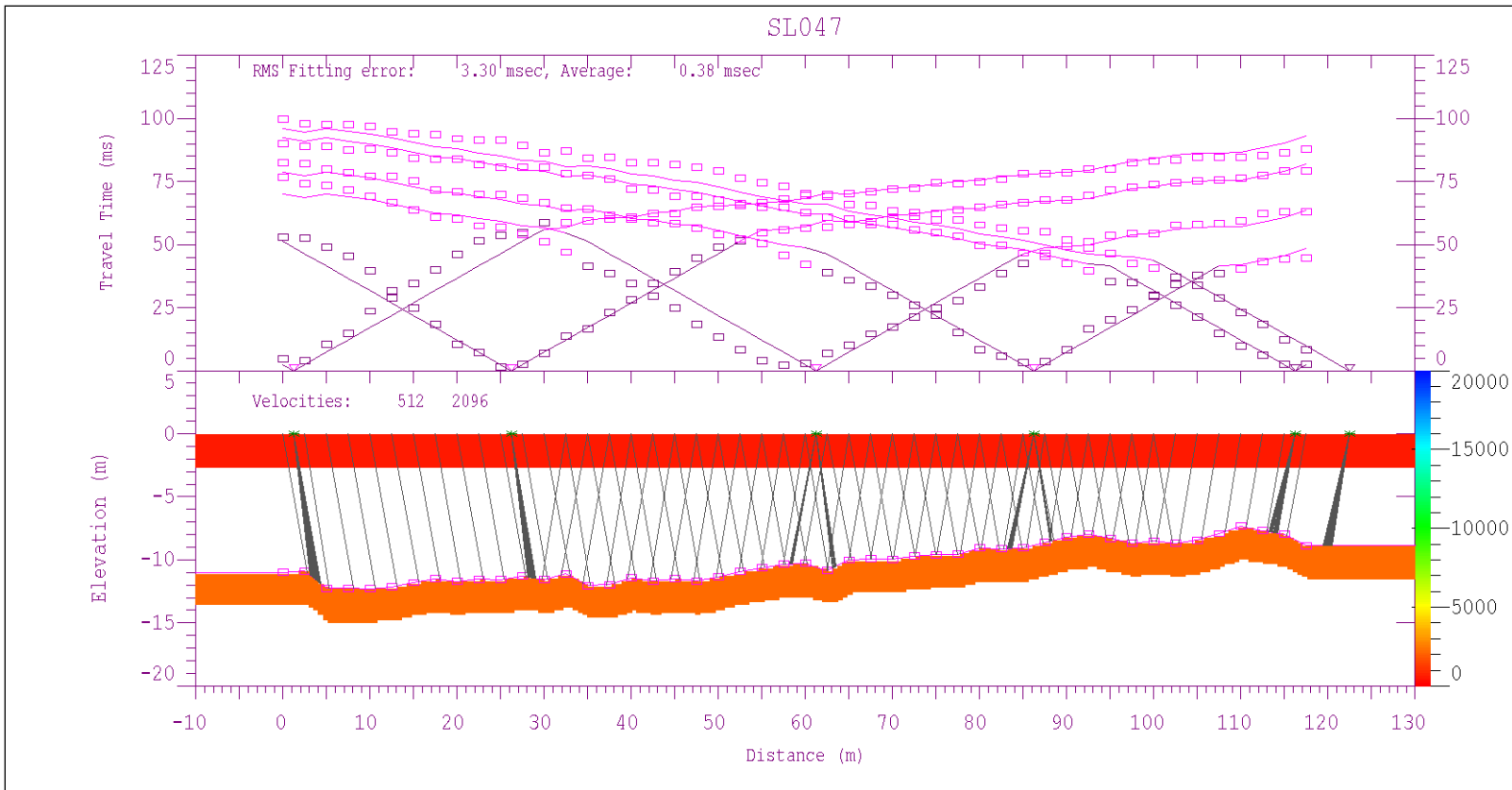


Figure 4.13 : 2D inverted model for line 47.

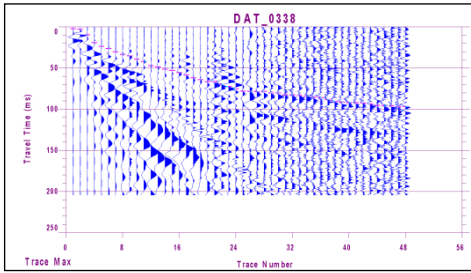


Figure 4.14: Shot point 1 in between geophone 1 and 2 for seismic line 3.

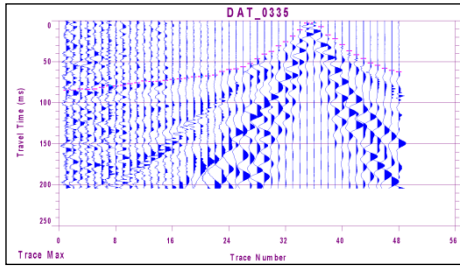


Figure 4. 15 : Shot point 4 in between geophone 35 and 36 for seismic line 3.

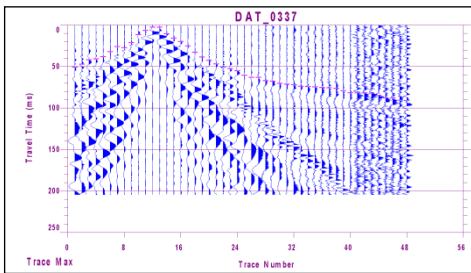


Figure 4.16: Shot point 2 in between geophone 12 and 13 for seismic line 3.

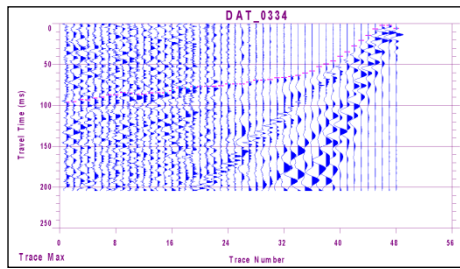


Figure 4. 17 : Shot point 5 in between geophone 46 and 47 for seismic line 3.

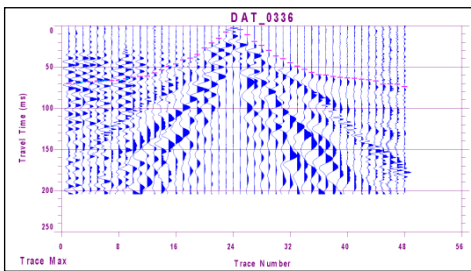


Figure 4. 18: Shot point 3 in between geophone 24 and 25 for seismic line 3.

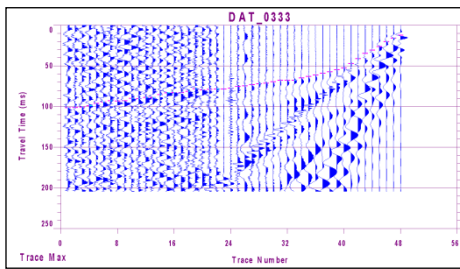


Figure 4.19 : Shot point 6 at 5 meters away from geophone 48 for seismic line 3.

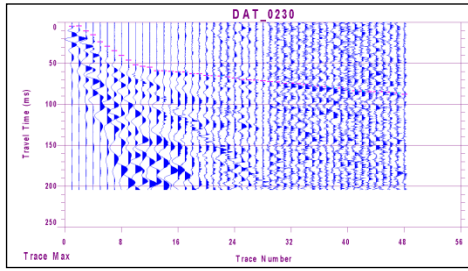


Figure 4.20 : Shot point 1 in between geophone 1 and 2 for seismic line 47.

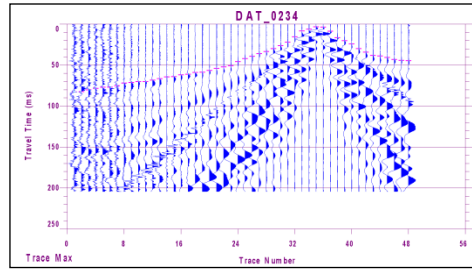


Figure 4.21: Shot point 4 in between geophone 35 and 36 for seismic line 47.

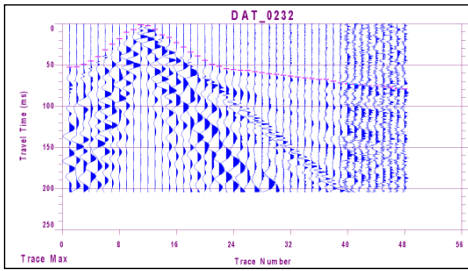


Figure 4.22 : Shot point 2 in between geophone 11 and 12 for seismic line 47.

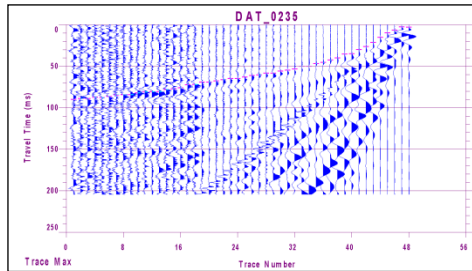


Figure 4.23 : Shot point 5 in between geophone 47 and 48 for seismic line 47.

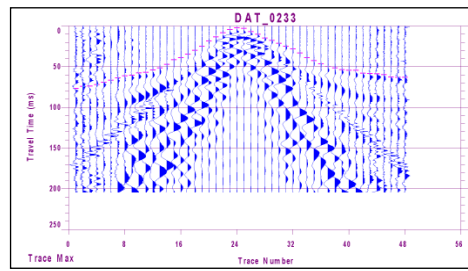


Figure 4.24 : Shot point 3 in between geophone 25 and 26 for seismic line 47.

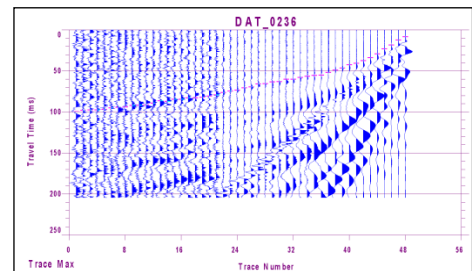


Figure 4.25 : Shot point 6 at 5 meters away from geophone 48 for seismic line 47.

## **4.4 Advanced Data Improvement**

Three different techniques were developed and the result of each developed techniques was compared. The first arriving signal or known as first break arrival is the most important signal in seismic refraction survey. Therefore, the development of the new technique is focusing on the enhancement of these signals. The techniques developed are subtraction technique, addition technique and frequency scaling technique.

### **4.4.1 Subtraction Technique and Addition Technique**

Figure 4.26 and Figure 4.27 show the recorded data and noisy data at that particular shot point respectively before any data enhancement application. The GRM interpreted depth model and 2D inverted depth model for this seismic line, line number 35 is shown by Figure 4.28 and Figure 4.29. From these models, the RMS fitting error is 2.02 millisecond and the average error is 0.07 millisecond. Figure 4.30 shows the product of seismic record after applying the subtraction technique. Figure 4.31 in the other hand shows the seismic record after applying the addition technique. The GRM interpreted depth model and 2D inverted depth modeling for both are shown in Figure 4.32 and Figure 4.33.

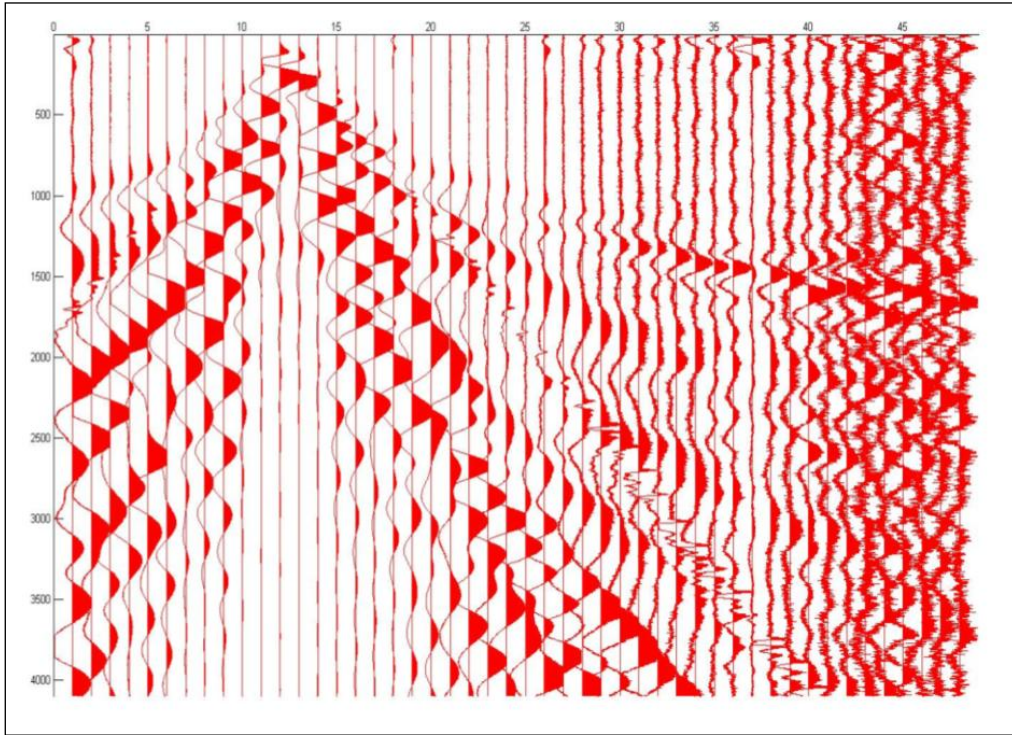
After the application of subtraction technique, the RMS fitting error is reduced to 0.92 millisecond and the average error is 0.03 millisecond compared to the value of the same error before the application. These values were obtained after the processing by the software using the new seismic record after applying the subtraction technique. The visualize view (Figure 4.30) from the traces obtain after the application are noisier in between geophone number 40 and 48 when compared to the original traces (Figure 4.26) before the application. It is also hard to see the first break signal, thus making it difficult to do the first break picking.

The addition technique on the other hand gives clearer seismic traces after the application of the technique in between geophone number 40 and 48 when compared to the subtraction technique as shown in Figure 4.31. RMS fitting error and average error for this technique is 0.70 millisecond and 0.22 millisecond respectively. The first break signals is clearly visible and make it easier to do the first break picking

compared to the same on the subtraction technique seismic traces. Table 4.4 shows the RMS fitting error value and average error value for original data and after the application of subtraction and addition technique.

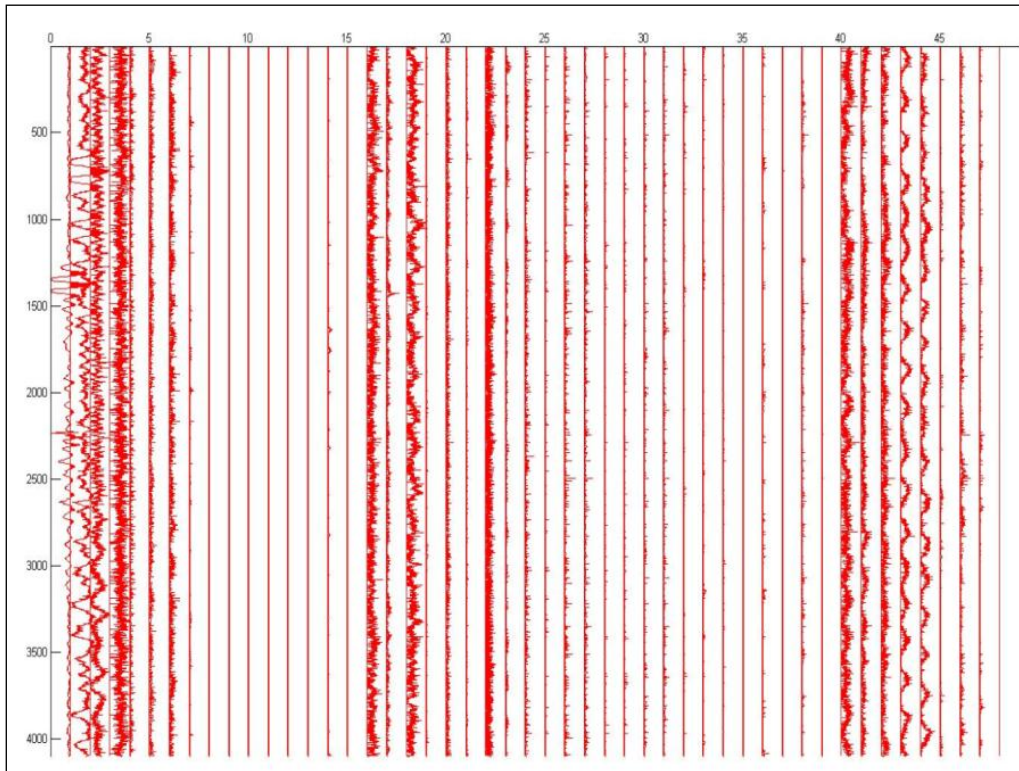
Table 4.4: RMS fitting error and average error values for original data and after application of subtraction and addition technique.

Traces number	RMS fitting error value (msec)	Average error value (msec)
Original	2.02	0.07
Subtraction	0.7	0.02
Addition	1.18	0.01



(a)

Figure 4.26: Recorded seismic signal data at shot point 2 for seismic line number 35.



(b)

Figure 4.27: Recorded noisy data at shot point 2 for seismic line number 35.

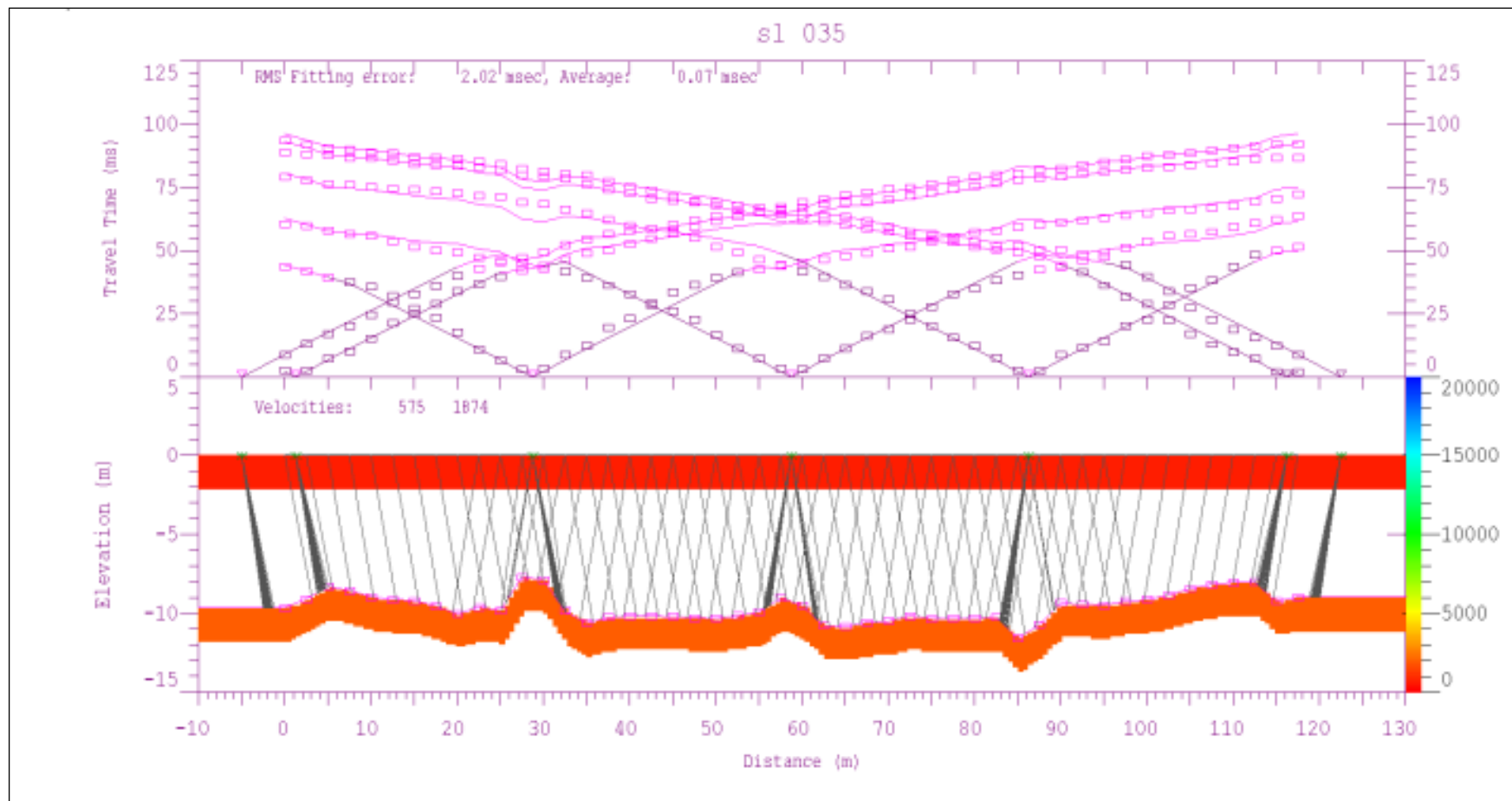


Figure 4.28: 2D inverted model for seismic line number 35.

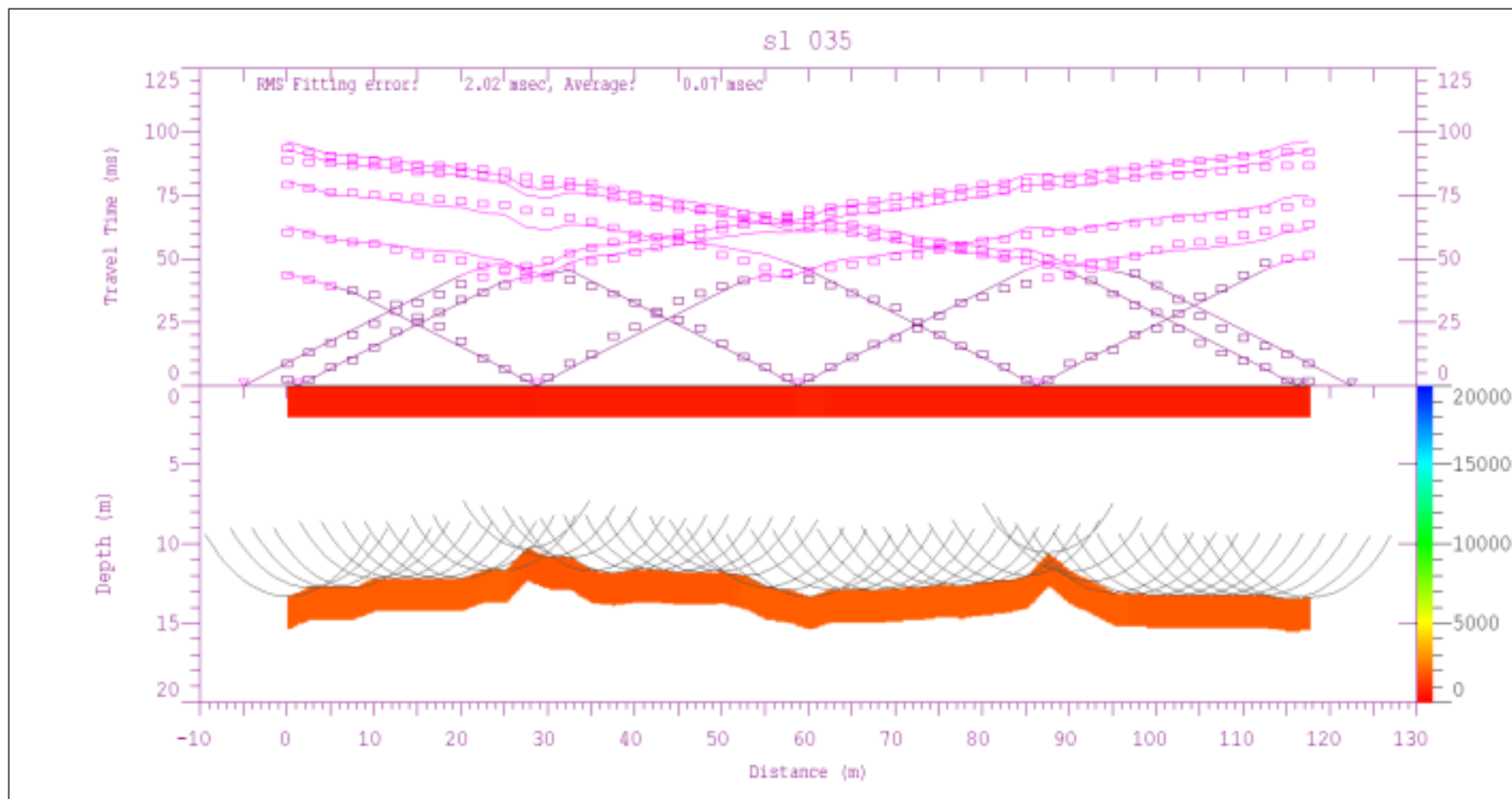
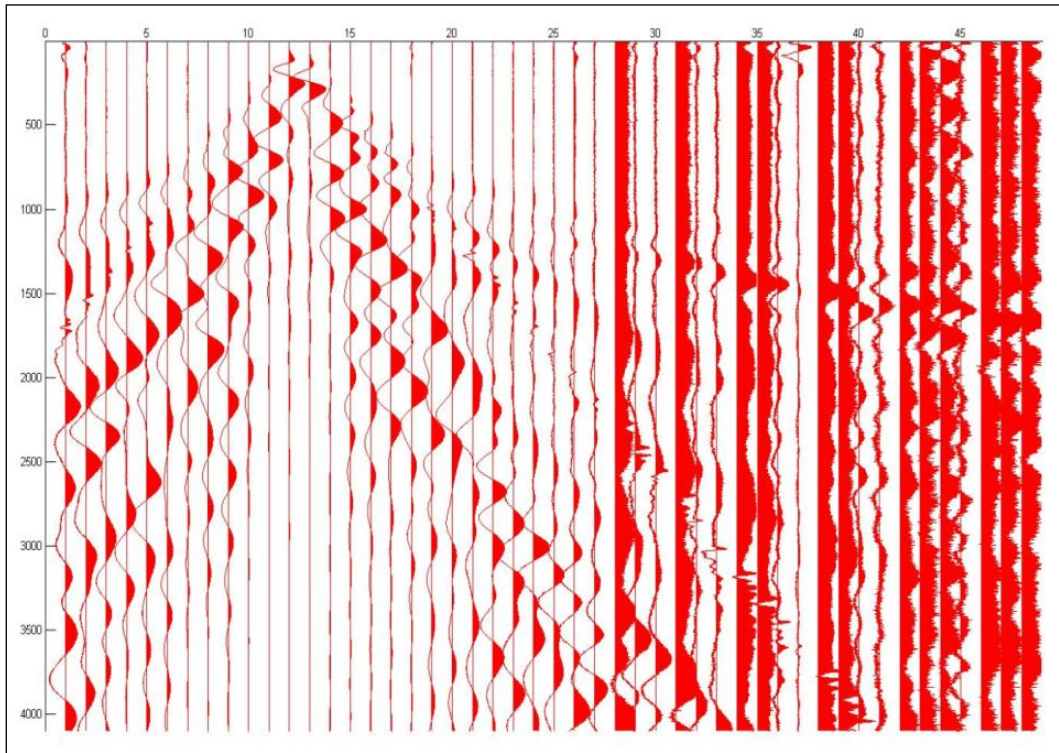
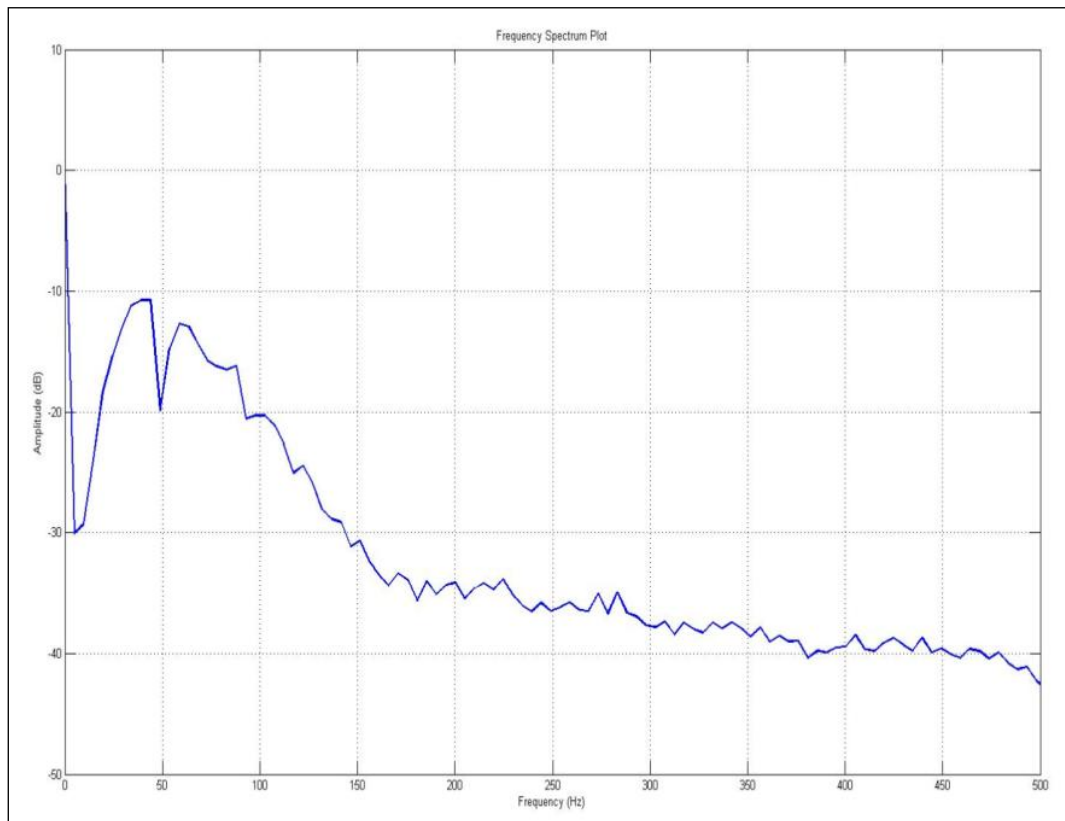


Figure 4.29: GRM interpreted depth model for seismic line number 35.

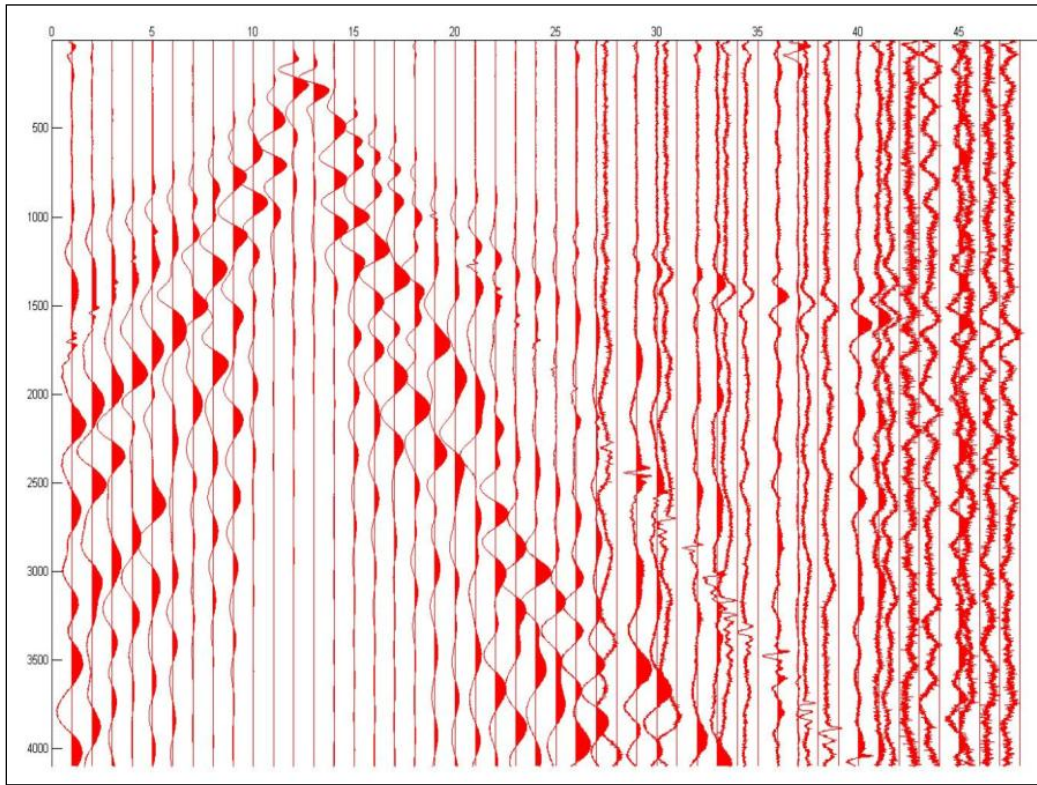


(a)

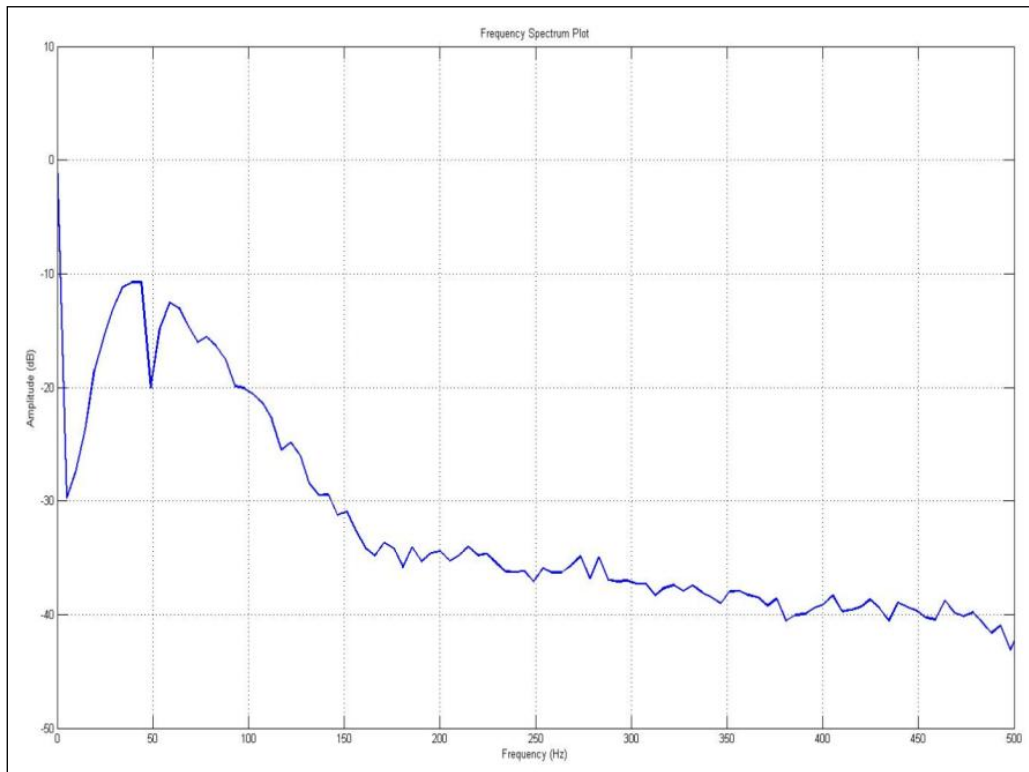


(b)

Figure 4.30: (a) Shot point record after subtraction technique (b) Spectrum plot.



(a)



(b)

Figure 4.31: (a) Shot point record after addition technique (b) Spectrum plot.

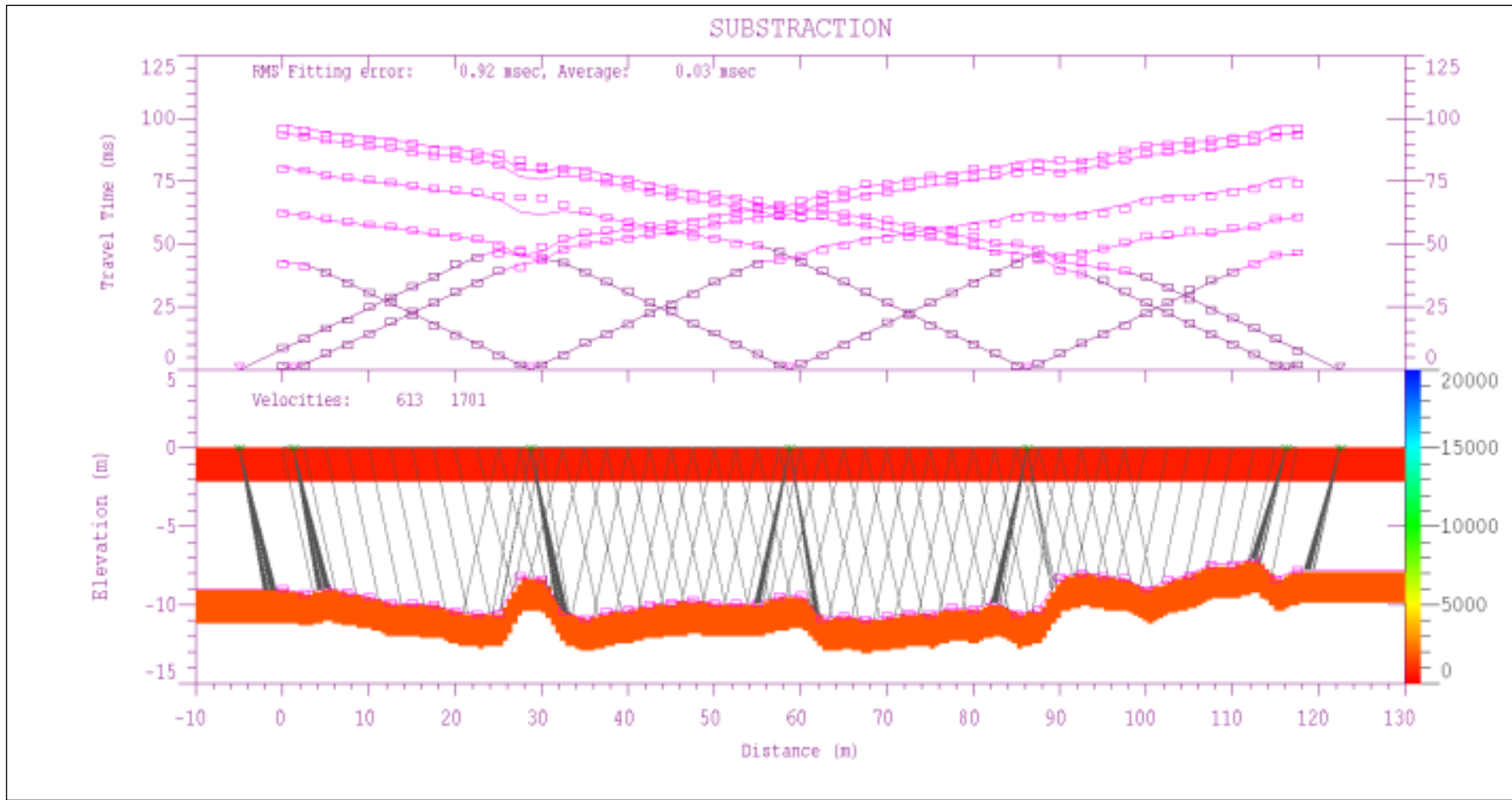


Figure 4.32: 2D inverted model after subtraction technique.

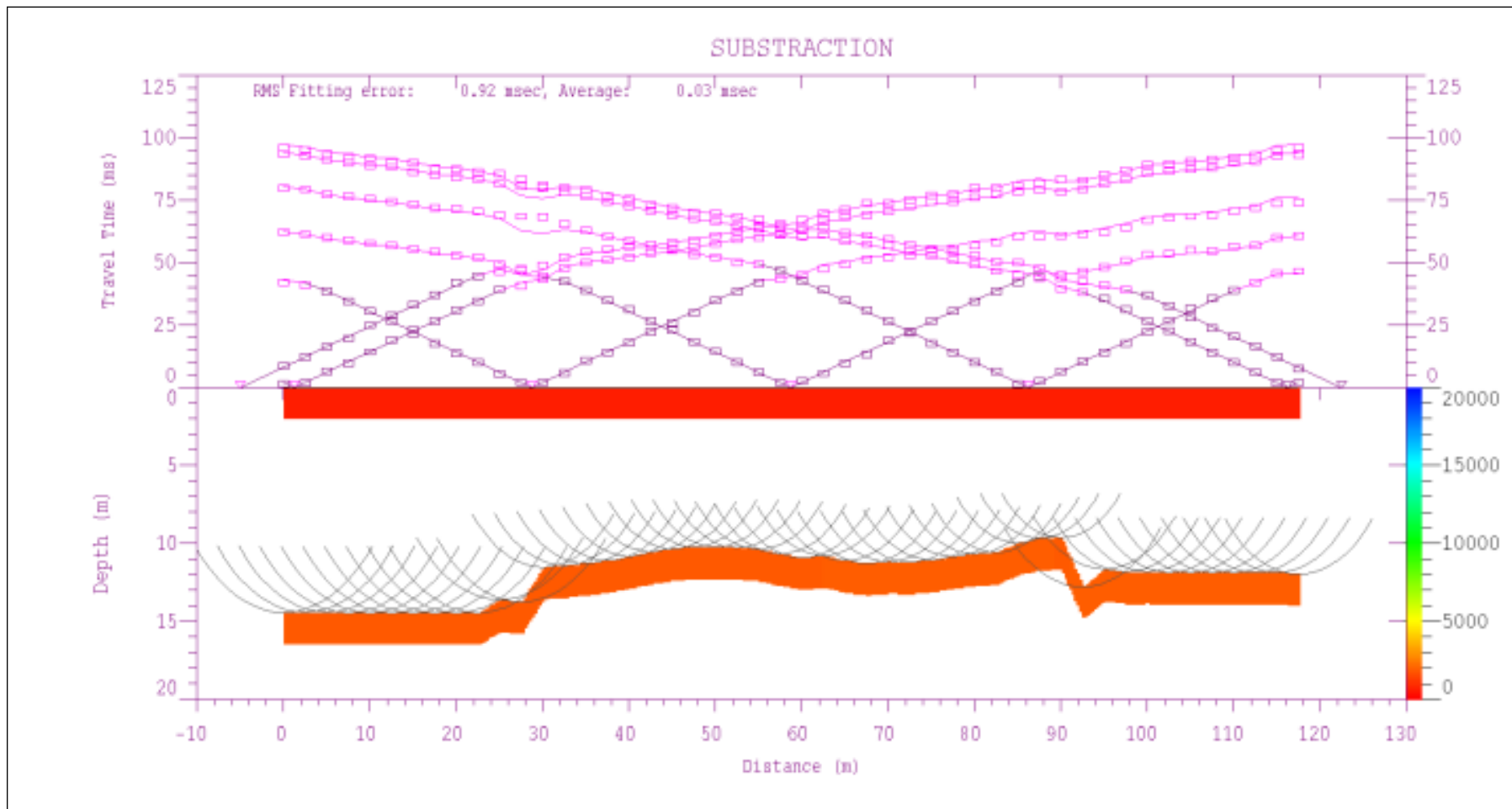


Figure 4.33: GRM interpreted depth model after subtraction technique.

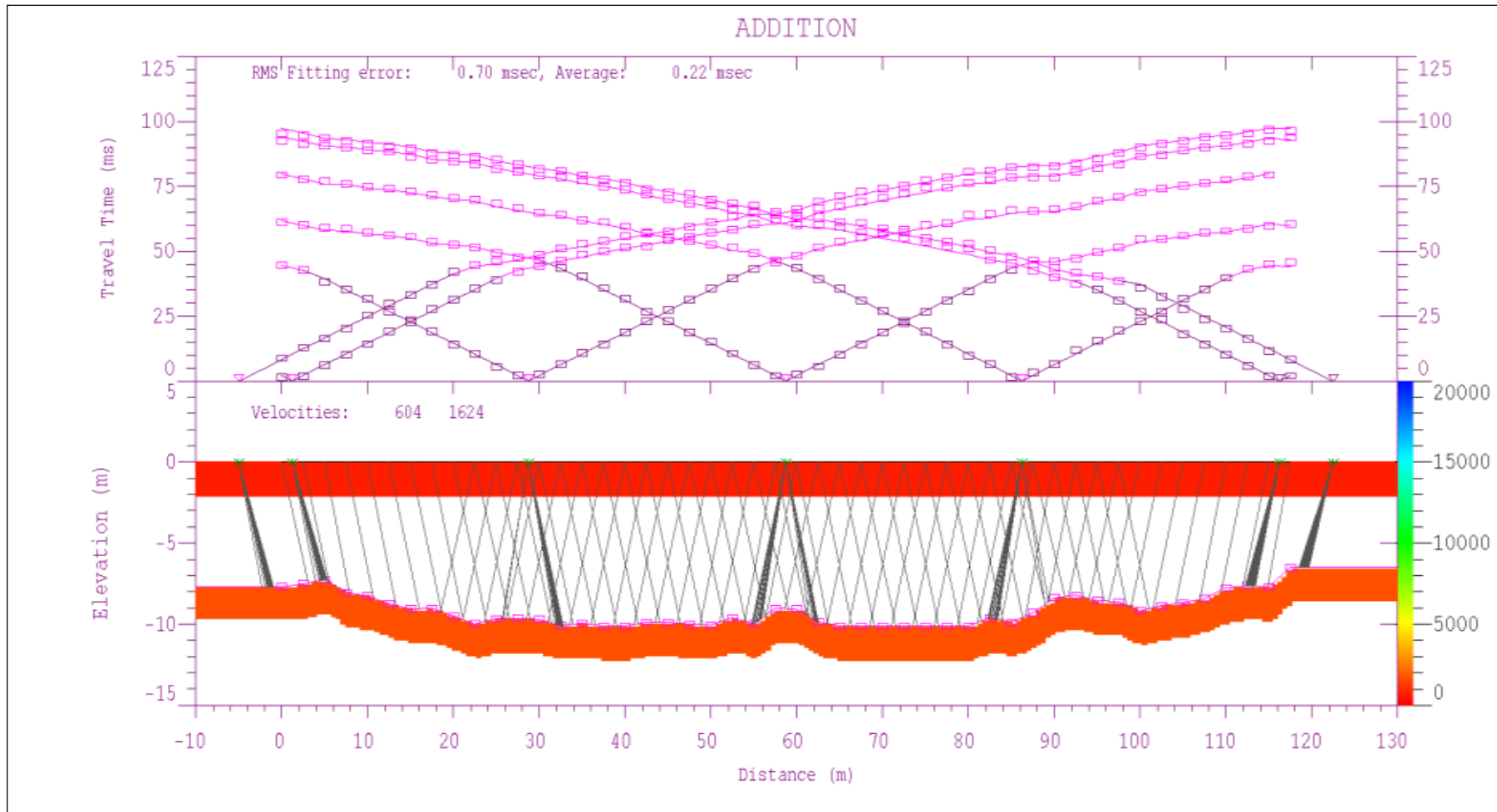


Figure 4.34: 2D inverted model after addition technique.

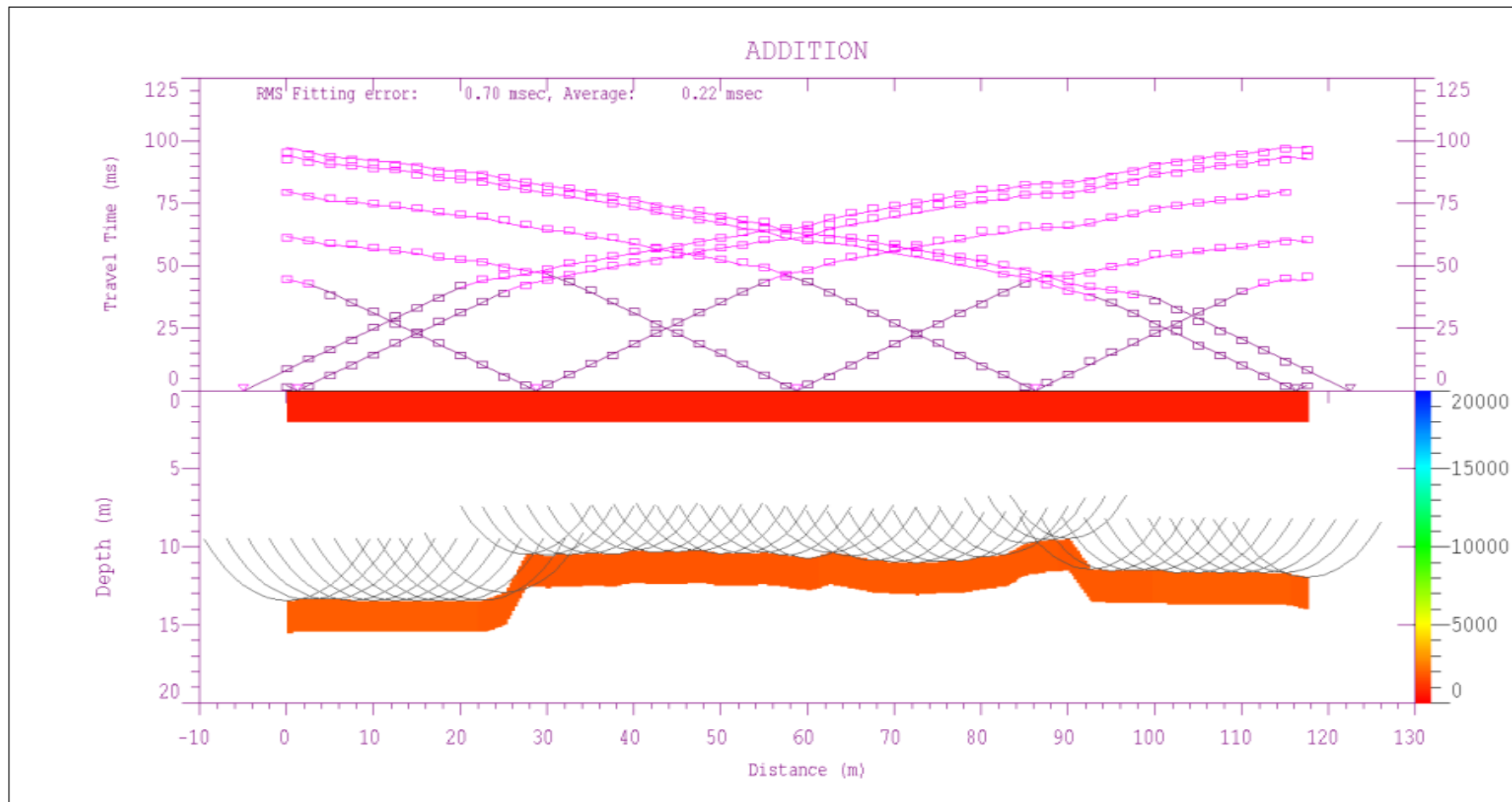


Figure 4.35: GRM interpreted depth model after addition technique.

#### 4.4.2 Frequency Scaling Technique

Seismic line number 35 was used as the example in this discussion. The shot record involved is shown in Figure 4.26. From the seismic trace, we can see that the noisy part is more dominant in between geophone number 40 and geophone number 48. The treatment is done using the MatLab algorithm developed (Appendix A) with trace number 40 to 48 used as the noisy trace for each time of treatment in turn. The seismic record after applying each traces as the noisy trace will be use later in the next step of this technique.

The differences between original RMS fitting error and average error and the selected noisy traces are ranging from 0.62 to 1.29. These values were obtained from the software processing via GRM interpreted depth model. The lowest and highest difference is by using trace number 43 and trace number 47 respectively as the noisy trace. Trace number 42 and 45 are giving the same medium different value when used as the noisy trace.

Figure 4.36 (a) shows the seismic traces after frequency scaling technique using trace number 43 as the noisy trace. For the noisy traces, trace number 40 to trace number 48, we can see the reduction of noise in those trace after applying trace number 43 as the noisy trace. The noise above the first break signals also reduced. Software processing then carried out again, using the seismic trace after applying trace number 43 as the noisy trace. The 2D inverted model and GRM interpreted model were obtained from this processing. From the 2D inverted model in Figure 4.37 and GRM interpreted depth model in Figure 4.38, the RMS fitting error value of the model is 1.40 and the average error value is 0.03.

The result of using trace number 42 as the noisy trace is shown by Figure 4.39 (a). The noisy traces, trace number 40 to trace number 48 is clearer as the noise on that trace is reduced tremendously and the first break signal is clearly seen. The noise above the first break signals also reduced. The 2D inverted model and GRM interpreted depth model after the software processing using the new seismic record with trace number 42 as the noisy trace is show in Figure 4.40 and Figure 4.41 respectively.

When using seismic trace number 47, the result of 2D inverted model and GRM interpreted depth model is giving medium difference of RMS fitting error value when compared to the other traces after the software processing was carried out. Both of the models are shown in Figure 4.43 and Figure 4.44. The noise at the noisy traces and above the first break signal is reduced.

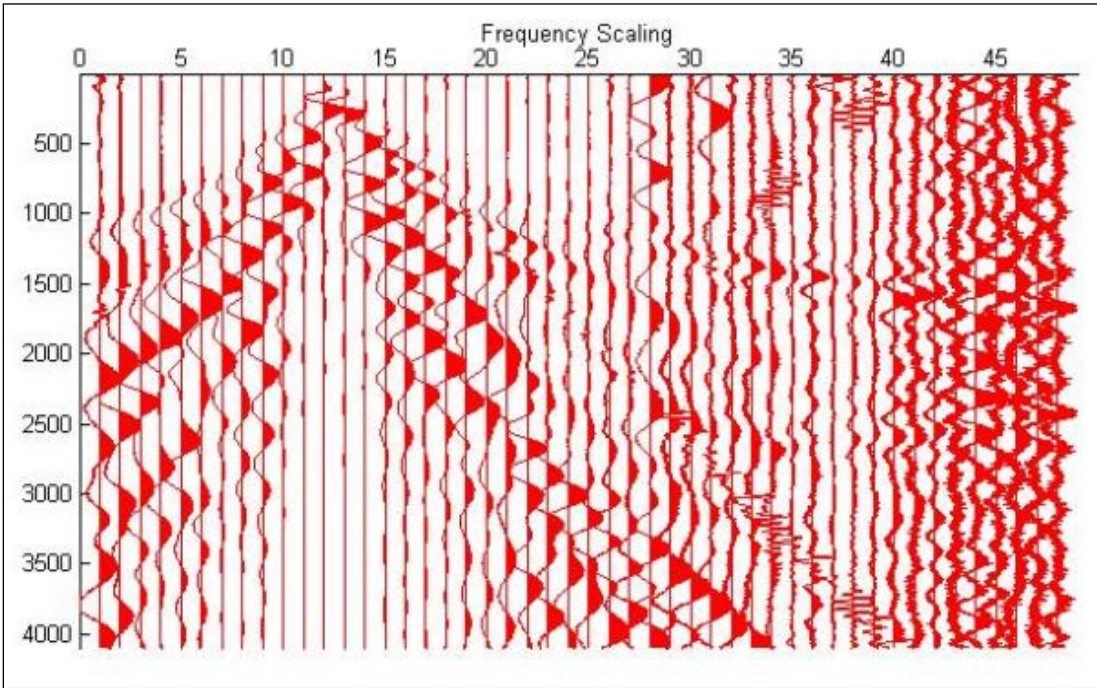
The same procedure is done for the other traces. Each of the traces is giving the same behavior of result. The RMS fitting error value and average value are lesser than the value given by the original data. Table 4.5 shows the RMS fitting error values and average error values given by the original data and after the application of frequency scaling technique to identified noisy trace, trace number 40 to trace number 48.

From this frequency scaling, the RMS fitting error value is reduced with percentage range of 31% to 61% when compared to the original values. The average error value in the other hand is reduced with percentage range of 14% to 129% when compare to the original values.

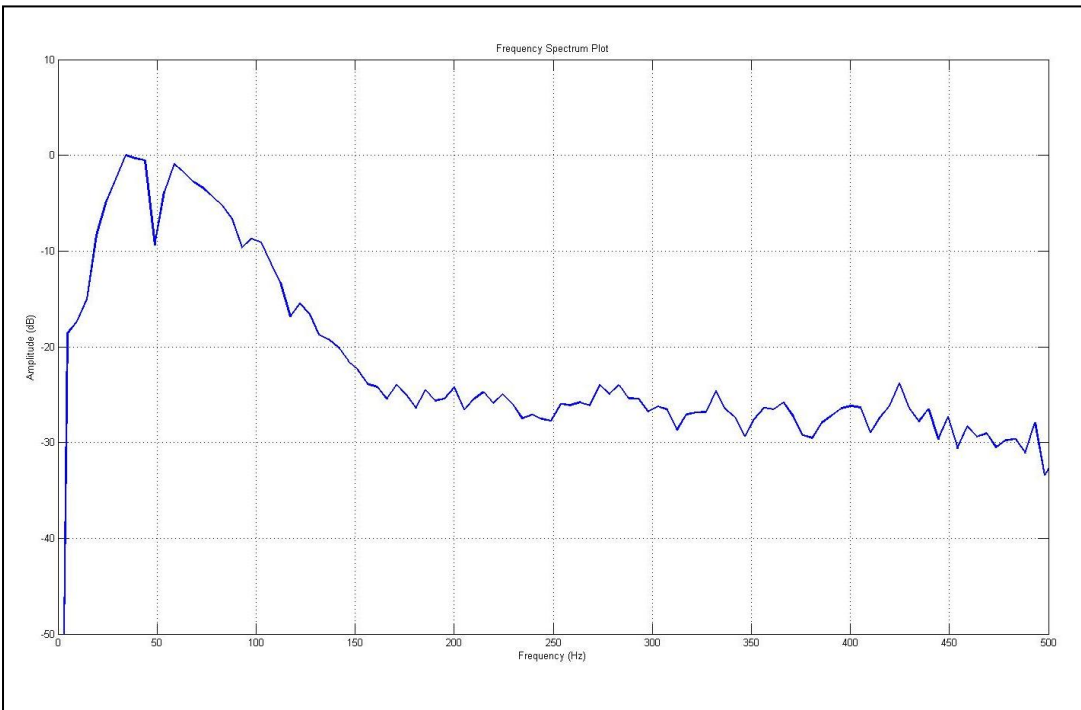
The frequency spectrum plot when using trace number 43, 42 and 47 as the noisy traces is shown in Figure 4.36 (b), Figure 4.39 (b) and Figure 4.42 (b) respectively. From this plot, we can see there are two different peaks which correspond to two different dominant frequencies that appear in this seismic record. The dominant frequency is appeared at 20 Hz to 50Hz and 50 Hz to 90 Hz at amplitude between for amplitude between -10 dB to 0 dB.

Table 4.5: RMS fitting error and average error values for original data and after frequency scaling technique's application.

Traces number	RMS fitting error value	Average error value
Original	2.02	0.07
40	1.09	0.02
41	1.18	0.01
42	1.08	0.0
43	1.40	0.03
44	0.95	0.02
45	1.08	0.02
46	1.27	-0.02
47	0.73	0.06
48	0.78	0.03



(a)



(b)

Figure 4.36: (a) Frequency scaling technique using trace number 43 as the noisy trace

(b) Spectrum plot.

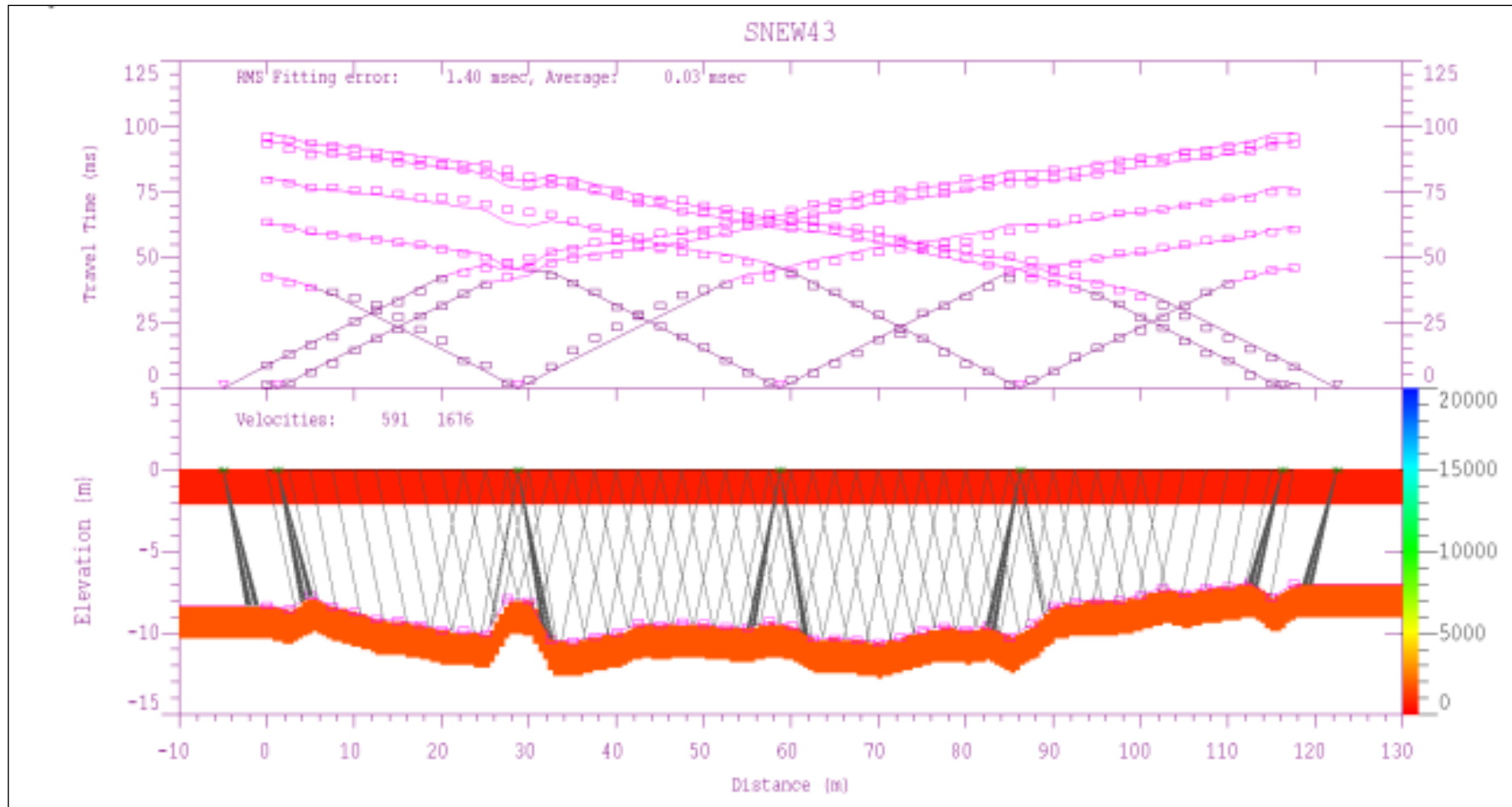


Figure 4.37: 2D inverted model after frequency scaling technique using trace number 43 as noisy trace.

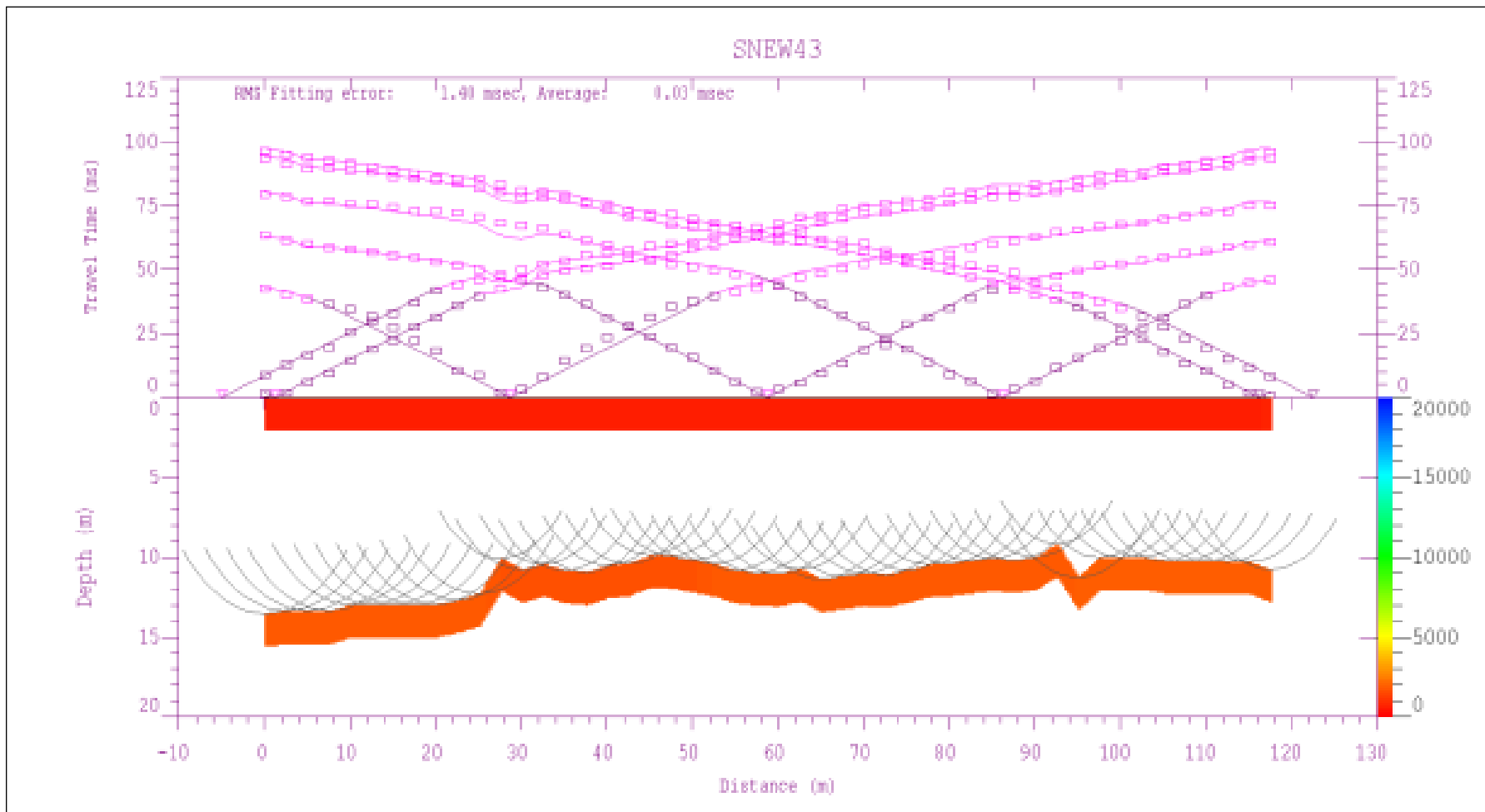
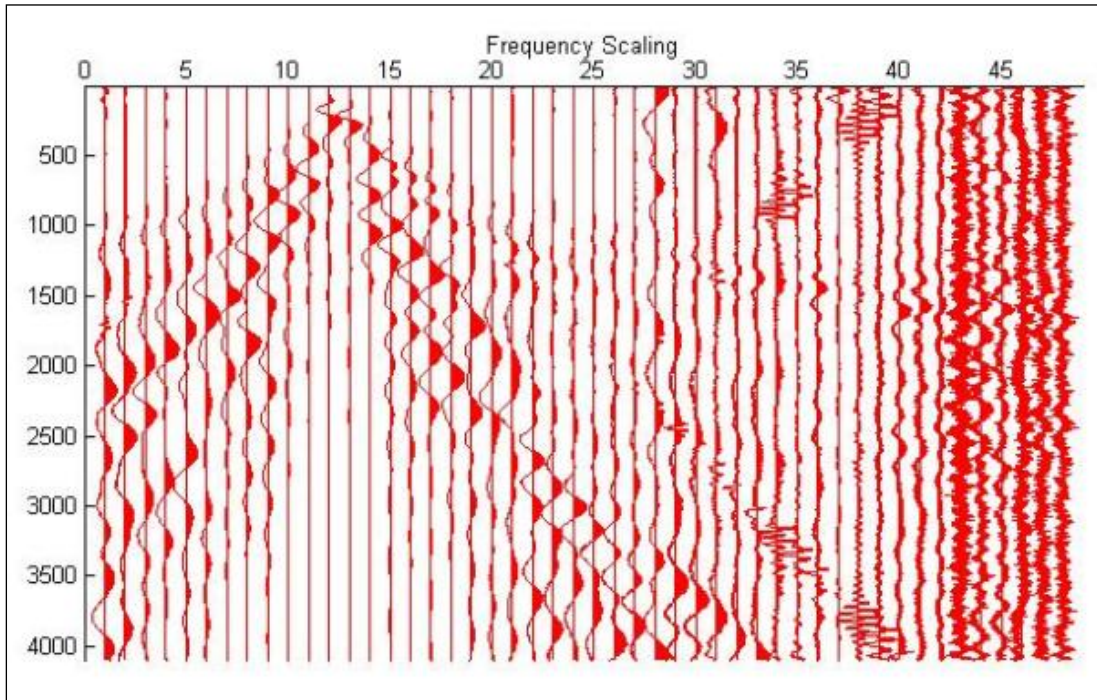
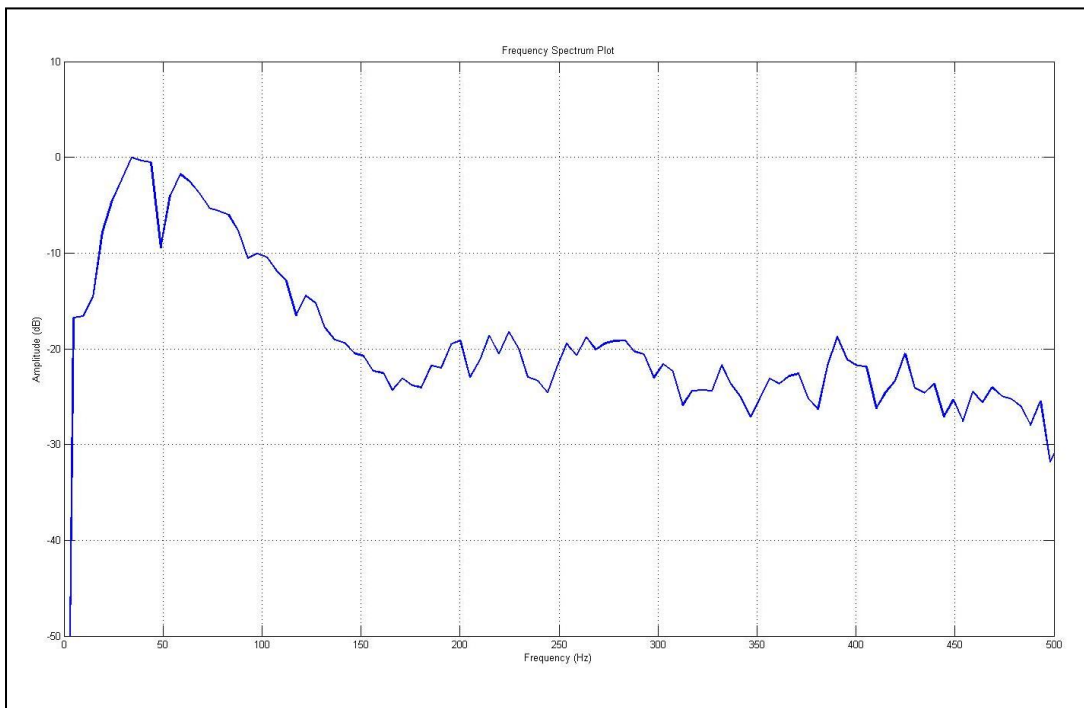


Figure 4.38: GRM interpreted depth model after frequency scaling technique using trace number 43 as noisy trace.



(a)



(b)

Figure 4.39: (a) Frequency scaling technique using trace number 42 as the noisy trace  
 (b) Spectrum plot.

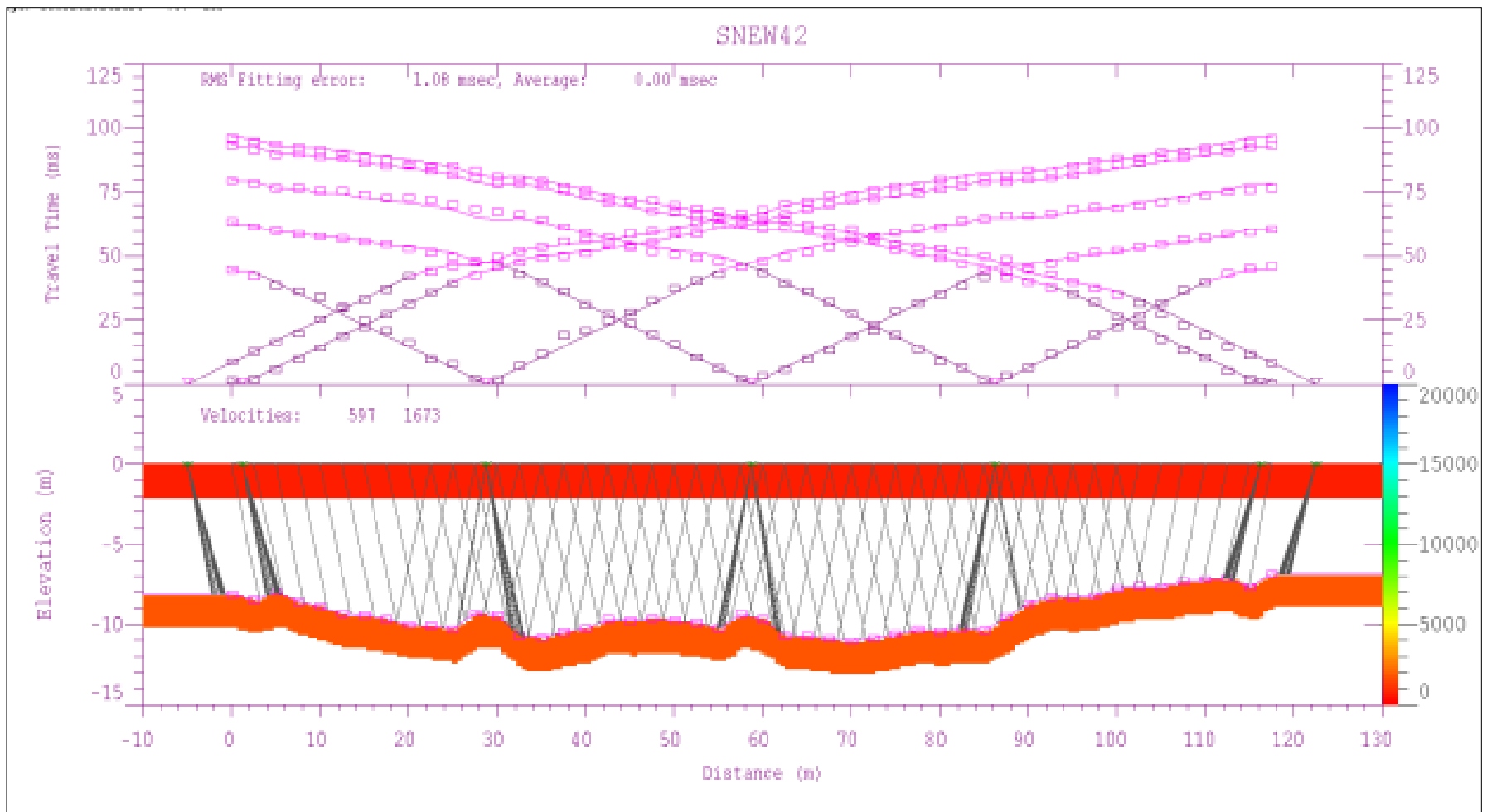


Figure 4.40: 2D inverted model after frequency scaling technique using trace number 42 as noisy trace.

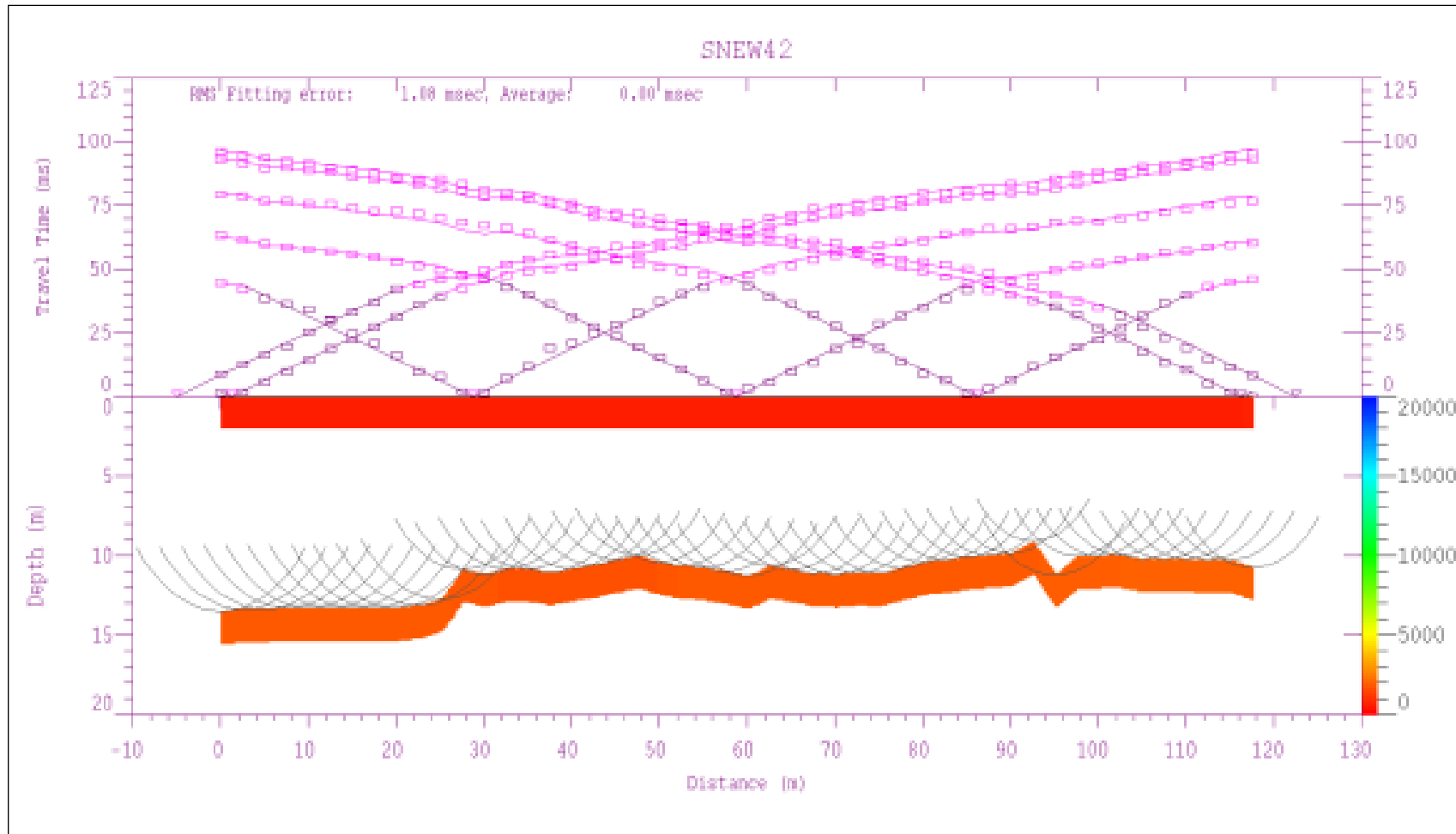
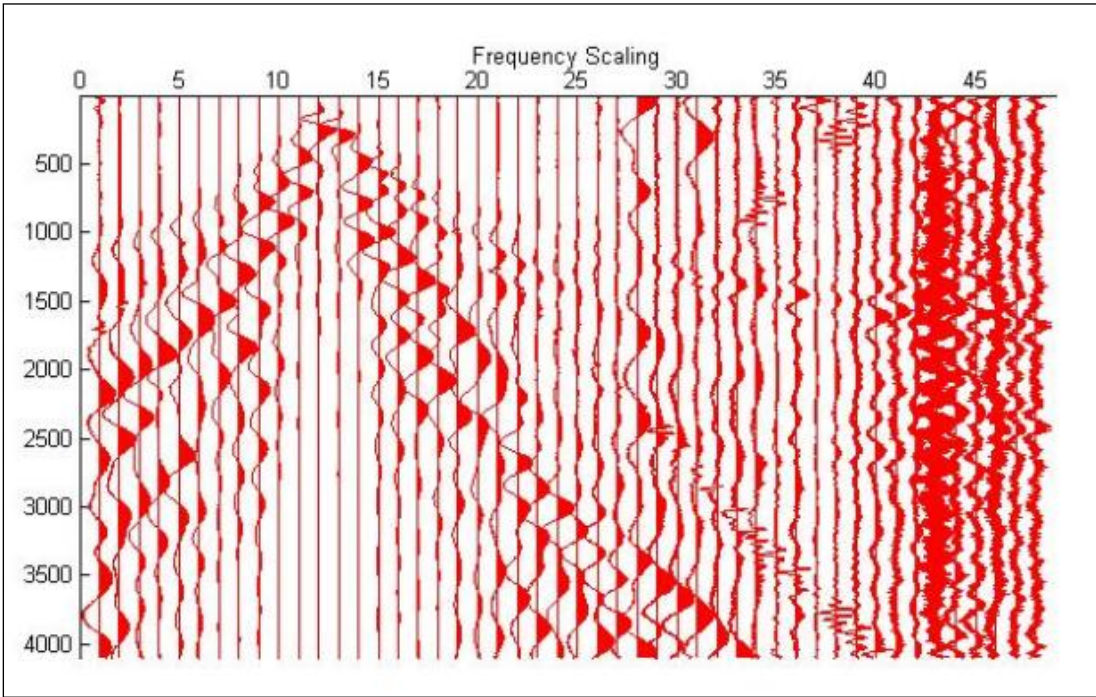
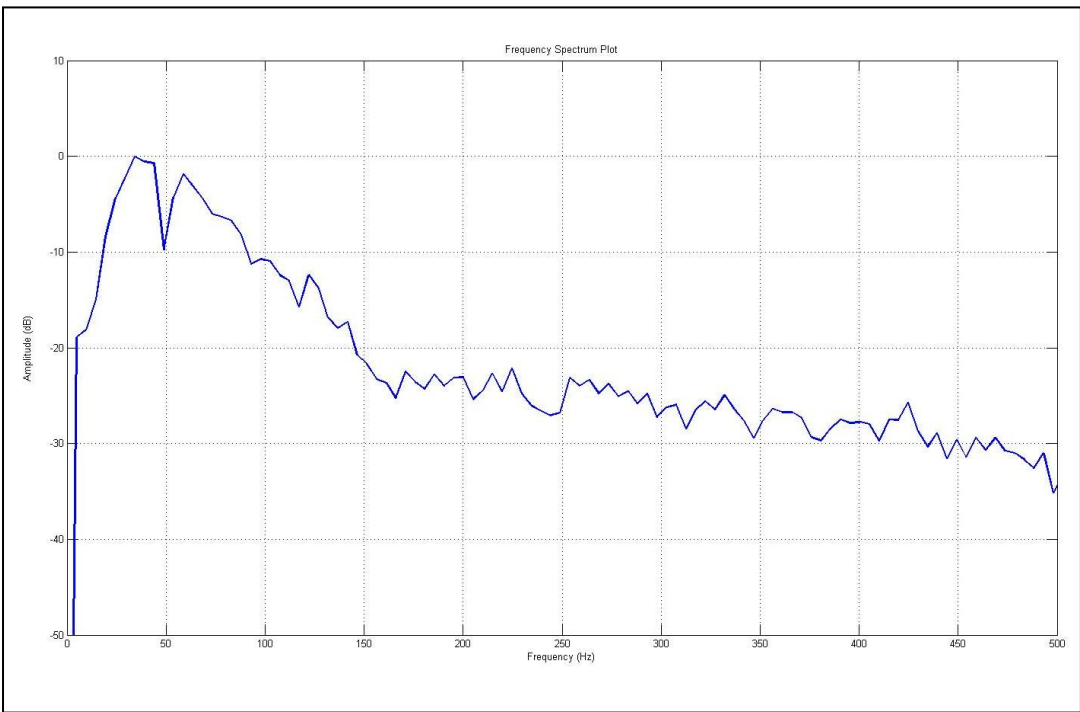


Figure 4.41: GRM interpreted depth model after frequency scaling technique using trace number 42 as noisy trace.



(a)



(b)

Figure 4.42: (a) Frequency scaling technique using trace number 47 as the noisy trace  
(b) Spectrum plot.

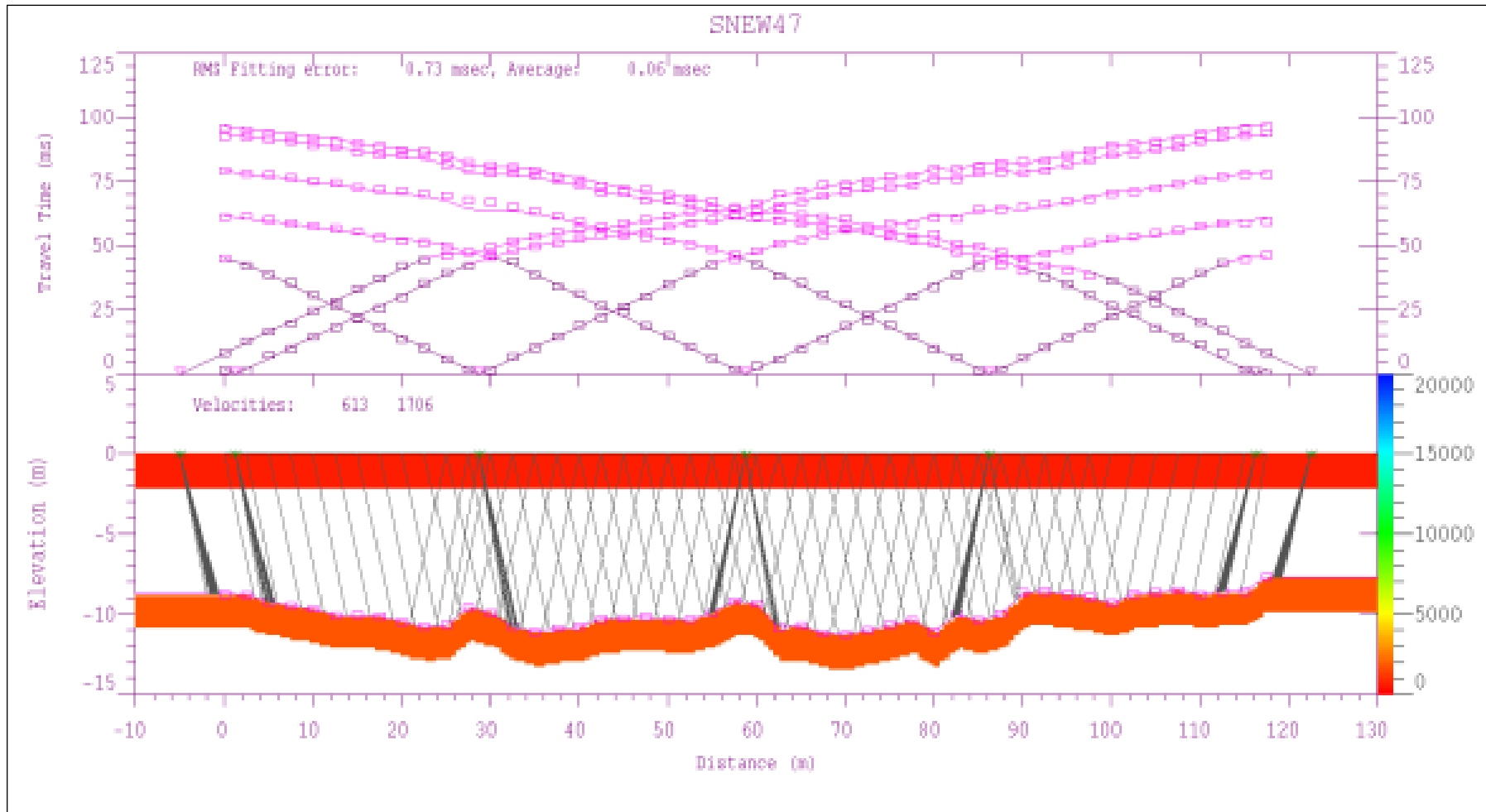


Figure 4.43: 2D inverted model after frequency scaling technique using trace number 47 as noisy trace.

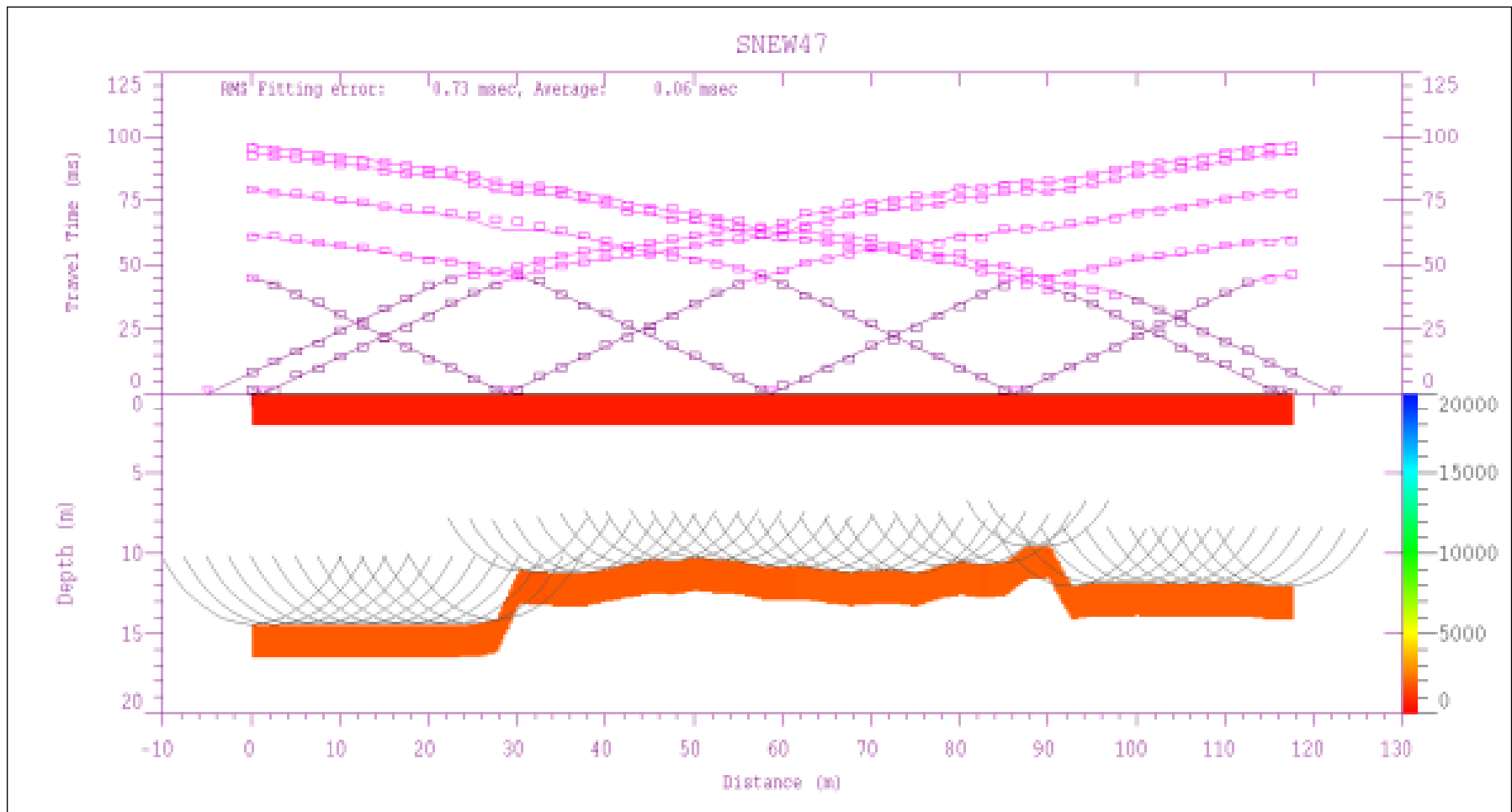


Figure 4.44: GRM interpreted depth model after frequency scaling technique using trace number 47 as noisy trace.

#### **4.4.3 Comparison between Subtraction and Addition Technique with Frequency Scaling Technique**

With simple mathematical expression, the subtraction and addition technique is built. The noisy traces after the subtraction technique are noisier than before and make the picking the first break of signals difficult. The result after addition technique on the other hand gives a good and promising result as the first break signals is easy to pick when compared with subtraction technique.

With frequency scaling technique, the identification of noisy traces and any trace which exceed the threshold value will undergo the treatment. After the treatment using one noisy trace as the reference, we can deduce that there is no significant difference when the noisy trace reference is changed.

From these three data enhancement technique, the frequency scaling is the best new approach of data enhancement technique since its capabilities in preserving the original state of signals when it is not used in part of the technique. This technique has helped in making the first break signal visible and reduces the noisy data that appeared above the first break. As a conclusion, the frequency scaling technique is the best new approached of new noise reduction technique.

#### **4.5 3D Subsurface Images after Data Enhancement**

After the processing and treatment of the data was completely done, the re-picking of FB and interpretation of the section were repeated. The result of this will be used to construct the subsurface image of the research area. With the information obtain from the seismic interpretation, 3D view of the research area with seismic lines superimposed is shown in Figure 4.45. This figure shows the position of the seismic lines and the elevation of this area varies in between 52 and 59 meters with ground surface being highest at northwestern part and gently dips to the south and lowest at the southern part of the area.

Figure 4.46 shows the isopach map 1 which represents the thickness of the unsaturated soil layer. This layer corresponds to the second refractor computed from the seismic analysis. The thickness of this layer varies between 7 meters to 16 meters.

The thicker regions are found in northeastern and southern parts of the area and denotes by blue zones. The shallowest region are found two third along the western part and southeastern part of the area, denotes by green zones. The other regions show a uniform thickness between 9 and 12 meters. The degree of accuracy of the result reaches up to 75% - 90% when correlate with boreholes data. The velocity of this layer ranges between 500 m/s to 600 m/s. The velocity range below this layer up to the bedrock surface is range in between 1600 m/s to 2000 m/s.

The isobach map in Figure 4.47 shows the bedrock elevation reduced to NGVD. The bedrock elevation ranges between 25 to 50 meters. Generally, the bedrock dips to the east on the half northern part of the area and showing gently dipping bedrock on the southern half of the area with the area dips toward the south. The lowest bedrock reliefs are found in the southern and western part of the area.

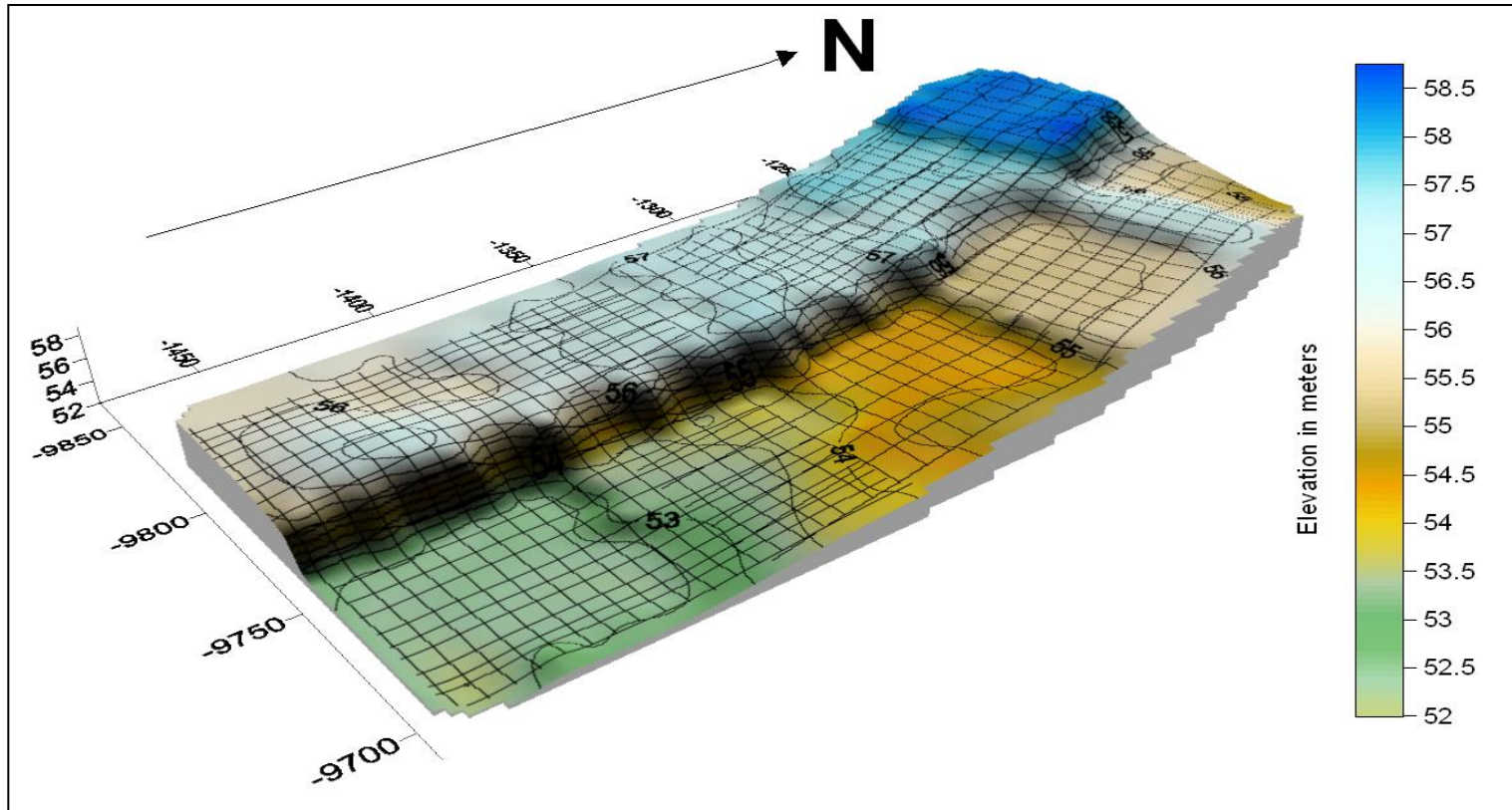


Figure 4.45: View of the research area with seismic lines superimposed.

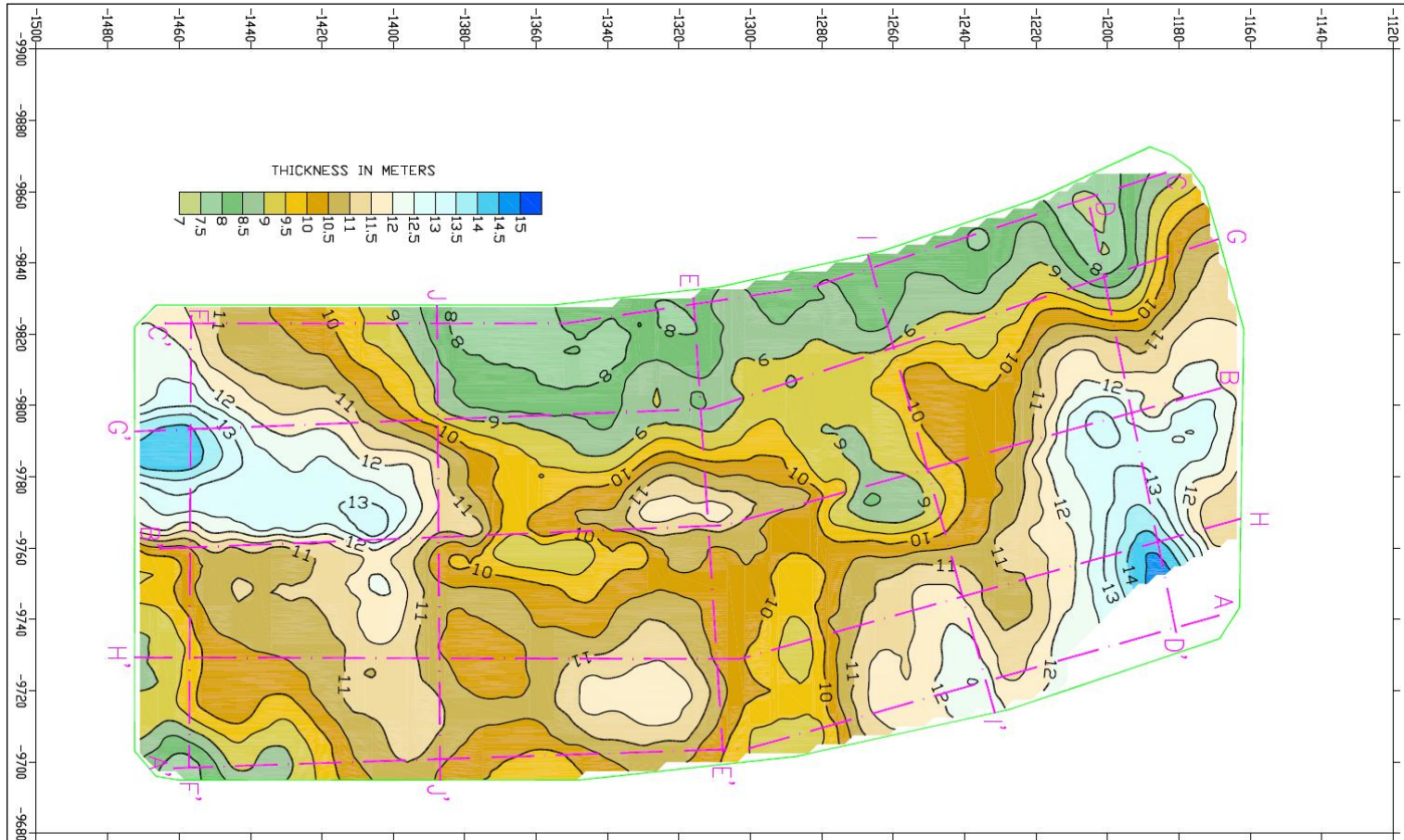


Figure 4.46: Isopach map 1 represents the thickness of the unsaturated soil based on the seismic data.

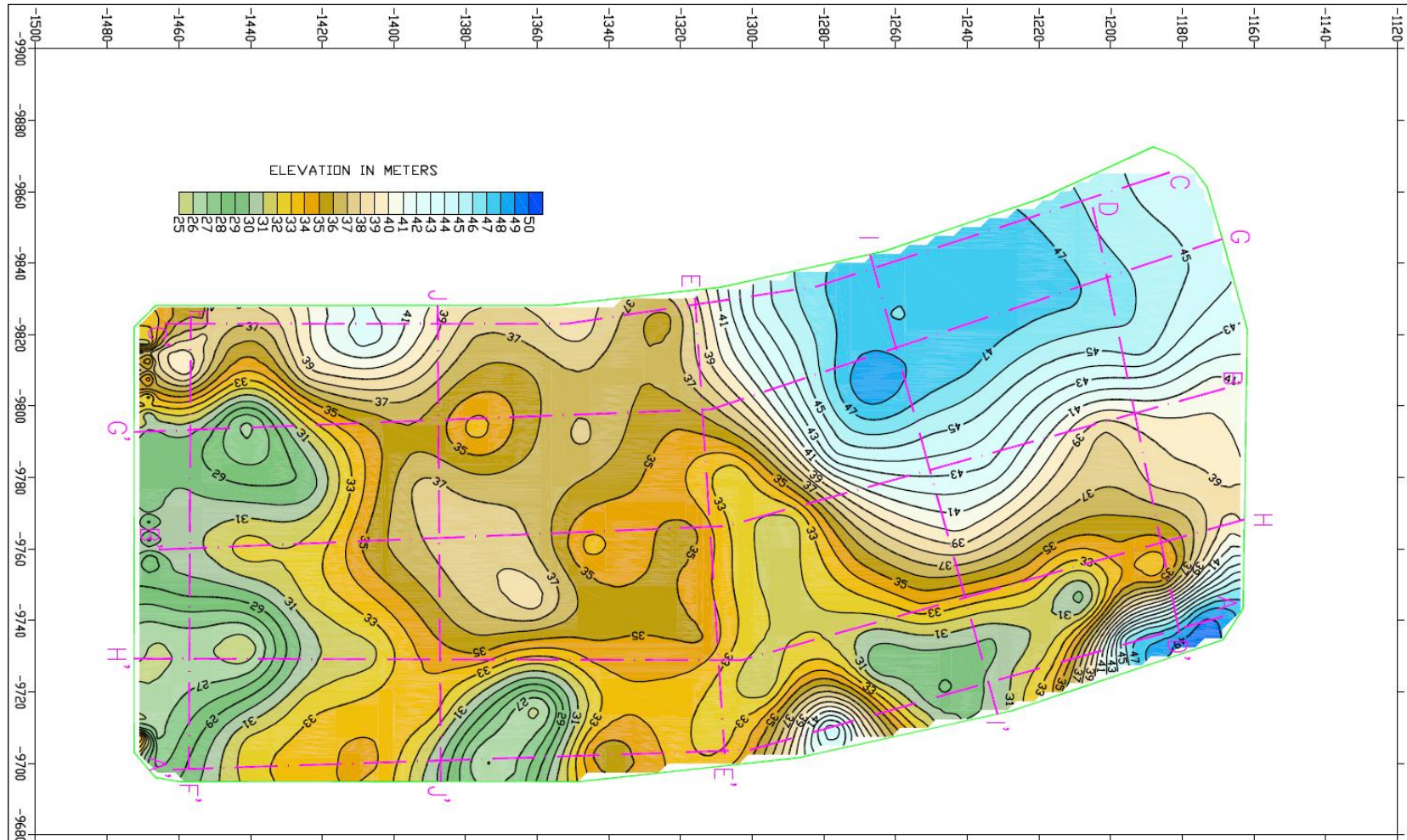


Figure 4.47: Isobach map represents the bedrock elevation based on the borehole data.

#### 4.6 Correlation between Standard Penetration Tests (SPT) with Seismic Velocity

The research area is located on Kuala Lumpur granite formation. From the borehole survey, the granite bedrock is generally 25 to 50 meters below the ground level. The granite appears to moderately weathered and boulders are not found. The overlaying layer on top of the granite consists of soil material with soft to very stiff and/or sand with gravel.

Other than seismic survey, borehole survey also done in the area. The position of the borehole superimposed with seismic line is shown in Figure 4.48. The start of line for seismic survey is marked by white circle and the black circle denotes the end of line. Figure 4.49 shows the isopach 2 map which represents the thickness of the overburden from the ground level to the bedrock surface. The thickness is varies between 5 to 30 meters. Generally, half of southern part is thicker than half of the northern part. Two shallowest regions (green regions) were found at northeast and part of northwest with thickness less than 10 meters. The thicker overburden with thickness between 20 to 30 meters is denoted by blue region in the map.

Figure 4.50 shows the example of processed data set of seismic line number 6. The velocities obtain from the GRM interpreted depth model gives the average value for first layer is 459.71 m/s and 1830.56 m/s for the second layer. Along this seismic line, there are two boreholes drilled down to the granite bedrock. The first borehole, name it borehole A is situated near to geophone number 2 of the seismic line. This borehole encountered the bedrock at depth of 19.6 meter. From the seismic data, the second layer is encountered at depth of 11.6 meter and the velocity of the first layer and second layer is 452.6 m/s and 2143.7 m/s respectively.

For the second borehole, borehole B, it is situated near to the geophone 13. This borehole encountered the bedrock at 26 meter. From the seismic data, the second layer is encountered at 11.6 meter and the velocity of first and second layer is 504.3 m/s and 2143.7 m/s respectively. Depth to the second layer from seismic survey acts as the cut off depth. The N-value fall above this depth will sum up and the average of this value is taking and consider as the average N-value for first layer. For N-value fall below this depth, the average of N-value will consider as the average value for second layer.

Graph 4.51 shows the result from the correlation between Standard Penetration Test (SPT) values with seismic velocities. The data plotting shows two dominant area of the plot. The upper grouping is corresponding to the second layer velocity while the lower grouping is corresponding to the first layer velocity. The correlation equation is  $y=53.57x + 324.3$  with correlation coefficient value is 0.355. With this relation, we can see there is a pattern between these two values. Unfortunately, it is too small and not conclusive enough for a correlation between these two values.

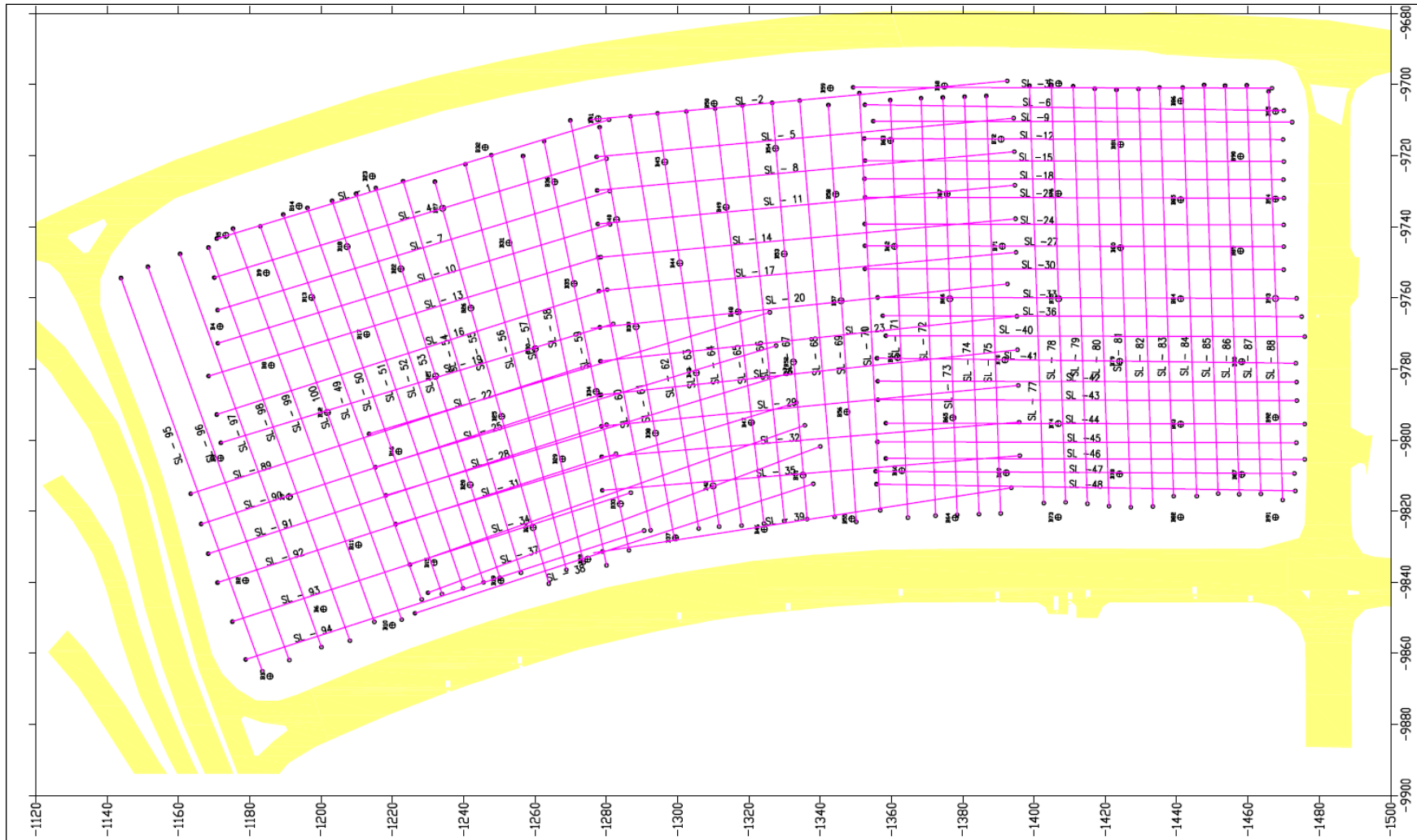


Figure 4.48: Location plan of seismic line superimposed with borehole survey.

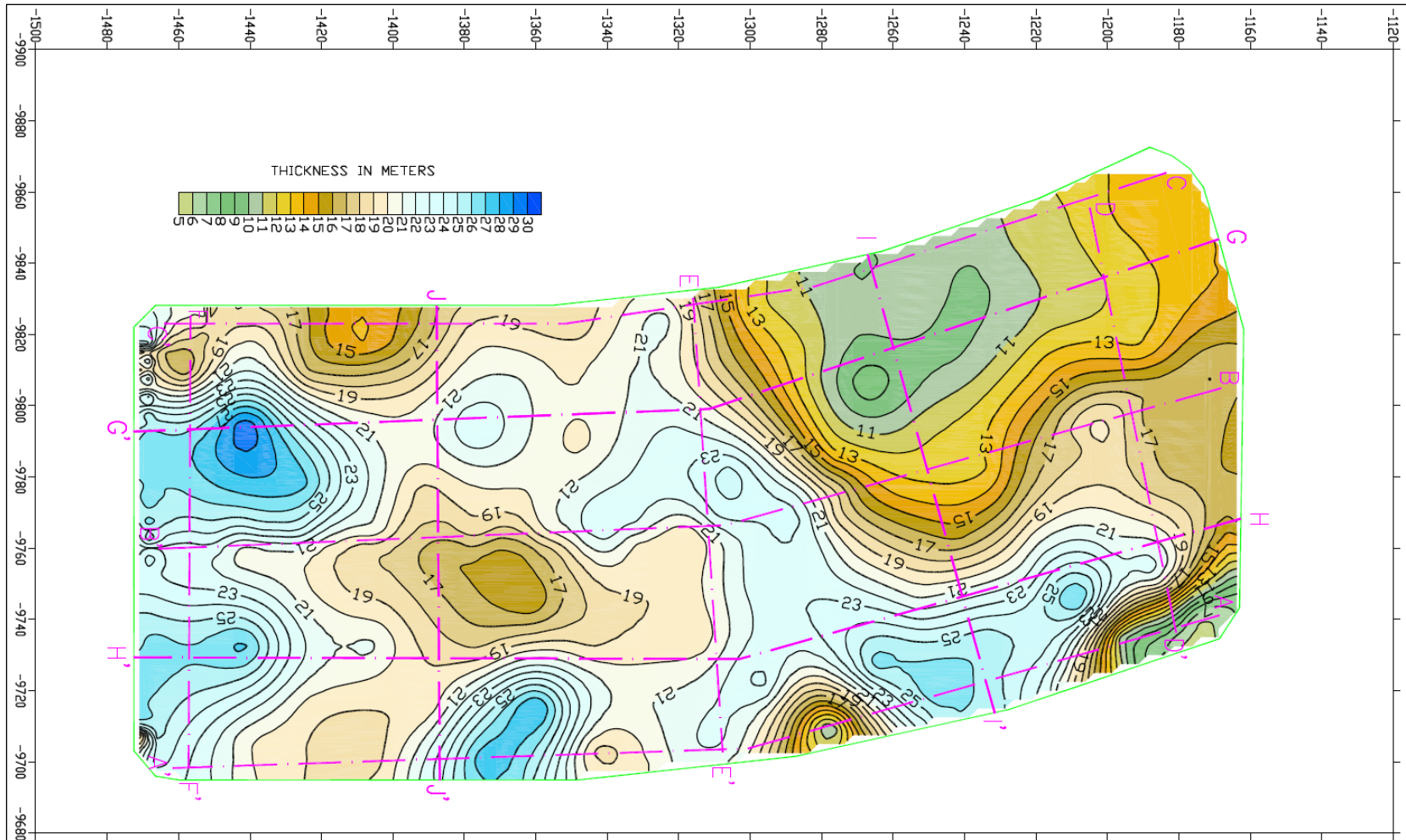


Figure 4.49: Isopach 2 map represents the thickness of overburden based on the boreholes data.

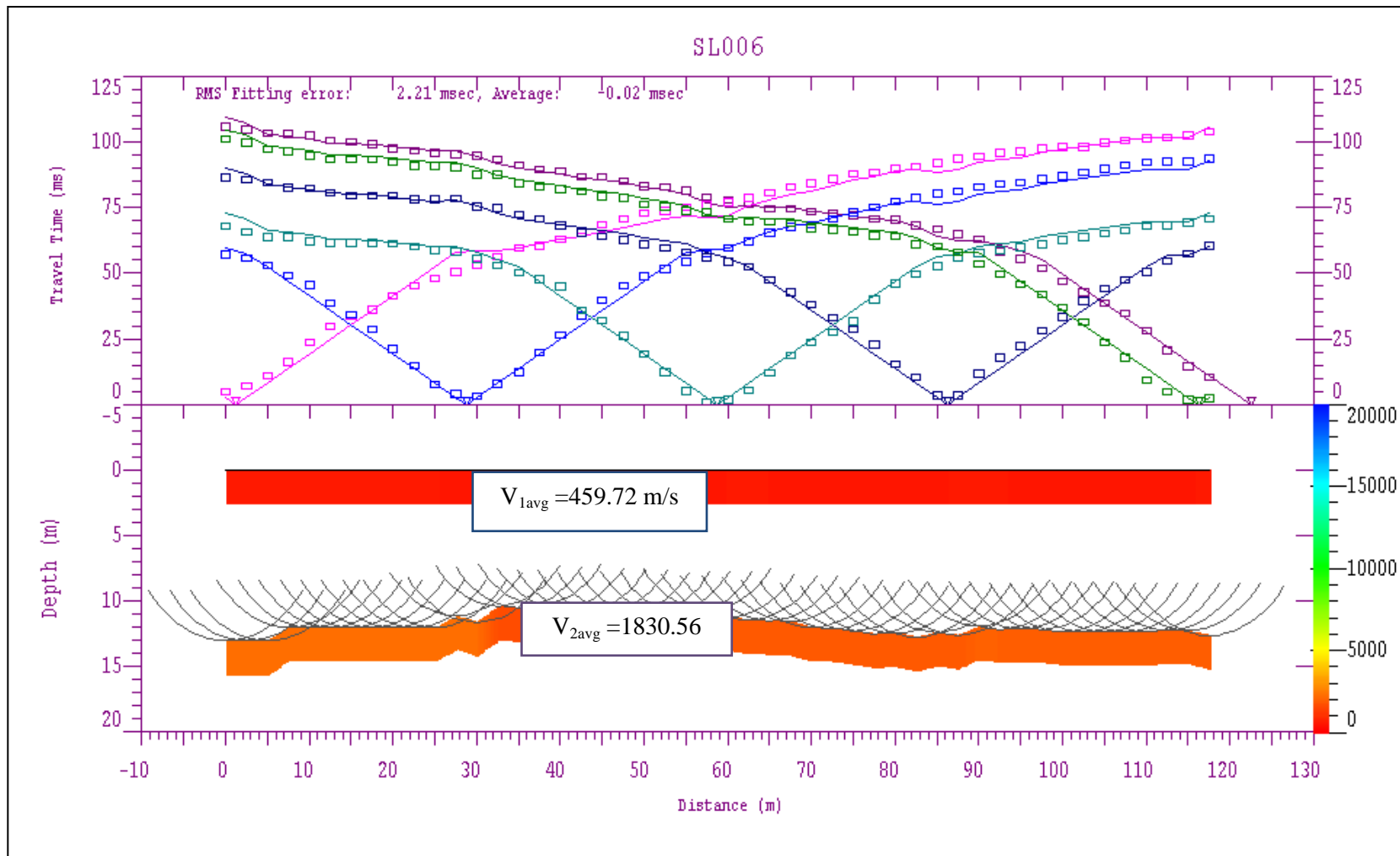


Figure 4.50 : Example of processed data.

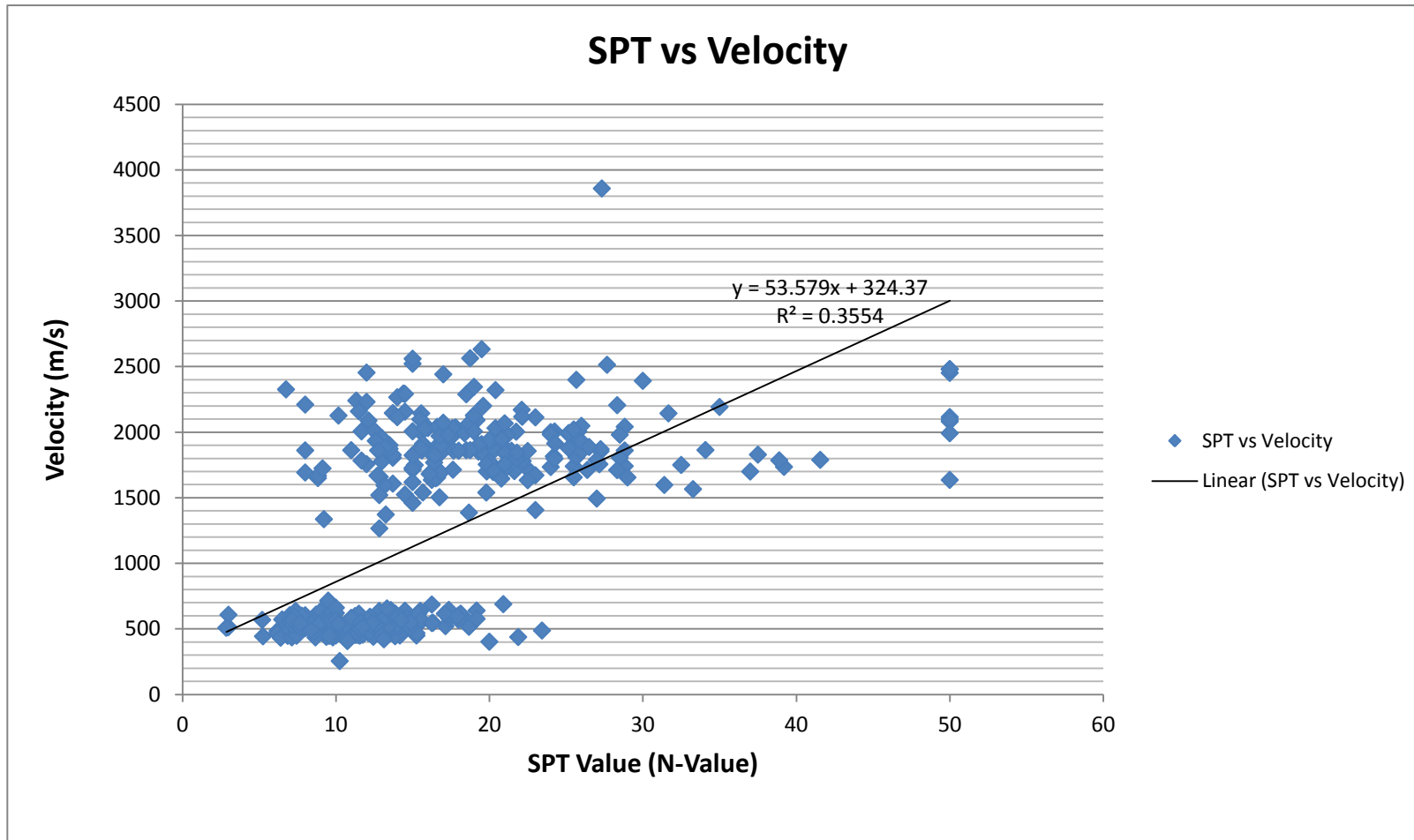


Figure 4.51: Correlation graph between SPT value and velocity value.

## CHAPTER 5

### CONCLUSIONS AND RECOMMENDATIONS

#### 5.1 Conclusions

Based on the field tests during the acquisition stage, the first objective of this research, to design the acquisition parameter for noisy area is fulfilled. Four different tests on the field parameter which are geophone array, source, equipment and trigger were CARRIED OUT. Two different geophone arrays consist of single geophone array and triple geophone array were tested. Frequency-amplitude spectrum was plotted for both geophone arrays and the results from the plots show very minimal changes of amplitude behavior for both geophone arrays. As a result, single geophone array was chosen over the triple geophone array as this geophone array gives a good signal record and shorter time needed in setting up, thus can help in speeding up the acquisition.

The safety, mobility and cost of the induce source for this research is taken into consideration due to the location of the research area. A sledge hammer was chosen as the primary induce source for this seismic acquisition. A test was carried out in determining which striker plate is the best to be pair with sledge hammer. Aluminium striker plate was chosen due to its ability to give good quality seismic data, medium rate of mobility and high level of toughness rate.

Analogue trigger was chosen over switch trigger as the main trigger for the acquisition. The analogue trigger required less time to revert back to its initial condition and low average time to complete one seismic line acquisition but having more time to move when compared to the switch trigger. The key factor is of choosing this trigger is because it has medium rate of sensitivity level which make the shooter more freedom to do the shooting.

Further investigation on affect of distance between planted trigger and striker plate was done. Distance of 1” and 6” away from striker plate is tested. From the spectrum plot, it shows there is no significant difference between planting the geophone 1” away or 6” away from the striker plate. One important factor is to make sure the geophone is planted properly and in firm contact with soil.

The spread layout was chosen and determined in the field itself. As there are two different sets of seismographs system used in the field, 24-channel seismographs system and 48-channel seismographs system the layout is designed to meet those two different seismographs characteristics. Other than that, the shot points also altered when needed to suits the area’s environment as the area is not a flat area. Both of the seismographs system, has the capabilities in help speeding up the acquisition process with a good to very good seismic record. Due to the time constraint, therefore, both seismographs are used during the acquisition processed.

From the testing, single geophone array, aluminium striker plate, analogue trigger and two sets of 24-channel seismograph system and 48-channel seismograph systems was chosen as the primary parameters.

The collected data during the acquisition phase was processed and interpreted using IXRefraX software. From the interpretation, the results shows two layer cases with average velocity value of first layer is 523 m/s. The average velocity for the second layer is 1933 m/s. The depth to the refractor is ranging from 7 m to 16 m. From this result, further investigation was carried on to fulfill the second objective of this research which is to formulate new technique for noise reduction using MatLab software. Three different techniques was developed and tested which are 1) subtraction technique, 2) addition technique and 3) frequency scaling technique as elaborated in Chapter 3. The result shows that the frequency scaling technique is the best approached. The results obtain from this technique are good and improved as the first break signal are easy to track and the picking can be done confidently.

The velocity values obtain from the processing using IXRefraX and Standard Penetration Test (SPT) value was used in order to fulfill the third objective of the research, to investigate for possible correlation between velocities value and SPT value. Graph of correlation between this two value was plotted and from the correlation, the correlation coefficient is measured at 0.355 with the correlation

equation value  $y=53.57x + 324.3$ . Even though there is a pattern between both of the values, it is not conclusive enough for a correlation relation.

## **5.2 Recommendations**

For future works, it is recommended to carry out the acquisition during the night time to avoid high noise contamination and compare the result with day time acquisition result. The using of other safe and reliable energy source is recommended in order to get a better signal in noisy environment. More stacking for each shot point may help in increasing the data quality. Further research on the new approach noise reduction technique might help in better understanding of the behavior of noise and giving clearer signals.

## REFERENCES

- [1] Ackermann, H. D., "Seismic Refraction Study of the Raft River Geothermal Area, Idaho," *Geophysics*, **44**, No. 2, Feb, 1979, pp. 216-225.
- [2] Burger, H. R., "Exploration Geophysics of the Shallow Subsurface," Prentice Hall, New Jersey, 1992.
- [3] Dobecki. T. L. and Romig, P.R., "Geotechnical and Groundwater Geophysics," *Geophysics*, **50**, No. 12, Dec, 1985, pp. 2621-2636.
- [4] Dobrin, M. B. and Savit, C. H., "Seismic Refraction Prospecting," in *Introduction to Geophysical Prospecting*", Fourth Edition, McGraw Hill International Editions, 1988, pp. 450-497.
- [5] Drijkoningen, G. G., "The Usefulness of Geophone Ground-coupling Experiments to Seismic Data," *Geophysics*, **65**, No. 6, Nov-Dec, 2000, pp. 1780-1787.
- [6] Durham, L. S., "3-D next Signal Hill Step: Urban Seismic Shoot Successful," *AAPG Explorer*, Oct, 2009, pp.10-12.
- [7] Gendzwill, D.J., "Underground Applications of Seismic Measurements in A Saskatchewan Potash Mine," *Geophysics*, **34**, No. 6, Dec, 1969, pp. 906-915.
- [8] Haeni F. P., "Application of Seismic Refraction Technique to Hydrologic Studies," *Techniques of Water-Resources Investigations of the United States Geological Survey*, Book 2, Collection of Environment Data, The U. S. Geological Survey, Denver, 1988.
- [9] Hagerdoon, J. G., "The Elusive First Arrival," *Geophysics*, **XXIX**, No. 5, Oct, 1964, pp. 806-813.
- [10] Hasancebi, N., " Empirical Correlation Between Sheer Wave Velocity and Penetration Resistance for Ground Shaking Assessments," *Bulletin of Engineering Geology and the Environment*, **66**, No 2, 2007, pp. 203-213.

- [11] Hatherly, P.J., "A Computer Method for Determining Seismic First Arrival Times," *Geophysics*, **47**, No. 10, Oct, 1982, pp. 1431-1436.
- [12] Hawkins, L. V. and Whiteley, R. J., "Shallow Seismic Refraction Methods in Exploration and Engineering," University of New South Wales
- [13] Hayashi, K. and Takahashi, T., "High Resolution Seismic Refraction Method Using Surface and Borehole Data for Site Characterization of Rock," *International Journal of Rock Mechanics & Mining Sciences*, **38**, 2001, pp. 807-813.
- [14] Hoover, G. M. and O'Brien, J. T., "The Influence of the Planted Geophone on Seismic Land Data," *Geophysics*, **45**, No. 8, Aug, 1980, pp. 1239-1253.
- [15] [http://www.abem.se/files/TERRALOC\\_Mk6v2\\_Mk8.pdf](http://www.abem.se/files/TERRALOC_Mk6v2_Mk8.pdf)
- [16] <http://www.hager-richter.com/seismic.html>
- [17] <http://www.interpex.com/IXRefraX/IXRefraX.htm>
- [18] Bujang, B. K. H., Ali, F. H., Abdullah, A., "Shear Strength Parameters of Unsaturated Tropical Residual Soils of Various Weathering Grades," available online at <http://www.ejge.com/2005/Ppr0564/Ppr0564.htm>
- [19] Inazaki, T., "Relationship between S-wave Velocities and Geotechnical Properties of Alluvial Sediments," SAGEEP2006: 19<sup>th</sup> Annual Symposium on the Application of Geophysics to Engineering and Environmental Problems, 2006.4.
- [20] Kaye, M. K., "Seismic Refraction Study In the Orinoco Basin of Deposition, Venezuela," *Geophysics*, **5**, No. 4, Oct, 1940, pp. 385-392.
- [21] Kilty, K. T., Norris, R. A., McLamore, W. R., Hennon, K. P., and Euge, K., "Seismic Refraction at Horse Mesa Dam: An Application of the Generalized Reciprocal Method," *Geophysics*, **51**, No. 2, Feb, 1986, pp. 266-275.
- [22] Knapp, R. W. and Steeples, D. W., "High-resolution Common-Depth-Point Reflection profiling: Field Acquisition Parameter Design," *Geophysics*, **51**, No. 2, February, 1986, pp. 283-294.

- [23] Koukis, G., Sabatakakis, N., Tsiambaos, G., and Katrivesis, N., "Engineering Geological Approach to the Evaluation of Seismic Risk in Metropolitan regions: Case Study of Patras, Greece, Bulletin of Engineering Geology and the Environment, **64**, No. 3, 2005, pp.219-235.
- [24] Krohn, C. E., "Geophone Ground Coupling," Geophysics, **49**, No. 6, Jun, 1984, pp. 722-731.
- [25] Lankston, R. W., "High-Resolution Refraction Seismic Data Acquisition and Interpretation," Geo Compu Graph, Inc., pp. 45-73.
- [26] Lankston, R. W., "The Seismic Refraction Method: A Viable Tool for Mapping Shallow Targets into 1990's," Geophysics, **54**, No. 12, Dec, 1989, pp. 1535-1542.
- [27] Li, X. and Couzens, R., "Attacking Localized High Amplitude Noise in Seismic Data –A Method for AVO Complaint Noise Attenuation," Sensor Geophysical Ltd., CSEG Recorder, Jan, 2006, pp. 32-36.
- [28] Linehan, D., S. J., and Murphy, V. J., "Engineering Seismology Applications in Metropolitan Areas," Geophysics, **XXVII**, No. 2, Apr, 1962, pp. 213-220.
- [29] Maheswari R. U., Boominathan A., and Dodagoudar G. R., "Use of Surface Waves in Statistical Correlations of Shear Wave Velocity and Penetration Resistance of Chennai Soils," Geotechnical and Geological Engineering, **28**, No 2, 2010, pp.119-137.
- [30] Mangriotis, M. D., Rector, J. W. and E. F. Herkenhoff, "Effects of the Near-Field on Shallow Seismic Studies," Geophysics, **76**, No. 1, Jan-Feb, 2011, pp. B9-B18.
- [31] Martí, D., Carbonell, R., Flecha, I., Font-Capó, J., Vázquez-Suñé, E., and Pérez-Estaún, A., "High-resolution Seismic Characterization in an Urban Area: Subway Tunnel Construction in Barcelona, Spain," Geophysics, **73**, No. 2, Mar-Apr, 2008, pp. B41-B50.

- [32] Miller, R. D., Pullan, S. E., Steeples, D. W., and Hunter, J. A., "Field Comparison of Shallow Seismic Sources Near Chino," *California Geophysics*, **57**, No. 5, May, 1992, pp.693-709.
- [33] Miller, R. D., Pullan, S. E., Waldner, J. S. and Haeni, F. P., "Field Comparison of Shallow Seismic Source," *Geophysics*, **51**, No. 11, Nov, 1986, pp. 2067-2092.
- [34] Mossman, R. W., Heim, G. E., and Dalton, F. E., "Vibroseis Applications to Engineering Work in Urban Area," *Geophysics*, **38**, No. 3, Jun, 1973, pp. 489-499.
- [35] Palmer, D., "An Introduction To The Generalized Reciprocal Method of Seismic Refraction Interpretation," *Geophysics*, **46**, No. 11, Nov, 1981, pp. 1508-1518.
- [36] Rademakers, F., Drijkoningen, G. G., and Fokkema, J. T., "Geophone Ground Coupling: New Elastic Approach," 66<sup>th</sup> Annual International Meeting, Society of Exploration Geophysics, Expanded Abstracts, Paper 4.6.
- [37] Redpath, B. B., "Seismic Refraction Exploration for Engineering Site Investigations," Technical Report E-13-4, U. S. Army Engineer Waterways Experiment Station Explosive Excavation Research Laboratory, California, 1973.
- [38] Ricker, N., "The Form and Laws of Propagation of Seismic Wavelets," *Geophysics*, **18**, No. 10, Jan, 1953, pp. 10-40.
- [39] Glenn, J. R., "Comparison of In Situ and Standard Penetration Tests in Residual Soils for Determining Site Class in Seismic Building Codes," Proceedings, 19th Symposium on the Application of Geophysics to Engineering and Environmental Problems, 2006, pp. 1316-1324.
- [40] Scales, J. A. and Snieder, R., "What is noise?," *Geophysics*, **63**, No. 4, Jul-Aug, 1998, pp. 1112-1124.
- [41] Sjögren, B., "Shallow Refraction Seismic," Chapman and Hall, New York, 1984, pp. 1-8.

- [42] Stam, J. C., "Modern Developments in Shallow Seismic Refraction Techniques," *Geophysics*, **XXVII**, No. 2, Apr, 1962, pp. 198-212.
- [43] Tan, T. H., "Reciprocity Theorem Applied to The Geophone-ground Coupling Problem," *Geophysics*, **52**, No. 12, Dec, 1987, pp. 1715-1717.
- [44] Telford, W. M., Geldart, L.P., and Sheriff, R. E., "Applied Geophysics," Second Edition, Cambridge University Press, New York, 1990, pp. 136-282.
- [45] Washburn, H. and Wiley, H., "The Effect of the Placement of A Seismometer on Its Response Characteristics," *Geophysics*, **6**, No. 2, Apr, 1941, pp. 116-131.
- [46] Wolf A., "The Equation of Motion of A Geophone On The Surface of An Elastic Earth," *Geophysics*, **9**, No. 1, Jan, 1944, pp. 29-35.
- [47] <http://www.britannica.com/EBchecked/media/91336/The-law-of-refraction-or-Snells-law-predicts-the-angle>
- [48] <http://www.dvssel.gov.my/cms/index.php?pt=749>
- [49] <http://www.jkr.gov.my/page/112>

## APPENDIX A

### MatLab Code for Advanced Data Improvement

```
clear all
dt=0.005;

[noiseori,STH,SH]=ReadSegy('DAT_0132.SGY');

[noise,STH,SH]=ReadSegy('DAT_0132.SGY');
[signal,STH,SH]=ReadSegy('DAT_0133.SGY');
ori=signal;
    fre(1:800,:)=ori(1:800,20:48);
B1=smooth(abs(fft(ori(:,47))));%trace with most noise
%B2=smooth(abs(fft(ori(:,12))));%trace without noise
%A=B2./B1;
    nt=length(ori(:,1));
sumnoise=sum(ori,2);
% spectrum
s=abs(fft(sumnoise(:,1),nt)); % noise recorded
spec=s(1:round(nt/2),:);
sp1=spec;
db=20*log10(spec/max(max(spec)));
db1=smooth(db);

s2=abs(fft(ori(:,12),nt)); % clean trace
spec=s2(1:round(nt/2),:);
sp2=spec;
db=20*log10(spec/max(max(spec)));
db2=smooth(db);

s3=abs(fft(ori(:,47),nt)); % noisy trace
spec=s3(1:round(nt/2),:);
sp3=spec;
db=20*log10(spec/max(max(spec)));
db3=smooth(db);

fn=1./(2*dt);
f=linspace(0.,fn,round(nt/2));
figure(1)
subplot(3,1,1)
plot(f,db1);
title('sum noise')
```

```

subplot(3,1,2)
plot(f,db2);
title('clean trace')

subplot(3,1,3)
plot(f,db3);
title('noisy trace')

t=0:dt:nt-1;

signal1=ori;
signal2=ori;
snew=ori;
%sumnoise=zeros(4096,1);

Fn=real(fft(sumnoise));
Fs=(fft2(ori));
signal2=ori;
av=mean(signal);
aav=mean(av);
bav=av/aav;
% {
for i=1:48
    if bav(i)>3
        %a(i)=3;
        %signal(:,i)=ori(:,i)-noise(:,i);
        %signal2(:,i)=ori(:,i)+noise(:,i);
        B2=smooth(abs(fft(ori(:,i))));%trace without noise
        A=B2./B1;
        S1=abs(fft(ori(:,i)));
        Fs(:,i)=A.*S1;
        %ssnew=real(ifft(FFs));
        %snew(:,i)=ssnew;
    end

end

% }

for i=1:48
    if abs(bav(i))>3
        signal1(:,i)=ori(:,i)-noise(:,i);
        signal2(:,i)=ori(:,i)+noise(:,i);
        %snew(:,i)=snew(:,i)+noise(:,i);
        B2=smooth(abs(fft(ori(:,i))));%trace without noise
        A=1.1*B2./B1;
        S1=real(fft(ori(:,i)));
        AFs=A.*S1;
        snew(:,i)=real(ifft(AFs));
    end
end

```

```

end
% ss=real(iff2(AFs))
% snew=ss+snew;
% snew=real(iff2(Fs));
figure(2)
subplot(2,2,1)
plotseis(ori)
title('Original')
subplot(2,2,2)
plotseis(snew)
title('Frequency Scaling')
subplot(2,2,3)
plotseis(signal1)
title('Subtraction')
subplot(2,2,4)
plotseis(signal2)
title('Addition')

% plotseis(snew)

trace1=ori(:,1);
% freq=abs(fft(ori));
% spec=20*log10(Fn);
% figure(2)
%
% subplot(2,1,1)
% plot(f,db)
% title('Noise spectrum');
%
% freq2=abs(fft(noise));
% spec2=20*log10(freq);
% plot(spec2(1:nt/2))

% try
% clear all
% [Data,SegyTraceHeaders,SegyHeader]= ReadSegy('DAT_0133.SGY');
clear f spec a b a2
Data=signal;
t = SH.time;
dt = t(2)-t(1);
%Data = bp_filter(Data,dt,10,20,150,200);

%t = t; %SegyHeader.time;

for i = 1:size(Data,2);
% Data(:,i)= Data(:,i)/max(abs(Data(:,i)));
[spec(:,i),f] = fftrl(Data(:,i),t);

```

```
a = abs(spec(:,i));
b(:,i)= a;
end

a2 = mean(b,2);
Adb=real(todb(a2));

hold on
figure(7);
plot(f,Adb,'b','linewidth',2); set(gca,'xlim',[0 500]); grid on;
    %ylim([0 500000000]);

    ylim([-50 10]);
title('Frequency Spectrum Plot');
```

APPENDIX B

Borehole Log Example (Borehole B86)

				BOREHOLE NO	BH - B86				
				STARTING DATE	14/1/2010				
TYPE OF BORING		Rotary Wash-boring/Coring		COORDINATE	E -9704.629				
TYPE OF RIG		YBM-2JES		FINISHING DATE	15/1/2010				
DIA. OF BORING		0.0875m (NW)		WATER LEVEL	3.20m.b.g.l.				
		EDUCED LEVEL (g)		52.28		SUPERVISOR	Azlan		
Date & Time	W.Level (M)	Drilling Method	Depth (M)	Sample & Test		RecRQD (%) (%)	Legend	Description	
				Number	Result				
			0.00					Top Soil Dark grey, sandy SILT with some	
			1.00						
			1.50	SPT1/ DS1	2,3,3,2,3,3 N=11	●			
			1.95		Rec=0.20/0.45		44	1.50m	
			2.00					Stiff, dark brown, sandy SILT.	
			3.00	SPT2/ DS2	2,3,2,3,2,3 N=10	●		- Ditto -	
			3.45		Rec=0.21/0.45		47		
			4.00						
			4.50	SPT3/ DS3	3,2,3,3,3,2 N=11	●		- Ditto -	
			4.95		Rec=0.18/0.45		40		
			5.00						
14/1/2010 1700hrs	1.80m	NW							
			6.00	SPT4/ DS4	4,3,3,3,2,3 N=11	●		- Ditto -	
			6.45		Rec=0.25/0.45		56		
			7.00						
			7.50	SPT5/ DS5	2,3,3,4,3,4 N=14	●		- Ditto -	
			7.95		Rec=0.20/0.45		44		
			8.00						
			9.00	SPT6/ DS6	2,3,3,2,2,2 N=9	●		9.00m	
			9.45		Rec=0.18/0.45		40	Loose, medium brown, silty SAND.	
			10.00						
Cohesive soil (N)		0 - 2 = V.Soft 2 - 4 = Soft 4 - 8 = M.Stiff 8 - 15 = Stiff 15 - 30 = V.Stiff > 30 = Hard		Legend		Standard Penetration Test ●		Remarks	
Non Cohesive Soil (N)		0 - 4 = V. loose 4 - 10 = Loose 10 - 30 = M.dense 30 - 50 = Dense > 50 = V. dense				Undisturbed Sample ○			
						Mazier Sample X			
						Vane Shear Test □			
						Coring into Rock ▣			



			20.00	C1	Rec=1.00/1.50 RQD=0/1.50	67	0	+++++	Light brown to grey, highly weathered, GRANITE, very weak.
			21.00					+++++	
			21.10					+++++	
		NMLC	22.00	C2	Rec=1.30/1.50 RQD=0.60/1.50	87	40	+++++	- Ditto - (weak)
			22.60					+++++	
			23.00					+++++	
			24.00	C3	Rec=1.35/1.50 RQD=0.65/1.50	90	43	+++++	- Ditto -
15/1/2010 1700hrs	2.80m		24.10					+++++	
16/1/2010	3.20m		24.10					+++++	END OF BOREHOLE AT 24.10m
			25.00						
			26.00						
			27.00						
			28.00						
			29.00						
			30.00						
Cohesive soil (N)		0 - 2 = V. Soft 2 - 4 = Soft 4 - 8 = M. Stiff 8 - 15 = Stiff 15 - 30 = V. Stiff > 30 = Hard	Legend		Standard Penetration Test	●	Remarks		
Non Cohesive Soil (N)		0 - 4 = V. loose 4 - 10 = Loose 10 - 30 = M. dense 30 - 50 = Dense > 50 = V. dense			Undisturbed Sample	○			
					Mazier Sample	⊗			
					Vane Shear Test	☐			
					Coring into Rock	⊠			







16/1/2010		NMLC	30.00				+++++	
1245hrs	4.23m		30.50				+++++	
17/1/2010	4.26m		31.00				+++++	END OF BOREHOLE AT 30.50m
			32.00					
			33.00					
			34.00					
			35.00					
			36.00					
			37.00					
			38.00					
			39.00					
			40.00					
Cohesive soil (N) 0 - 2 = V. Soft 2 - 4 = Soft 4 - 8 = M. Stiff 8 - 15 = Stiff 15 - 30 = V. Stiff > 30 = Hard			<b>Legend</b> Standard Penetration Test  Undisturbed Sample  Mazier Sample  Vane Shear Test  Coring into Rock 		<b>Remarks</b>			
Non Cohesive Soil (N) 0 - 4 = V. loose 4 - 10 = Loose 10 - 30 = M. dense 30 - 50 = Dense > 50 = V. dense								